THE DISTRIBUTION OF DISSOLVED SILICA IN THE DEEP WESTERN NORTH ATLANTIC OCEAN

by

Gerald J. Needell

B.S., Northeastern University
(1975)

SUBMITTED IN PARTIAL FULFILLMENT OF THE REQUIREMENTS FOR THE DEGREE OF MASTER OF SCIENCE

at the

MASSACHUSETTS INSTITUTE OF TECHNOLOGY

and the

WOODS HOLE OCEANOGRAPHIC INSTITUTION

November, 1978

Signature of Author.....Gerald J. Needell.....
Joint Program in Oceanography, Massachusetts Institute of Technology - Woods Hole Oceanographic Institution, Department of Meteorology, Massachusetts Institute of Technology, November, 1978.

Certified by.....James R. Luyten.....
Thesis Supervisor

.....Glenn R. Flierl.....
Thesis Supervisor

Accepted by.....
Chairman, Joint Oceanography Committee in the Earth Sciences, Massachusetts Institute of Technology - Woods Hole Oceanographic Institution.

THE DISTRIBUTION OF DISSOLVED SILICA IN THE DEEP WESTERN NORTH ATLANTIC OCEAN

by

Gerald J. Needell

B.S., Northeastern University
(1975)

SUBMITTED IN PARTIAL FULFILLMENT
OF THE REQUIREMENTS FOR THE
DEGREE OF

MASTER OF SCIENCE

at the

MASSACHUSETTS INSTITUTE OF TECHNOLOGY

November 1978

Signature of Author.....Gerald J. Needell.....
Department of Meteorology, November 1978

Certified by.....James R. Chamberlain.....
Thesis Supervisor

.....Glenn R. Flierl.....
Thesis Supervisor

Accepted by.....
Chairman, Department Committee

To Sally - who is my inspiration

ABSTRACT

The distribution of dissolved silica in the deep western North Atlantic Ocean is presented. The potential temperature-dissolved silica relationship is compared with the potential temperature salinity relationship in the North Atlantic Deep Water. Geographical variations in the potential temperature-dissolved silica relationship are discussed with particular emphasis on the low silica signal of the Western Boundary Undercurrent (WBUC). The WBUC is shown to have a significant influence on the potential temperature-dissolved silica relationship from the tail of the Grand Banks of Newfoundland to Cape Hatteras.

It is suggested that a region of enhanced mixing is present west of 65°W that is responsible for the observed changes in the dissolved silica distribution.

THE DISTRIBUTION OF DISSOLVED SILICA IN THE DEEP WESTERN NORTH ATLANTIC OCEAN

by

Gerald J. Needell

Submitted to the Department of Meteorology
on November 13, 1978 in partial fulfillment of the requirements
for the Degree of Master of Science

ABSTRACT

The distribution of dissolved silica in the deep western North Atlantic Ocean is presented. The potential temperature-dissolved silica relationship is compared with the potential temperature salinity relationship in the North Atlantic Deep Water. Geographical variations in the potential temperature-dissolved silica relationship are discussed with particular emphasis on the low silica signal of the Western Boundary Undercurrent (WBUC). The WBUC is shown to have a significant influence on the potential temperature-dissolved silica relationship from the tail of the Grand Banks of Newfoundland to Cape Hatteras.

It is suggested that a region of enhanced mixing is present west of 65°W that is responsible for the observed changes in the dissolved silica distribtution.

Thesis Supervisor: Dr. J. R. Luyten, Associate Scientist

Table of Contents

I. Introduction

The distribution of dissolved silica in the deep western North Atlantic Ocean may be used to identify water masses with distinct characteristics within the potential temperature and salinity range of the ubiquitous North Atlantic deep water.

The most prominent feature of the silica distribution is a narrow band of low silica along the continental rise. This low silica feature shall be identified as the Western Boundary Undercurrent (WBUC) in keeping with the literature (Richardson (1977)). It shall be demonstrated that the WBUC can be traced from the tail of the Grand Banks of Newfoundland to Cape Hatteras. With the data presented below, a "global" view of the WBUC shall be provided.

In the past, observations of the WBUC have consisted of hydrographic sections across the continental rise for which the geostrophic transport was computed. Either neutrally buoyant floats or moored current meters were used to set absolute velocities (Swallow and Worthington (1961), Volkmann (1962), Richardson (1977), Clarke, Hill, Reiniger, and Warren (1978)). Occasionally, dissolved silica was measured and it could be demonstrated that the water observed did have a northern origin (Richardson (1977), Clarke, Hill, Reiniger, and Warren (1978)).

Eight month long current meter records along 70°W show a steady westward flow on the upper continental rise (Luyten,

1977). Unfortunately, one cannot be sure whether the westward flow is the WBUC (i.e., low silica) or is part of a broad westward flow in the slope water region (Webster (1969)).

This brings up an important problem with the historical observations of WBUC. Stommel (1957) postulated the existence of a deep southward flowing western boundary current in the Atlantic Ocean. His model was based on the hypothesis that some thermohaline process caused sinking of water in arctic regions and upwelling in antarctic regions. To conserve mass, he argued that a deep flow would be present along the western boundary.

In the following year, Swallow and Worthington (1961) occupied hydrographic sections and tracked neutrally buoyant floats near Cape Romaine, North Carolina. In the hydrographic data, they found that the deep isotherms sloped downward off shore indicating the presence of westward shear. When they observed that the neutrally buoyant floats moved westward, it was assumed that the WBUC had been found. The current meter data from 70°W shows that even where the flow is relatively steady toward the west, it is not always so. Occasional reversals in the flow are not uncommon. Thus one must be cautious in the interpretation of few day-long float tracks.

It should also be noted that the spatial coverage of the data from which we can observe the WBUC is not uniform. The only long-term current meters on the continental rise were at 70°W. Hydrographic sections with some method of determining absolute velocities are only available near 70°W and Cape

Hatteras. The results of a section at 50°W are not considered realistic for reasons discussed in the text. Thus we are left with only a limited set of observations of the WBUC. There is no direct evidence for a continuously flowing current that passes around the tail of the Grand Banks of Newfoundland and follows the continental rise toward the west. To the contrary, the current meter data and the variations in the transport calculations suggest that whatever flow there is, is not steady.

The distribution of dissolved silica will be used to demonstrate that the WBUC can be identified in terms of its water mass characteristics. The effects of the WBUC can be traced along the continental rise from the tail of the Grand Banks of Newfoundland to Cape Hatteras. However, the structure of the flow cannot be determined from the available data.

Evidence is presented below which suggests that a region of enhanced mixing is present west of 65°W and has a pronounced effect upon the dissolved silica distribution.

II. Background

2.1 Historical uses of dissolved silica as a water mass tracer

It has only been in the past three decades that one has been able to map out the distribution of dissolved silica. On the basis of sparse data, Sverdrup, Johnson, and Fleming (1942) concluded that the concentration of dissolved silica

increased monotonically with depth everywhere in the world oceans. They pointed out that the silica values in the Atlantic Ocean were in general, lower than those of the other oceans. Cooper (1952) examined the sources and sinks of dissolved silica and suggested that the concentration of silica in the deep water should be in equilibrium and might be useful as a water mass tracer. Without any observations to rely on, Cooper assumed that the tundra drainage in the Arctic would result in a high silica content of the waters of the North Polar Sea. He then reasoned that there would be a flow of high silica water in the Greenland and Irminger Currents which could be easily detected by its silica content. While recent observations have indeed shown that there exists high silica water in the Baffin Basin (SiO_2 > 80µg A/ℓ - Corwin and McGill (1963), Grant (1970)), there is no evidence of it getting over the sill and into the Labrador Basin. In fact, the Norwegian and Labrador Seas are characterized by a low silica signal (SiO_2 ∿ 10-15 µg A/ℓ). As it shall be demonstrated, these waters are easily detected along the western boundary of the western North Atlantic Ocean.

Armstrong (1965) showed the distinctly lower concentrations of silica in the deep Atlantic Ocean, when compared to the world oceans. He concluded that this was a result of the unique exchange of bottom waters that occurs in the Atlantic Ocean and suggested that "...our understanding of water movements and of mixing processes in the Atlantic Ocean would be greatly increased by more knowledge of the silica content of Arctic waters."

Metcalf (1969) showed that the concentration of dissolved silica could be used to identify Antarctic Bottom Water, North Atlantic Deep Water, and Antarctic Intermediate Water. He also suggested that silica might be useful in studying the NADW where little variation in the potential temperature-salinity relationship is found.

Carmack (1973) found that silica was a valuable tracer in the Antarctic. He found that he could distinguish between water masses that appeared indistinguishable on the basis of θ-S data alone.

2.2 The deep western North Atlantic Ocean

It is well known that there is a tight correlation between potential temperature and salinity in the deep western North Atlantic Ocean for potential temperatures below 3.0°C (Worthington and Metcalf (1961), Wright and Worthington (1970)). Most of the water characterized by this θ-S correlation for $\theta > 1.9$°C have been classified as North Atlantic Deep Water (NADW) (Wright and Worthington (1970)). There is little geographic variation in the θ-S distribution of the western North Atlantic in this potential temperature range (Worthington and Wright (1970)). This has made it difficult for physical oceanographers to study the deep general circulation in terms of potential temperature and salinity characteristics.

Near the continental rise, geostrophic calculations and direct velocity measurements (neutrally buoyant float and

moored current meters) allowed observers to deduce the existence of a deep southward flowing current (Swallow and Worthington (1961); Volkmann (1962); Richardson (1977)). This flow has become known as the Western Boundary Undercurrent and is responsible for the equatorward movement of deep water from the Norwegian and Labrador Seas (Stommel (1957); Richardson (1977); Clarke, Reiniger, Hill, and Warren (1978)).

Metcalf (1969) demonstrated the usefulness of the dissolved silica content of deep water as a water mass tracer. Using the available data, he constructed a map of the concentration of dissolved silica on the 2.0°C potential temperature surface. His figure is reproduced as Fig. 1. The principal feature of this map is the general north-south gradient of dissolved silica. The paucity of data prevents a detailed analysis of the distribution but this map does suggest that dissolved silica is a useful tracer of the general circulation of the North Atlantic Ocean.

Richardson (1977) and Worthington (personal communication) found that there is a drop in the silica concentration along potential isotherms as one approaches the continental rise.

Worthington (1976) has proposed a model of the general circulation of the North Atlantic Ocean, in which he postulated the existence of two anti-cyclonic gyres. One to the north of the Grand Banks of Newfoundland, and the second comprised of the Gulf Stream and its return flow bounded to

the south by the Mediterranean salt tongue. In the deep water Worthington based his interpretation partly on the change in the dissolved silica distribution in the deep water across the proposed boundary between the two gyres. His figure showing characteristic deep θ-SiO_2 plots for the two gyres is reproduced as Fig. 2. Worthington's model also allows for a WBUC passing around the tail of the Grand Banks of Newfoundland and along the continental rise until it crosses beneath the Gulf Stream near Cape Hatteras. He allows for no exchange of water between the WBUC and the southern gyre.

Clarke, Hill, Reiniger, and Warren (1978) have criticized Worthington's model. They claim that in the deep water, no evidence exists for two distinct gyres, and that the silica distribution (from a survey of their own) indicates that there is an exchange of water between the "Northern Gyre" area and the Sargasso Sea.

In this work the distribution of dissolved silica in the deep western North Atlantic Ocean, based on several sections occupied during the last two decades, shall be presented. A large portion of the data is from the last six years. After presenting a summary of the data and methods of analysis used, we shall describe the water mass characteristics present and form a consistent picture of the geographical variations in the silica distribution. It shall be demonstrated that there are significant variations of the silica distribution within the NADW. These variations

will allow us to trace the origins of some components of the NADW which cannot be distinguished on the basis of θ-S characteristics. The distribution of silica on potential temperature surfaces shall be examined and these distributions compared with models of the general circulation. In addition the WBUC shall be examined by following its silica signal along the continental rise from the tail of the Grand Banks to Cape Hatteras. Evidence shall be presented for isopycnal mixing along the WBUC path, resulting in downstream dilution of the low silica WBUC water.

The data coverage of the western North Atlantic Ocean has expanded greatly over that which was available to Metcalf (1969) and Worthington and Wright (1972). More structure in the silica distribution can be discerned here than was possible previously. The time span over which the data was collected must certainly be kept in mind. Little is known of the temporal variations of the deep water properties. That a consistent picture of the deep silica distribution can be presented is taken to indicate that these temporal variations are indeed small.

It must, of course, be kept in mind that local anomalies do exist. They may be either due to temporal, spatial, or possibly instrumental effects. As discussed in Appendix I large anomalies which contradict surrounding data must be suspect, but more reasonable local features are retained in the data set and are accepted as essential characteristics of the ocean. Where these features stand out they will be noted.

III. Data and Methods

The data used in this report was obtained by searching the WHOI and NODC oceanographic files for cruises in which temperature, salinity, and dissolved silica were measured. Only those cruises where salinities were measured by a conductivity bridge (i.e., three decimal place precision) were used. This basically restricted the data set to cruises since 1958. The data used is summarized in Table 1 (Fig. 3). The data from one cruise, KNORR 12, was rejected for reasons given in Appendix I.

In a few cases, duplicate sections (i.e., two or more sections at the same location) existed in the data. The section with more closely spaced stations was used. In addition, cruises for which samples were analyzed at sea were preferred to those during which the samples were frozen. All of the data used in this report was analyzed at sea with either a spectrophotometer or autoanalyzer.

For all cruises except AII 100 (see below) the data were accepted as they existed in the files. Observations denoted as questionable by the observers were discarded. Plots of θ-SiO_2 and S-SiO_2 were formed and observations which disagreed with the main body of data were rejected (see discussion of θ-SiO_2 data). All of the data (again with the exception of AII 100 as noted below) were from previously published sources (see Table I) and had been edited on the basis of the mean θ-S distribution of the North Atlantic Ocean.

Table I.

Year	Ship	Cruise	Location	Previous Publication
1958	DISCOVERY II	I.G.Y. 2	24° 30' N* 32° 15' N*	Metcalf (1969) Worthington and Wright (1970)
1961	ATLANTIS	265	40° 15' N*	
1961	CHAIN	20	Woods Hole-Bermuda	Worthington and Wright (1970)
1966	ATLANTIS II	18	near 36°N,66°W and 36°N,63°w	Metcalf(1969)
1971	TRIDENT		Cape Hatteras	Richardson (1977)
1972	HUDSON		50°W and around the tail of the Grand Banks	Clarke, Hill, Reiniger and Warren (1978)
1972	CHAIN	104	around the tail of the Grand Banks	Clarke, Hill, Reiniger and Warren (1978)
1972	KNORR	30	GEOSECS stations* 27-34	Broeker, Takahashi and Li(1976)
1975	KNORR	48	64° 30'W	Worthington(in preparation)
1977	KNORR	66	55°W	Worthington(in preparation)
1978	ATLANTIS II	100	70°W	

* used only in the preparation of the maps of dissolved silica on potential temperature surfaces

The section from cruise AII 100 was occupied by the author in the spring of 1978. The samples were collected with a 24-bottle rosette of Niskin bottles on a Neil Brown CTD. For this work only the temperature data from the CTD was used. The salinities were determined at sea on a Guildline Autosal salinometer and the dissolved silica was determined with a spectrophotometer. The data were edited by plotting both salinity and silica versus pressure and removing those points from which both salinity and silica values indicated contamination of the sample. For the thirteen stations occupied, the worst had eight "contaminated" samples and the best had none (there were 24 samples per station). The final θ-S data set was then compared to the Worthington-Metcalf (1969) mean θ-S curve and no other questionable salinities were obvious below 4.0°C.

The contour plots presented in Section V were prepared by linearly interpolating the θ-SiO_2 data for each station to the θ values used.

IV. Water Mass Characteristics

4.1 Potential temperature salinity characteristics

As previously stated, the deep western North Atlantic Ocean is characterized by a tight potential temperature salinity correlation. Figure 4 is a composite plot of deep θ-S observations for those stations indicated. The boundaries of the North Atlantic Deep Water are indicated (Worthington

and Wright (1970)). Below the inflection point at $\theta \sim 1.85°C$ a low salinity tail is present indicating the effects of Antarctic Bottom Water (Wright and Worthington (1970); Broeker, Takahashi, and Li (1976)).

4.2 Potential temperature-silica characteristics

Figure 5 is a composite plot of deep observations of potential temperature and dissolved silica for those stations indicated. It should be noted that within the potential temperature range of the North Atlantic Deep Water ($\theta > 1.9°C$), we find the maximum scatter in the θ-SiO_2 plot.

Note also that for $\theta < 1.85°C$ there is a sharply increasing silica tail corresponding to the low salinity tail of the Antarctic Bottom Water (AABW) (Broeker, Takahashi, and Li (1976)). This high silica branch is confined to the south of the tail of the Grand Banks of Newfoundland. One can see the difference clearly when the data are separated into groups of data from either side of the tail of the Grand Banks (see Figures 6a and 6b). Those stations east of 50°W show no AABW. This geographical limit to the northward influence of the AABW is similar to that used by Wright and Worthington (1970) in their volumetric potential temperature, salinity census of the North Atlantic Ocean. The AABW was seen clearly in the North American Basin, but not in the Labrador Basin (Figures 7a and 7b were reproduced from Wright and Worthington (1970)).

Wright and Worthington (1970) also found that in the Labrador Basin (but absent in the North American Basin) there

was a relatively saline (with respect to the Antarctic Bottom Water) and cold ($\theta < 1.9°C$) water mass (Denmark Straits, Overflow Water (DSOW)). In agreement with this we find that for $\theta < 1.9°C$, east of 50°W (Figure 6b), there is a low silica branch on the θ-SiO_2 plot. This water is not generally observed west of 50°W (see exception noted below).

The two branches of the θ-SiO_2 plot come together at $\theta \sim 1.9°C$ as did the two branches of the θ-S distribution (Wright and Worthington (1970)). Worthington and Wright (1970) showed that at 1.8°C and below there is no direct path between the AABW and the DSOW. It is between 1.8°C and 1.9°C a direct path first exists (Figures 8a and 8b).

The data presented above suggest that for $\theta < 1.9°C$ both salinity and dissolved silica can be used to identify the AABW and the DSOW.

In the range of the NADW ($\theta > 1.9°C$) one may take advantage of the wide variation of dissolved silica (whereas there is very little variation of salinity) to distinguish between water masses of different origin within the NADW.

In the data from east of 50°W (Figure 6b) there is a distinct gap in the data from $\theta = 1.9°$ to 3.4°C. The higher silica branch runs from $\theta \sim 3.4°C$ and $SiO_2 \sim 18$ µg A/ℓ to $\theta \sim 1.9°C$ and $SiO_2 \sim 32$ µg A/ℓ where it joins in with the AABW and the DSOW. In this same potential temperature range, there exists a lower silica branch running from $\theta \sim 3.4°C$, $SiO_2 \sim 16$ µg A/ℓ to $\theta \sim 1.9°C$, $SiO_2 \sim 18$ µg A/ℓ. This lower silica water may be traced back into the Labrador and

Norwegian Seas (Grant (1970)), and is presumed to be the source of the Western Boundary Undercurrent (WBUC) (Richardson (1976); Clarke, Hill, Reiniger, and Warren (1978)).

West of 50°W, the distribution is quite different (Figure 6a) in the NADW range of potential temperature. There are only a few observations to the low side of the majority of the observations. The distinct gap seen to the east is not evident here. In fact, most of the "anomalous" observations come from two cruises. The section along 50°W shows the two branched distributions clearly and also shows some of the DSOW water at $\theta \sim 1.8°C$ (Figure 9). This section was grouped with the western group because of the AABW seen for $\theta < 1.9°C$ and $SiO_2 > 30$ µg A/ℓ. The other source of the anomalous data is AII 18 (Figure 10). These data also show evidence of DSOW ($\theta \sim 1.85°C$, $SiO_2 \sim 24$ µg A/ℓ). These are the only observations of the water mass at a point so far west. Since these observations of the DSOW are so isolated, it is assumed that there was an intrusion of this water mass into the area at the time these data were collected.

With the two sections discussed above deleted, the θ - SiO_2 distribution west of 50°W consists of a broad line of values from $\theta = 3.5°C$ and $SiO_2 = 14$ µg A/ℓ to $\theta = 1.9°C$ $SiO_2 = 30$ µg A/ℓ where it meets the AABW (Figure 11).

We stated previously that it was, in general, the lower values of silica that were found closer inshore. This will become more clear when the charts of silica on constant

potential temperature surfaces are discussed in Section V. The reason for the lower values inshore is assumed to be the influence of the WBUC (Richardson (1977); Worthington (1976)).

Examination of the individual sections which extend from the abyssal plain up onto the continental rise reveals that while there is a general tendency toward lower values of silica inshore, the strength of the gradient and the extreme values vary considerably (Figures 12a-e). The figures may be divided into two categories. The first are those sections which show a distinct gap between the WBUC and the remainder of the NADW (HUDSON, KN 48). The second are those which show a continuous band of observations but are limited to a range of values within the extremes of HUDSON and KN 48 (AII 100, CH 20, TRIDENT). These types of distributions are grouped geographically, the two branched distributions being to the east (east of 65°W) and the more uniform distributions being to the west.

4.2.1 Polynomial fits to the potential temperature silica relationship

To quantify the differences between these distributions, polynomial fits to the data were made. It was found that little was gained for fits of higher than fourth order. The fits were obtained with a least square polynomial regression program for the Hewlett-Packard 9830 calculator. The fits and residuals are presented in Figures 13-17. Root mean square deviations for each of the fits were also computed

(Table 2). It should be noted that the r.m.s. deviations are lower to the west than to the east, the plots of the residuals show that for CH 20, AII 100, and TRIDENT, the residuals are evenly distributed between $\pm 2\sigma$ with an increase of the scatter toward lower potential temperatures. For both KN 48 and HUDSON, we find that the residuals are evenly distributed above $\theta = 3.0°C$ but break into two branches for $\theta < 3.0°C$. The low residuals can readily be identified in the WBUC water which forms the low silica branch of the θ - SiO_2 plots. To illustrate the effects of the WBUC on the fits, the inshore stations were removed (containing the WBUC observations) from the KN 48 and HUDSON sections and re-computed the fits (Figures 18, 19). The r.m.s. deviations are now 1.10 for HUDSON and 1.01 for KN 48. The plots of the residuals now show a more uniform distribution than did the fits including the WBUC. The curves fitted to the KN 48 (65°W) and HUDSON (50°W) sections with the WBUC removed are nearly identical (Figure 20). To the west of 65°W, the three fits produce similar curves. Above 2.0°C those for TRIDENT and AII 100 are nearly identical and CHAIN 20 shows a deviation from the other two between 2.5° and 4°C (Figure 21). In Figure 21 a 2 standard deviation envelope has been included to show that the discrepancies are not statistically significant even from 2.5 C → 4°C.

To demonstrate that the WBUC has an effect on the distribution of silica west of 65°C the fits for AII 100, CH 20,

Table II.

Cruise	Location	Standard Deviation (ugA/l)
HUDSON	50°W	2.72
KNORR 48	65°W	1.46
CHAIN 20	Woods Hole-Bermuda	1.41
ATLANTISII 100	70°W	1.10
TRIDENT	Cape Hatteras	1.21

and TRIDENT were plotted along with HUDSON and KN 48 (With WBUC removed) (Figure 22). The 2σ envelope is from KN 48. It can be shown that for $2.00 < \theta < 2.40°C$ there is a significant difference between the AII, CH 20, TRIDENT curves and the HUDSON and KN 48, indicating that the water of the WBUC has a significant effect west of 65°W.

It should be emphasized that the data being compared were collected over a span of several years. The three sections which show the effect of the WBUC west of 65°W were occupied in 1961, 1971, and 1978 (CH 20, TRIDENT and AII 100, respectively). The consistency of the data suggests that the conditions were not anomalous at the time of the observations.

For comparison, the $\theta \sim SiO_2$ plots for the sections discussed above are presented again with the KN 48 (without WBUC) curve and 2σ envelope (Figures 23a-h).

Thus it has been shown while there are dramatic changes in the $\theta - SiO_2$ distribution from the tail of the Grand Banks of Newfoundland to Cape Hatteras, one can demonstrate that the low silica signal of the WBUC can be traced throughout the region.

V. The Distribution of DIssolved Silica on Surface of Constant Potential Temperature

In the previous section, the plots of silica versus potential temperature demonstrated the existence of geographic variations in the silica distribution of the deep western North Atlantic Ocean. In particular, it was found that near

the tail of the Grand Banks of Newfoundland and along the continental rise as far west as 65°W, the North Atlantic deep water consisted of two distinct water masses, easily distinguished by their silica content. Further west, the water masses could not be so easily separated on the θ-SiO_2 plots, however, it was shown that the low silica water did have a significant effect on θ-SiO_2 relationship as far west as Cape Hatteras.

To illustrate further the geographic variability of the silica distribution, four potential temperature* surfaces were chosen upon which to prepare contour maps of the silica distribution (Figures 24-27).

The data base used in preparing these maps is presented in Table I.

For potential temperatures less than 1.9°C one cannot trace water continuously throughout the North Atlantic Ocean. Figures 8a,b (Worthington and Wright (1970)).

Between 1.8°C and 1.9°C the bottom waters from northern and southern origin come in direct contact.

---

*Due to the tight θ-S relationship in the deep western North Atlantic Ocean for $\theta < 3.0$°C (Wright and Worthington (1970); Worthington and Metcalf (1961)) potential temperature surfaces nearly coincide with potential density surfaces.

5.1 The 1.9° potential temperature surface

The distributions of dissolved silica on the 1.9°C surface (Figure 24) shows the general southward increase in silica noted by Metcalf (1969) on the 2.0°C surface (see Figure 1).

Along the mid-Atlantic Ridge, a tongue of high silica water is found to extend northward. This is AABW and was identified by Metcalf (1969) using the same IGY sections.

In the vicinity of the tail of the Grand Banks of Newfoundland, there is a sharp silica gradient, with the lowest values inshore, following the bottom topography. One should note that this sharp gradient cannot be traced westward around the tail of the Grand Banks. The lowest contours (<22.5 µg A/ℓ) are only resolved by a few observations and our interpretation of this as a continuous feature may not be justified. Since none of the very low silica water penetrates around the tail of the Grand Banks, it is <u>not</u> associated with the WBUC, but rather with the Denmark Straits overflow water that is usually observed to be confined to the Labrador Basin (Figure 2, Wright and Worthington (1970); Worthington (1976)). Away from the continental rise the silica values are uniformly high (>35 µg A/ℓ) and join with the plume of AABW extending north. It should be noted that 1.9°C is the potential temperature at which the θ-SiO_2 and θ-S (Wright and Worthington (1970)) plots show the joining of the DSOW and AABW (Figure 5).

West of 50°W, the silica distribution takes on a different character. There is a decrease in the silica values as

one approaches the continental rise but the sharp gradient of the DSOW is not present. After passing around the tail of the Grand Banks, the 30 and 32.5 µg A/ℓ contours diverge leaving a large area with little change in the silica concentration. This is the location of the deep anti-cyclonic gyre proposed by Worthington (1976).

It should also be noted that the 30 µg A/ℓ contour follows the topography of the continental rise until it disappears west of 70°W. It is commonly observed that the lowest silica contours will follow the topography until they end by running into the coast indicating some mixing process (Figures 24-27).

5.2 The 2.2°C potential temperature surface

On the 2.2°C potential temperature surface (Figure 25) the general north-south gradient is again present with a zonal gradient with the higher values of silica being found along the mid-Atlantic Ridge. There is a sharp gradient near the tail of the Grand Banks with the lowest value nearest the continental rise. This gradient may be traced along the continental rise and westward around the tail of the Grand Banks.

In contrast to the 1.9°C surface, the sharp gradient along the continental rise may be traced further west to 65°W. As it was previously defined, this is the WBUC transporting water southward from the deep Labrador Sea (Grant (1970)).

West of 65°W the gradient weakens. The 20 µg A/ℓ contour runs into the coast and the 22.5 and 25 µg A/ℓ contours diverge. Similar to the 1.9°C surface, the silica contours on the 2.2°C surface, away from the continental rise, near the Grand Banks diverge as one proceeds westward. Here the 25 and 27.5 µg A/ℓ contours diverge. The waters above the abyssal plain are characterized by a nearly uniform distribution of silica.

5.3 The 2.4°C potential temperature surface

The 2.4°C potential temperature surface, Figure 26, is similar to the 2.2°C surface. We see once again the northwest-southeast gradient with the highest values of silica found along the mid-Atlantic Ridge and the lowest along the continental rise.

One can trace a sharp silica gradient from the tail of the Grand Banks westward to 65°W where the 20 and 22.5 µg A/ℓ contours then diverge in a similar fashion to the 22.5 and 25 µg A/ℓ contours on the 2.2°C surface. Also similar to the 2.2°C surface, the 22.5 and 25 µg A/ℓ are close together near the tail of the Grand Banks but diverge when traced westward beyond 50°W. Thus it is found that the waters above the abyssal plain nearly uniform in silica.

The inshore gradient on the 2.4°C surface is not as sharp as that seen on the 2.2°C surface. As shown on the θ-SiO_2 plots (Figure 23a for example) the spread between the WBUC water and the remainder of the NADW increases with decreasing potential temperature.

5.4 The 3.0°C potential temperature surface

The 3.0° potential temperature surface (Figure 27) shows a departure from the contribution on the previous surfaces. There is the expected southward increase in silica but at this potential temperature, there is open communication across the mid-Atlantic Ridge. The data indicate a sharp gradient near 32°N with abrupt changes above the mid-Atlantic RIdge. These features are not well resolved and shall only be pointed out here without further comment.

Near the tail of the Grand Banks, and along the continental rise, the sharp gradients seen on the previous surfaces are no longer present. The distribution is nearly uniform throughout the entire region north of 35°N from the Grand Banks to Cape Hatteras. This was shown also in the θ-SiO_2 plots (see Figure 5) by the narrowing of the θ-SiO_2 scatter for $\theta \geq 3.0°C$.

VI. Discussion

6.1 The θ-SiO_2 relationship

In the preceding sections a silica minimum (on surfaces of constant potential temperature) was found along the continental rise. This feature has been associated with the WBUC (Richardson (1977); Clark, Hill, Reiniger, and Warren (1978)). It has been demonstrated that the low silica water can be traced from the tail of the Grand Banks of Newfoundland to Cape Hatteras. However, it was also found

that the θ-SiO_2 characteristics of the WBUC do not remain unchanged throughout the region of study. There is a marked change in the θ-SiO_2 relationship to the west of 65°W. The data suggest that a narrow band of low silica water comes around the tail of the Grand Banks and extends to 65°W along the continental rise. Further west, the silica minimum is less pronounced. The two branches of the θ-SiO_2 plot seen at 50°W are no longer distinguishable at 70°W where a more diffuse silica pattern exists. At 50°W the low silica branch was 8-10 µg A/ℓ lower in silica (for θ = 2°-2.2°C) than the high silica branch. When compared to the high silica branch at the KN 48 (65°W) station (or equivalently the high silica branch of the HUDSON section, see Figure 22), the TRIDENT, AII 100, and CH 20 sections all show a 2-4 µg A/ℓ silica deficit in the same potential temperature range.

The process(es) responsible for the alteration of the θ-SiO_2 relationship west of 65°W is not a simple one to identify. The distribution of dissolved silica has been described, but it has not been related to the flow field. It has been suggested that since the low silica water undoubtedly originated in the northern regions, its presence in a narrow band along the continental rise implies the existence of a WBUC.

6.2 Geostrophic transport measurements

Several observers have made hydrographic sections and computed the geostrophic transport of the WBUC. Richardson

(1977) compared the results and Table III is reproduced from his work. A wide range of values is found. How much of the variability represents changes in the mass flux of the WBUC and how much is due to the choice of stations or the method used to establish the absolute velocities is not known. Richardson (1977) has described the methods used in each computation and suggested possible error sources. All of the data listed in Table III came from sections to the west of 65°W.

There are few available calculations of the transport to the east. Clarke, Hill, Reiniger, and Warren (1978) found no evidence for the WBUC at 50°W but they suggested that this was due to unrealistic reference velocities used. The current meters used to adjust the geostrophic velocities were probably outside the WBUC (see further discussion below).

Worthington (1970), in his model of the circulation of the North Atlantic Ocean, allows only $6 \times 10^6 m^3/s$ to flow in the WBUC, although he suggests that the flow may be unsteady.

Although Worthington's $6 \times 10^{+6} m^3/s$ is smaller than most of the observations to the west of 65°W, it is not felt that any of the measurements are precise enough to be compared. Collectively, these data do suggest that the WBUC is present from the Grand Banks to Cape Hatteras. It cannot, from the available data, be determined if any changes in the transport are occurring to accompany the changes in the θ-SiO_2 relationship.

Table III.

(taken from Richardson (1977))

Volume transport estimates of the Western Boundary Undercurrent. The value in parenthesis is the r.m.s. deviation of the innividual transports about the mean.

Measured by	Transport ($10^6 m^3/sec$)	Latitude	Date
Swallow & Worthington(1961)	7	33	Mar 1957
Volkmann (1962)	50	38	Jul 1959
	17	38	Jul 1960
Barrett (1965)	4	35	Oct 1962
	12	35	Oct 1962
Worthington & Kawai (1972)	2	35	Nov 1966
Richardson & Knauss (1971)	12	35	Jul 1967
Amos,Gordon & Schneider(1971)	22	31	May 1968
Average	16 (14)		

6.3 Moored current meter observations

There have been several current meters moored in the WBUC. Along 70°W steady westward flow was observed for eight months on the upper continental rise (bottom depth <4000) (Luyten (1977)). Off Cape Hatteras, records less than one month long show flow to the southwest directly beneath the Gulf Stream (Richardson (1977)). Recent data from the Blake-Bahama Outer Ridge indicate the presence of a strong westward flow (Rhines, personal communication). To the east, at 50°W, a two-month record just to the south of the tail of the Grand Banks shows a predominently westward flow. In general, however, the current meter data along 50°W and along another line to the north of the Grand Banks running southeast, show little evidence of the WBUC. Clarke, Hill, Reiniger, and Warren (1978) remarked that "...our velocity vectors do not show a definite westward flow along the continental slope in conformity with the unequivocal evidence in the deep silica field for the western boundary undercurrent." They suggested that the disparity between the current meter and hydrographic data was due to a difference in the time scale to which the two types of data respond. While this may in fact be true, an alternative explanation is offered. In this case, it appears that the current meters were placed outside the WBUC. Some idea of the location of the WBUC may be gained from the deep silica data (Figure 28). The 2.0°C potential isotherm has been added to and one can identify the WBUC where the silica contours sharply turn downward and cross the isotherm. Note

also the slope of the 2.0°C isotherm indicating the presence of deep shear. Along the section running southeast (Figure 29) none of the instruments were in the low silica water. Along 50°W (Figure 28) one instrument is located clearly within the low silica water. The record from this instrument shows a predominantly westward flow for two months (Figure 30). Thus we feel that the disparity between the current meter and hydrographic data is due to the location of the instruments outside the WBUC.

Fortunately, it is along 50°W that the silica data provides the clearcut evidence for the WBUC. Along 70°W and near Cape Hatteras, the silica data alone suggests only that the WBUC has had some influence but the current meter data and the geostrophic transport calculations offer evidence that the undercurrent is present. It is from this observation that one may anticipate that the change in the silica distribution is not due to a fundamental change in the character of the flow, but rather is caused by some external effect which results in an exchange of water between the WBUC and the central basin.

6.4 Enhanced mixing west of 65°W

The current meter data may be used to offer a suggestion as to the nature of the process which provokes this exchange of water particles. Current meter measurements along both 70°W and 55°W indicate that the flow over the abyssal plain is characterized by energetic eddy activity (Schmitz (1976) (1978); Luyten (1977)). The effect of these eddies can be seen in the

silica distribution by the nearly uniform silica level over the abyssal plain (Figure 24).

When the WBUC rounds the tail of the Grand Banks, it follows the topography westward and effectively skirts around the deep eddy field. After passing through the New England seamount chain (near 65°W) the topography steers the WBUC southward and forces it to flow directly under the Gulf Stream and presumably into more vigorous contact with the deep eddy field. Thus the topography steers the flow into a region of enhanced mixing which exchanges the low silica water along isopycnal surfaces with the surrounding North Atlantic deep water, thus eroding the silica signal and providing the smoother distribution observed.

VII. Summary

The distribution of dissolved silica in the deep western North Atlantic Ocean has been presented. It has been found that the dissolved silica content can be used, in conjunction with potential temperature, to identify water masses.

For potential temperatures less than 1.9°C the dissolved silica-potential temperature relationship is similar to the salinity-potential temperature relationship. Both show two distinct branches which identify the Denmark Straits overflow and the Antarctic bottom water.

In the North Atlantic deep water, where the θ-S relationship forms a tight correlation, the θ-SiO_2 relationship shows

a wide range of values. It has been shown that a silica minimum, on surfaces of constant potential temperature, can be traced along the continental rise from the tail of the Grand Banks of Newfoundland to Cape Hatteras.

The low silica water has been termed the Western Boundary Undercurrent (for historical reasons), which has been interpreted as the mechanism by which water is transported from the Norwegian and Labrador Seas toward the equator.

Given this observed silica distribution, one is left with a difficult task of interpretation. The WBUC is the most prominent feature in the distribution yet little is known about the structure of the flow. What roles do advection and diffusion play in determining the observed silica distribution? It has been hypothesized that a region of enhanced mixing is present west of 65°W. It has been suggested that this enhanced mixing is due to the presence of the deep eddy field observed with moored current meters.

Appendix I. Rejected Data

The data collected on KNORR 12 has been rejected because of anomalous θ-S and θ-SiO_2 characteristics. This was unfortunate since the stations were located in the region between 55°W and 65°W where there is no other data (Figure 31).

The θ-S relationship from KN 12 shows a consistent bias toward lower salinities when compared to neighboring sections (Figure 32). The θ-SiO_2 relationship shows a consistent bias toward higher silica values (Figure 33).

It may be argued that the low salinity and high silica values imply an intrusion of water from the south. However, since these anomalous conditions were observed in the data from only a single cruise, it is felt that they should be suspect.

ACKNOWLEDGEMENTS

An advisor who is willing to give advice when sought and support when needed is extremely important to a graduate student. Jim Luyten has been such an advisor.

There are many people who have helped in the preparation of this thesis and in my training as an oceanographer. I would like to thank Val Worthington and Mike McCartney for teaching me the joys of collecting hydrographic data. Thanks are also due to all those who helped on ATLANTIS II 100.

Val Worthington and Bruce Warren generously allowed me to use their unpublished data.

I would like to thank Doris Haight for typing this manuscript.

Finally, I would like to express my thanks to the other students in the WHOI/MIT Joint Program in Oceanography who have been a constant source of encouragement and enjoyment. I am particularly indebted to Nan Bray, Dean Roemmich, Neal Pettigrew, and John Toole for being patient whenever I took to roaming the halls.

BIBLIOGRAPHY

Armstrong, F. A. J. (1965). Silicon. In: Chemical Oceanography, Vol. I. Eds. J. P. Riley and G. Skirrow.

Broecker, W. S., T. Takahashi, and Y.-H. Li (1976). Hydrography of the central Atlantic - I: The two degree discontinuity. Deep-Sea Research 23, pp. 1083-1104.

Carmack, E. C. (1973) Silicate and potential temperature in the deep and bottom waters of the western Weddell Sea. Deep-Sea Research 20, 927-932.

Clarke, R. A., H. W. Hill, R. F. Reiniger, and B. A. Warren (1978). Current system south and east of the Grand Banks of Newfoundland, in press.

Cooper, L. H. N. (1952) Factors affecting the distribution of silicate in the North Atlantic Ocean and the formation of North Atlantic deep water. J. Mar. Biol. Ass. U. K. 30, 511-526.

Corwin, N. A. and D. A. McGill (1963). Nutrient Distribution In the Labrador Sea and Baffin Bay. U. S. Coast Guard Bulletin #48.

Grant (1970) p. 25

Luyten, J. R. (1977). Scales of motion in the deep Gulf Stream and across the Continental Rise. JMR 35, 49-74.

Metcalf, W. G. (1969). Dissolved silicate in the deep North Atlantic. Deep-Sea Research 16 supplement, 139-145.

Richards, F. A. (1958). Dissolved silicate and related properties of some western North Atlantic Caribvean waters. JMR 17, 449-465.

Richardson, P. L. (1977). On the crossover between the Gulf stream and the western boundary undercurrent. Deep-Sea Research 24, 139-159.

Schmitz, W. J. (1977). On the deep general circulation in the western North Atlantic. JMR 35, 21-28.

Schmitz, W. J. (1978) Observations of the vertical distribution of low frequency kinetic energy in the western North Atlantic. JMR 36, 295-310.

Stommel, H. M. (1957). A survey of ocean current theory. Deep-Sea Research 4, 149-184.

Sverdrup, H. U., M. W. Johnson, and R. H. Fleming (1942). The Oceans: Their physics, chemistry and general biology. Prentice Hall, 1087 pp.

Swallow, J. C. and L. V. Worthington (1961). An observation of a deep countercurrent in the western North Atlantic. Deep-Sea Research 8, 1-19.

Volkmann, G. (1962). Deep current observations in the western North Atlantic. Deep-Sea Research 9, 493-500.

Webster, F. (1969). Vertical profiles of horizontal ocean currents. Deep-Sea Research 15, 85-98.

Worthington, L. V. (1976). On the North Atlantic circulation. The Johns Hopkins Oceanographic Studies 6, 110 p.

Worthington, L. V. and W. R. Wright (1970). North Atlantic Ocean atlas of potential temperature and salinity in the deep water including temperature, salinity, and oxygen profiles from the Erika Dan cruise of 1962. Woods Hole Oceanographic Institution Atlas Series, 2. 58 plates.

Worthington, L. V. and W. R. Wright (1971). Discussion of a paper by X. LePichon, S. Eittreim, and J. Ewing, "A sedimentary channel along Gibbs Fracture Zone." JGR 76, 6606-6608.

Wright, W. R. and L. V. Worthington (1970). The water masses of the North Atlantic Ocean; a volumetric census of temperature and salinity. Ser. Atlas Mar. Envir. 19, 8 p., 7 plates.

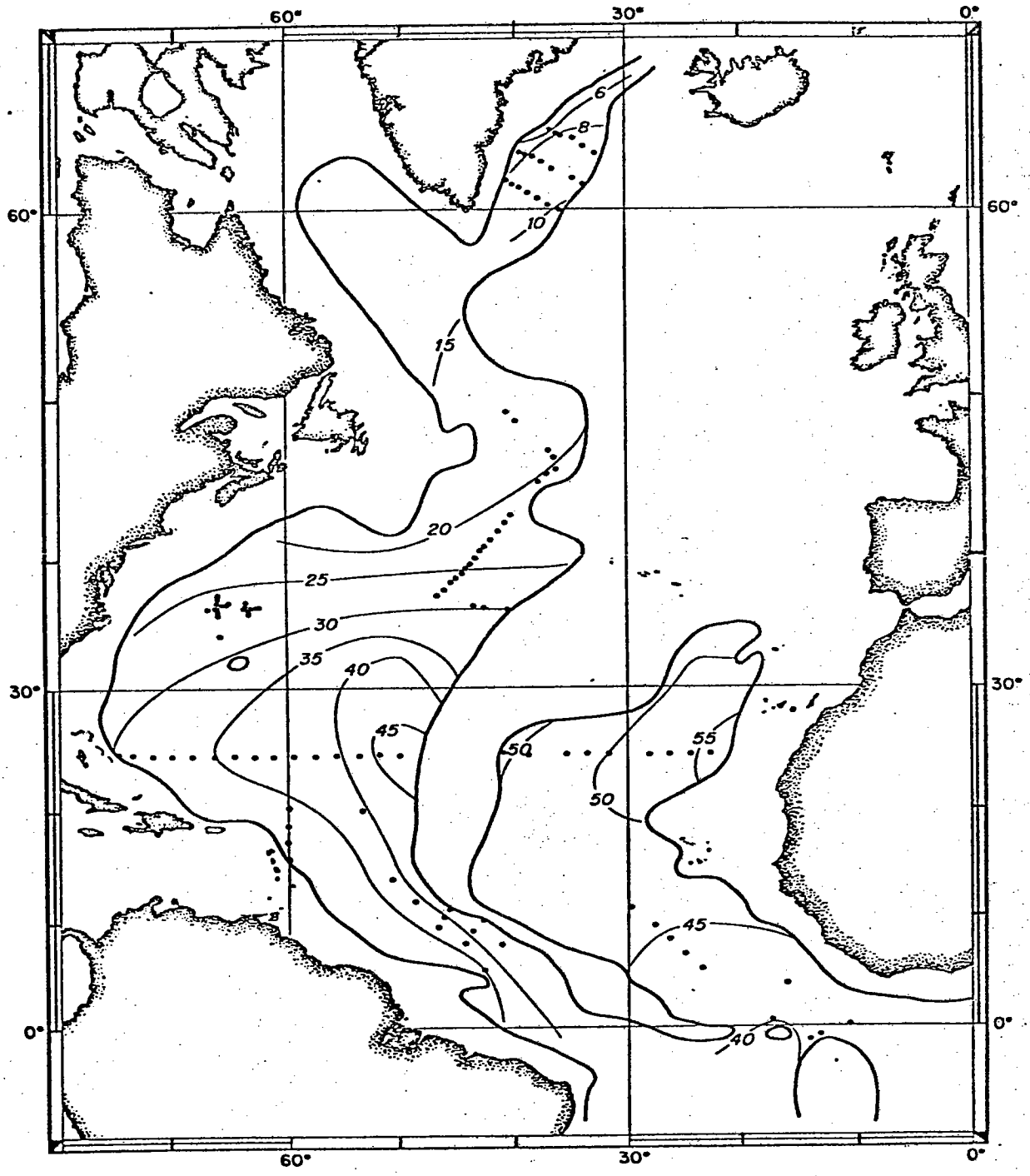

Fig. 1. Contours of dissolved silica (ugA/l) on the 2.0° c. potential temperature surface. (taken from Metcalf(1969))

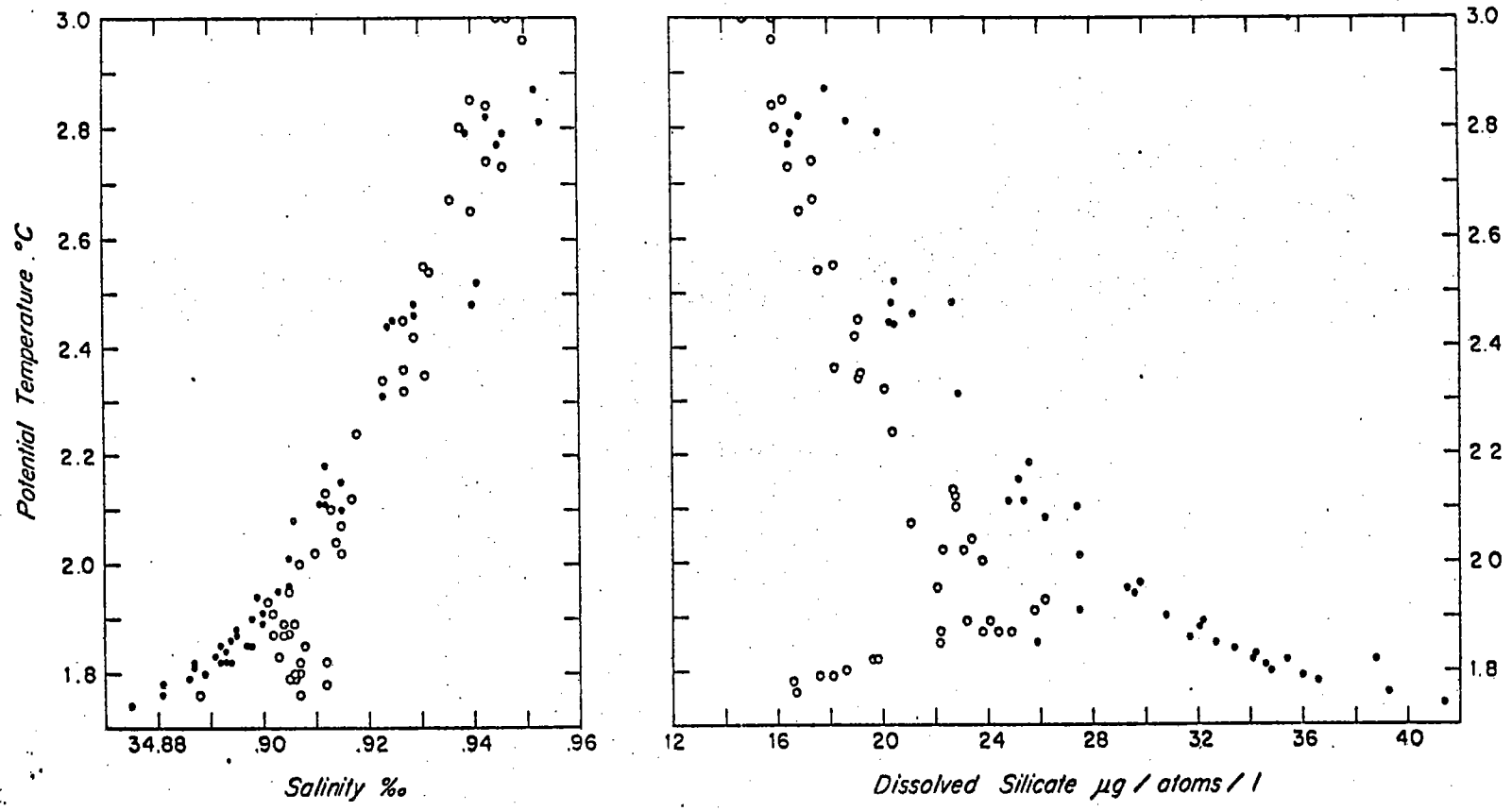

Fig. 2. Plots of potential temperature vs. salinity and potential temperature vs. dissolved silica for stations north (open circles) and south(filled circles) of the tail of the Grand Banks. (taken from Worthington(1976))

Fig. 3. Locations of stations used in this work. Stations denoted by * were used only in the preparation of the charts of silica on potential temperature surfaces.

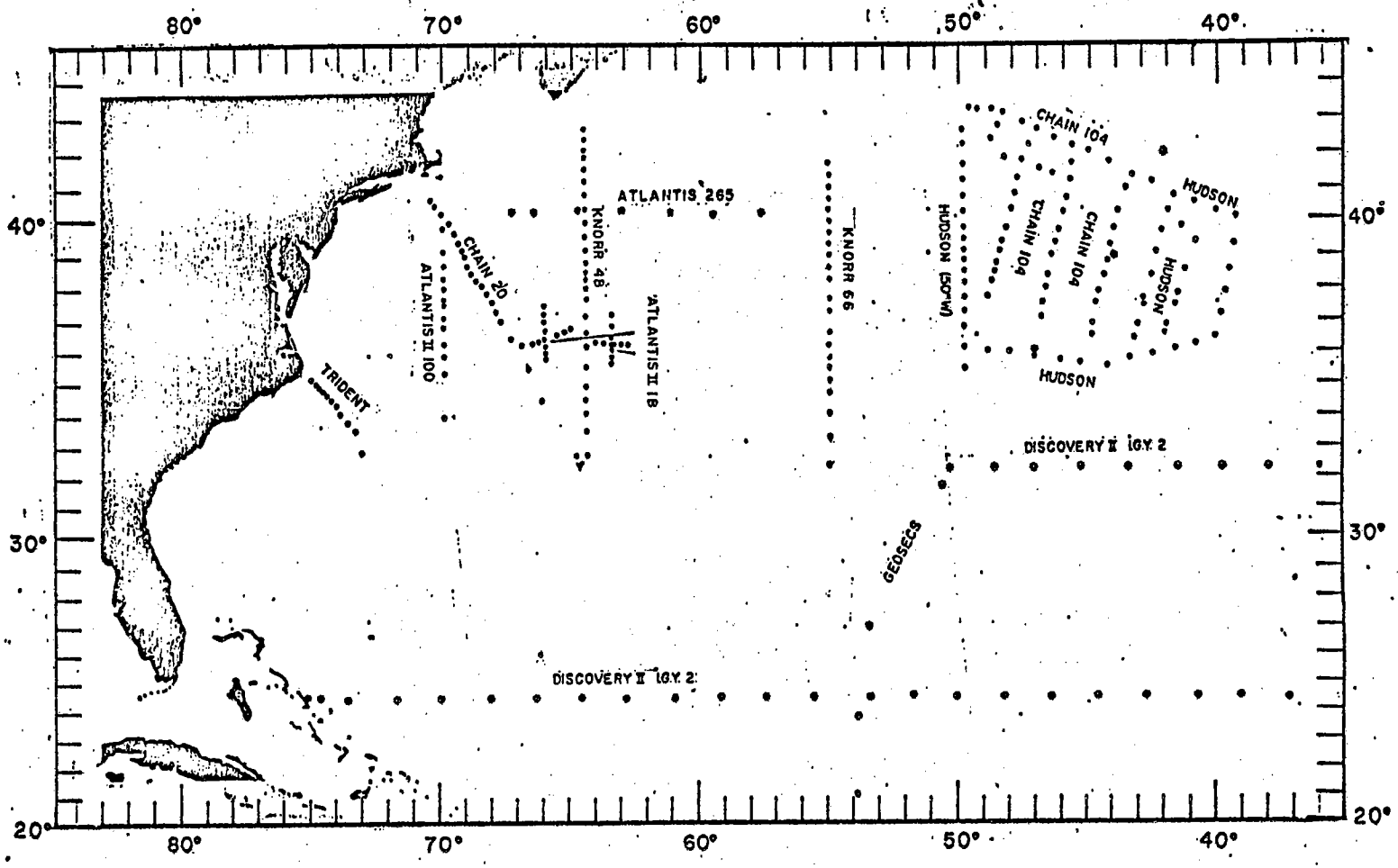

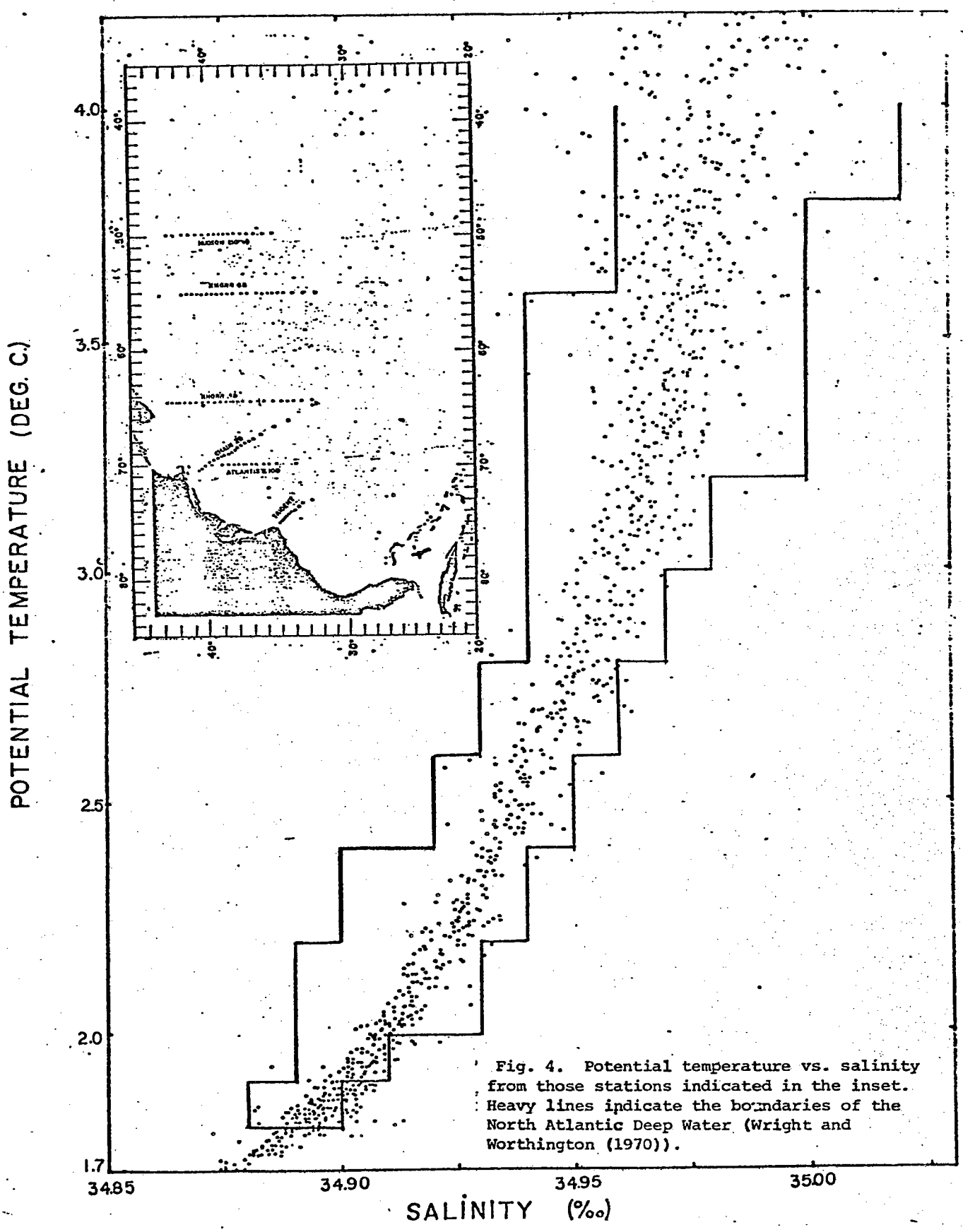

Fig. 4. Potential temperature vs. salinity from those stations indicated in the inset. Heavy lines indicate the boundaries of the North Atlantic Deep Water (Wright and Worthington (1970)).

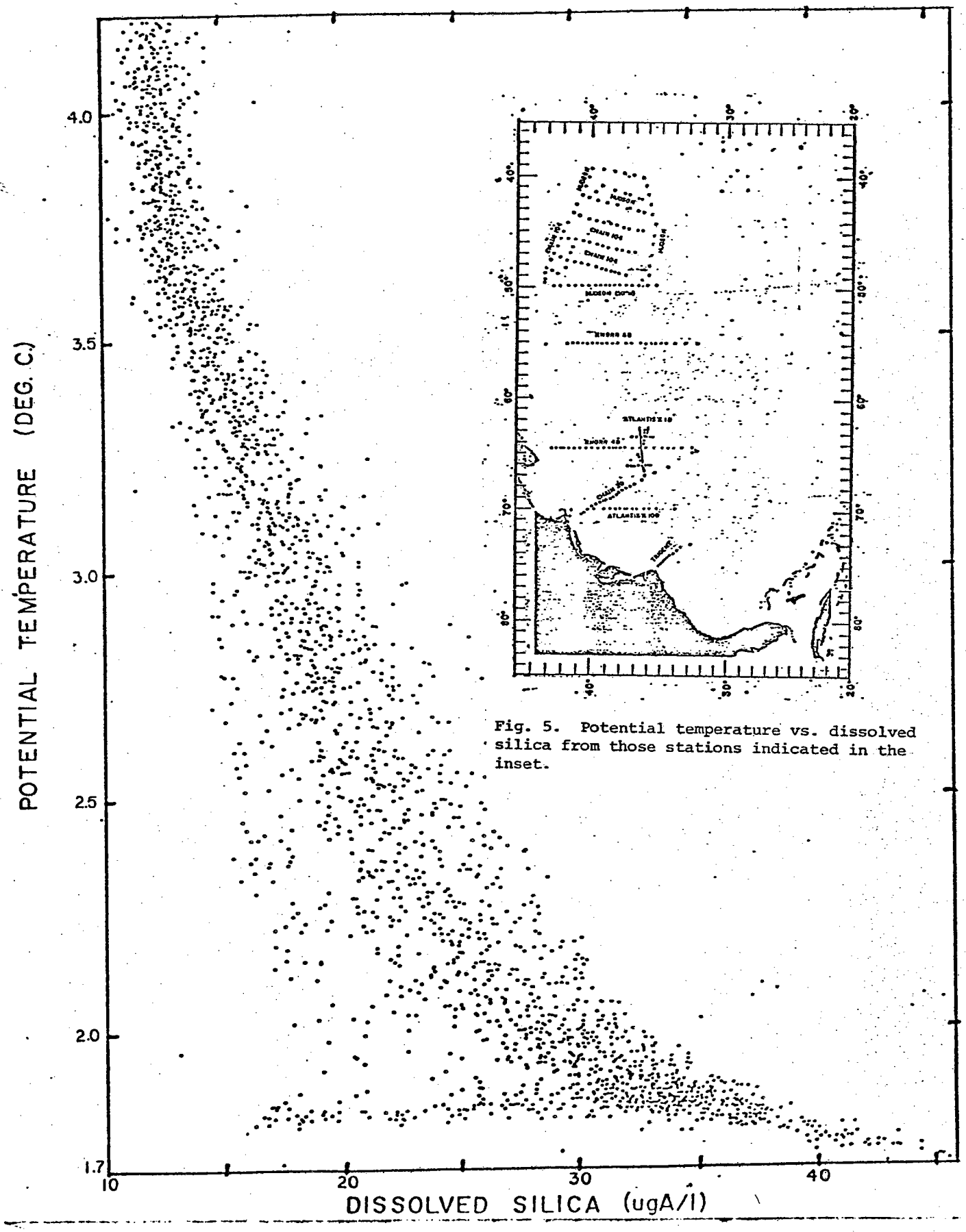

Fig. 5. Potential temperature vs. dissolved silica from those stations indicated in the inset.

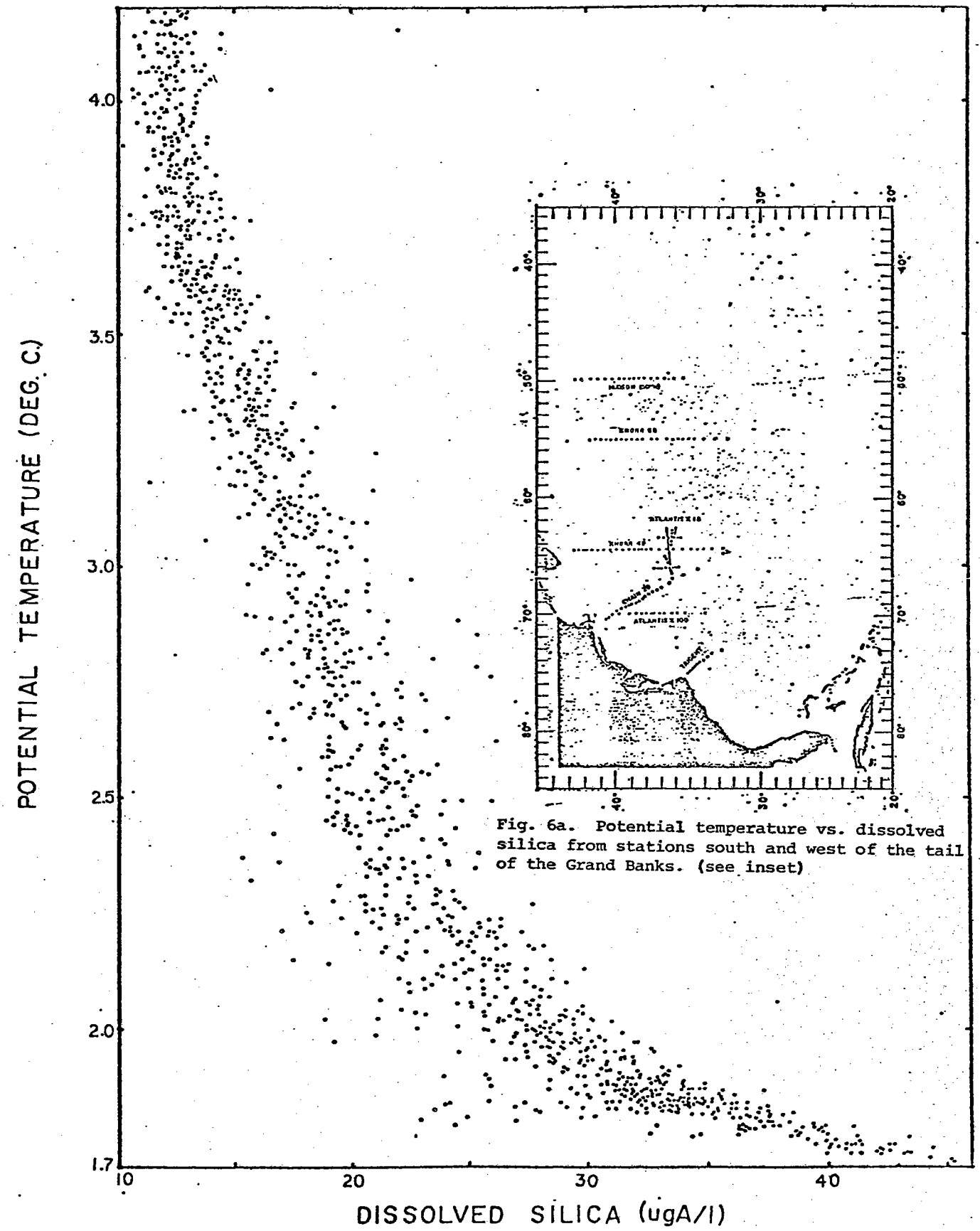

Fig. 6a. Potential temperature vs. dissolved silica from stations south and west of the tail of the Grand Banks. (see inset)

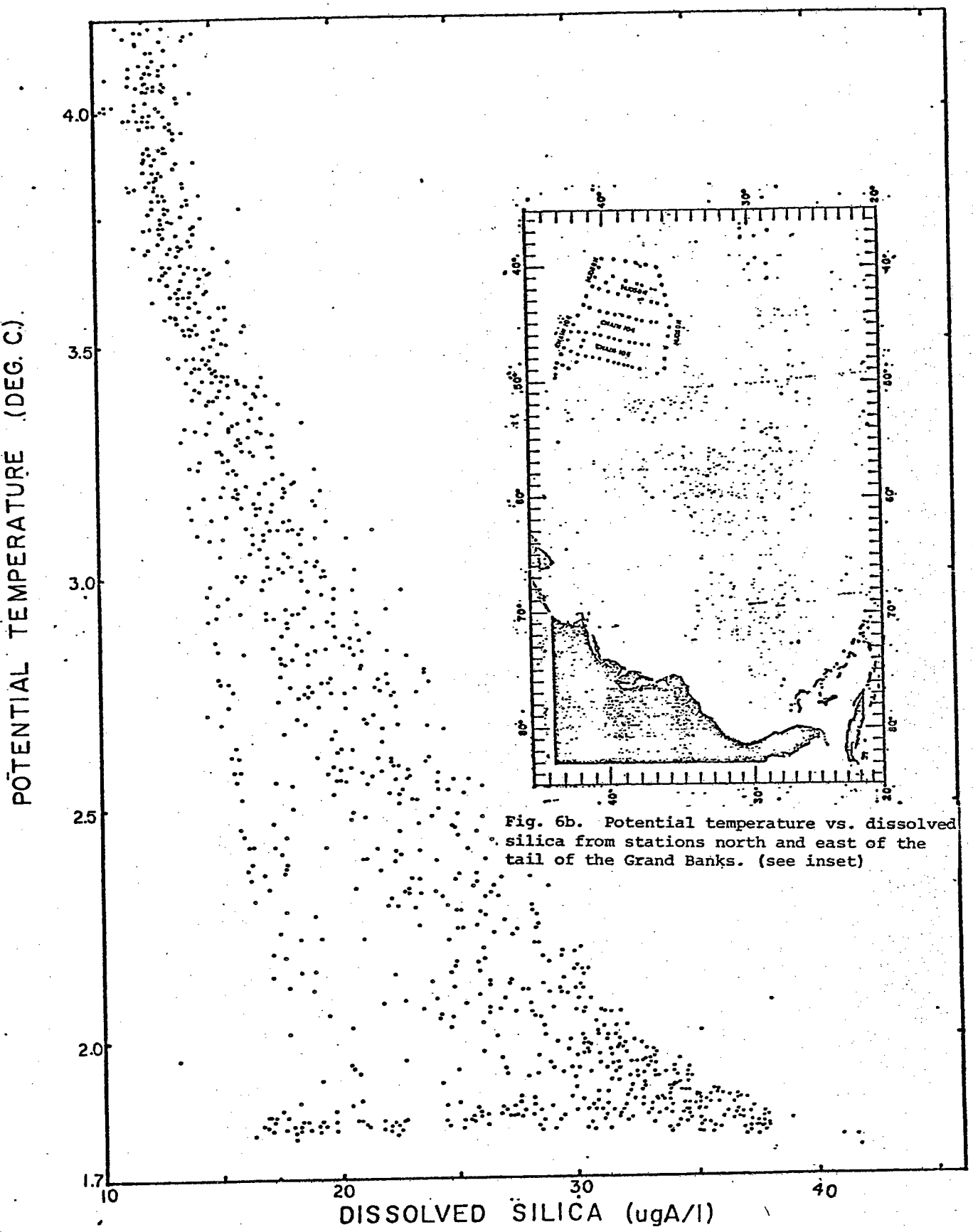

Fig. 6b. Potential temperature vs. dissolved silica from stations north and east of the tail of the Grand Banks. (see inset)

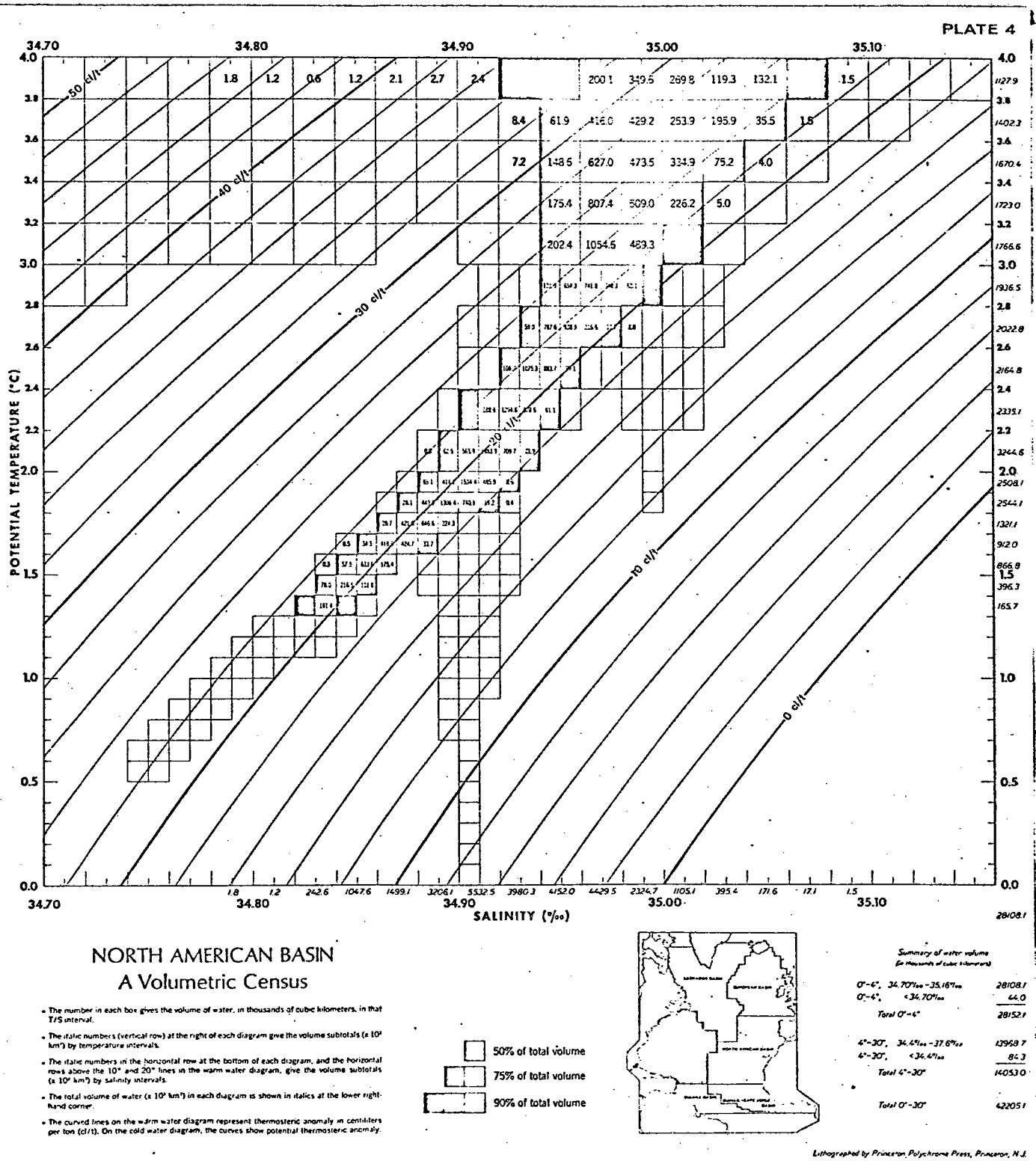

Fig. 7a.
(taken from Wright and Worthington (1970))

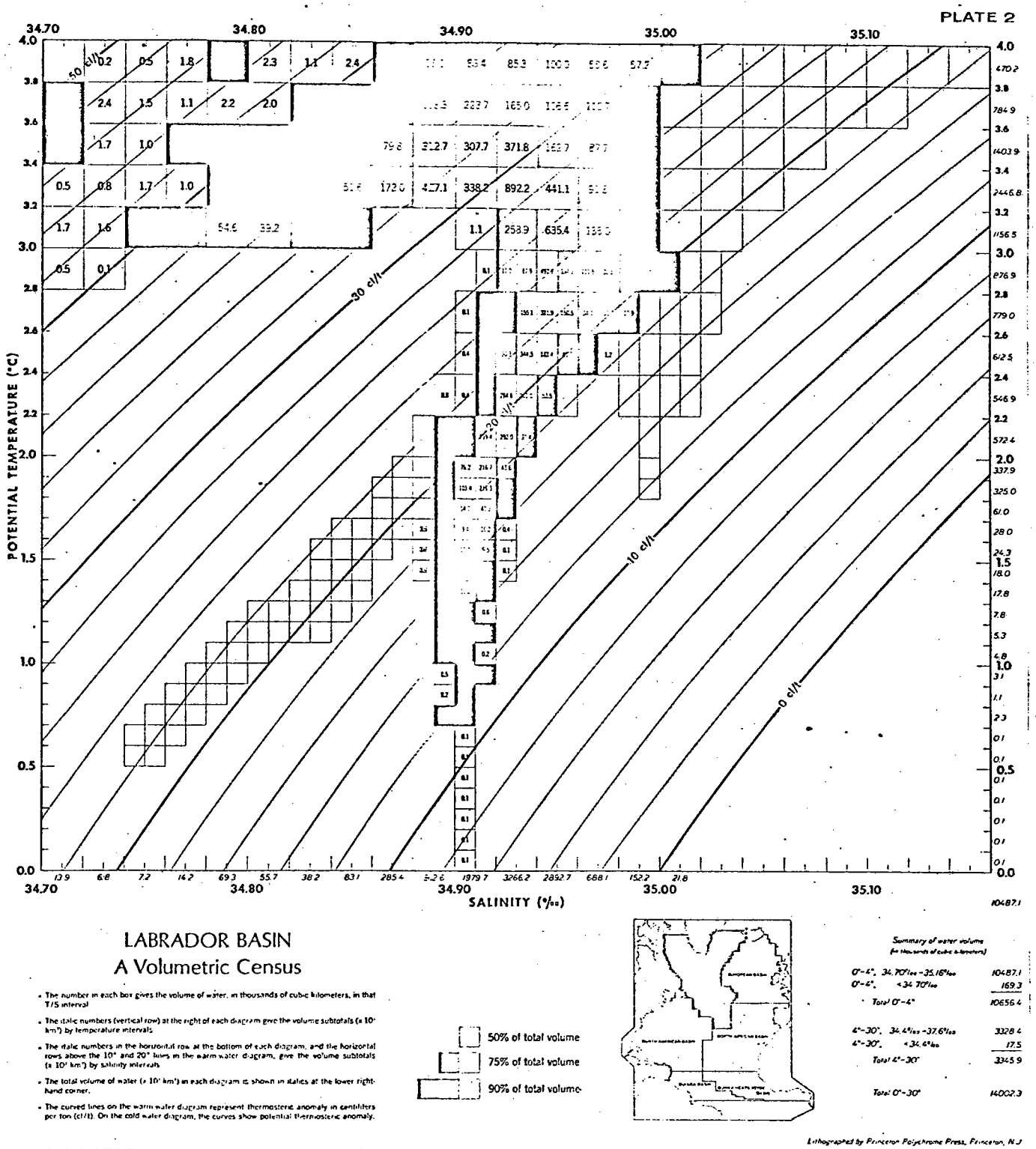

Fig. 7b.
(taken from Wright and Worthington(1970))

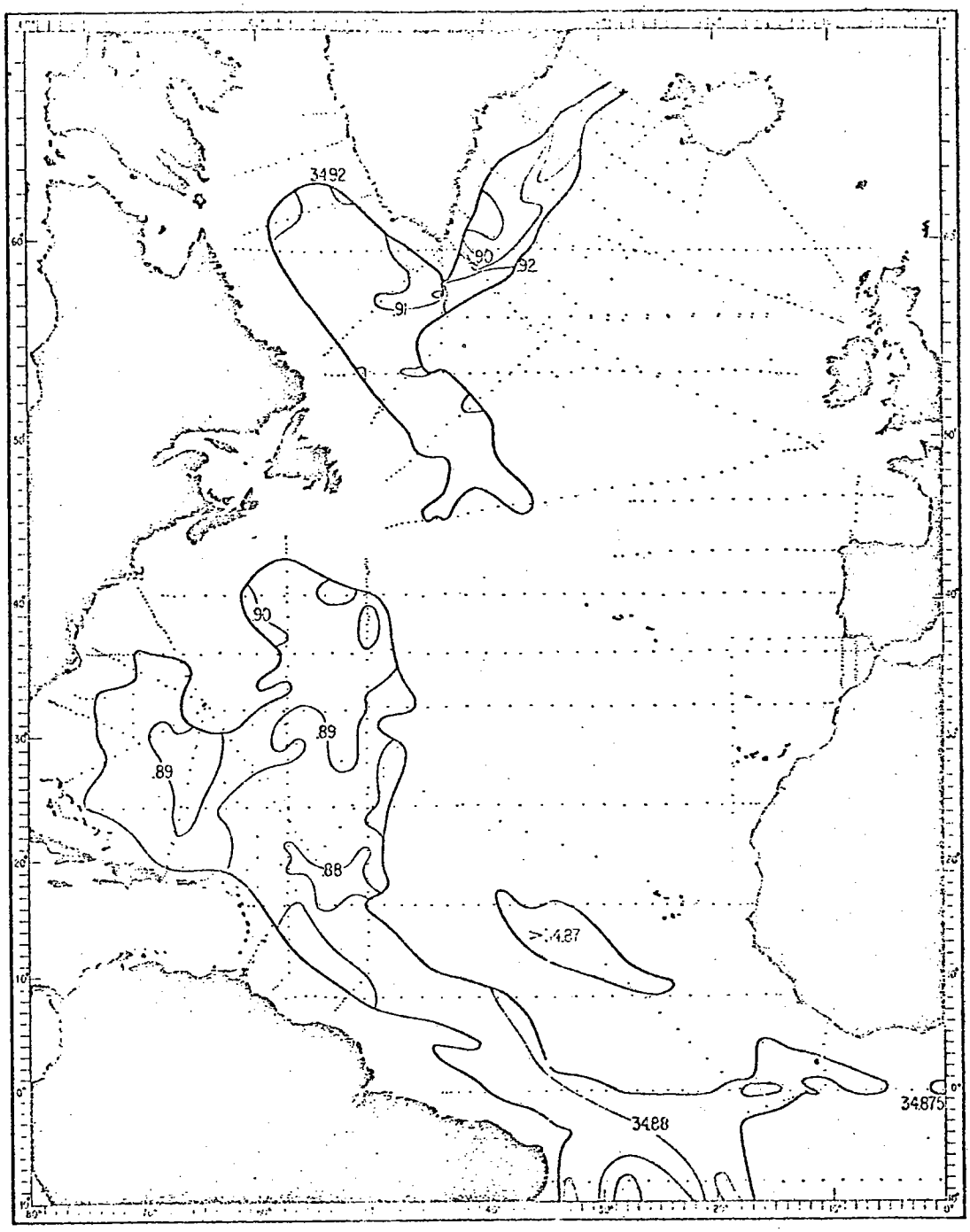

SALINITY (‰) AT THE 1.8°C POTENTIAL TEMPERATURE SURFACE

Fig. 8a.
(taken from Worthington and Wright (1970))

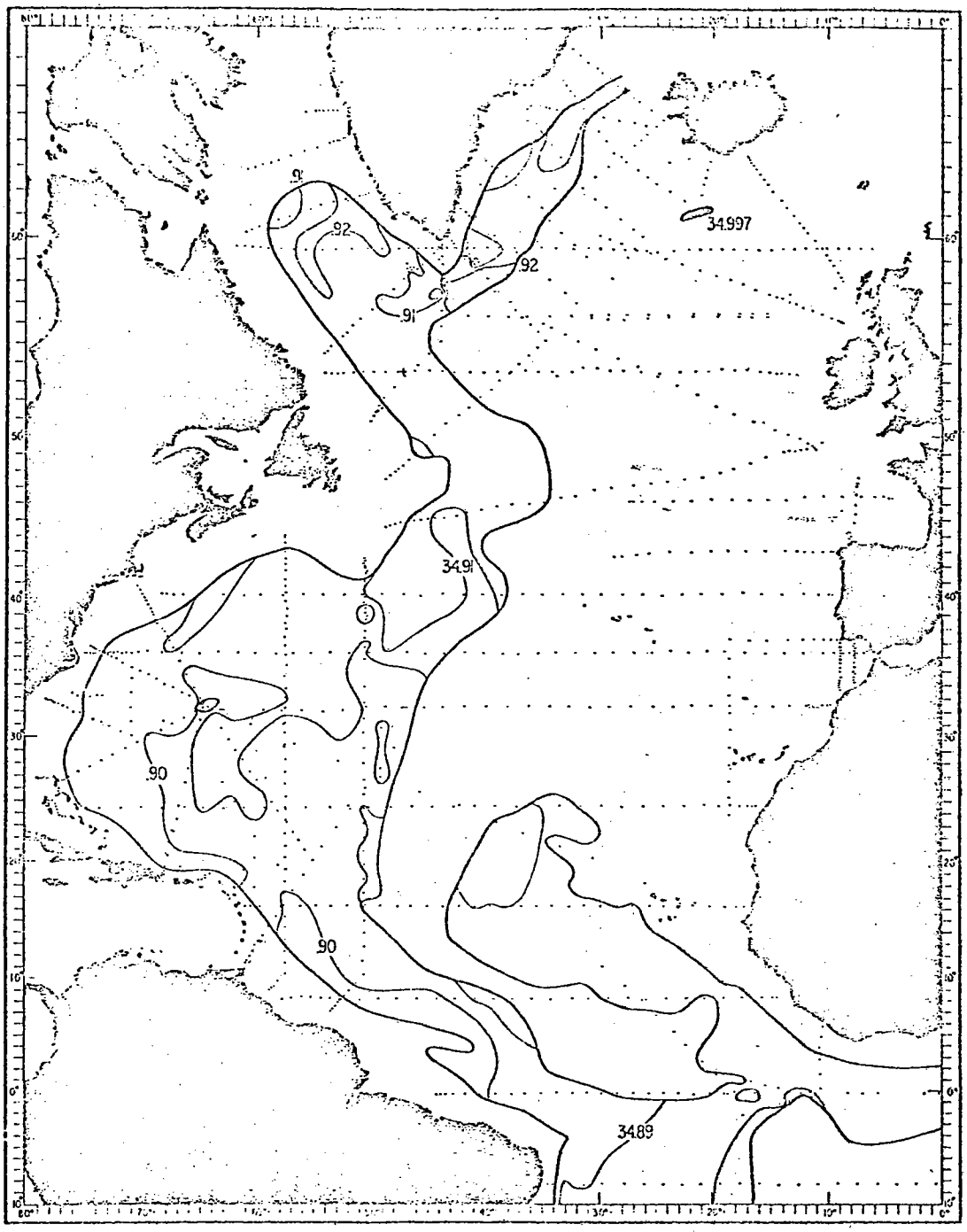

SALINITY (‰) AT THE 1.9°C POTENTIAL TEMPERATURE SURFACE

Fig. 8b.
(taken from Worthington and Wright (1970))

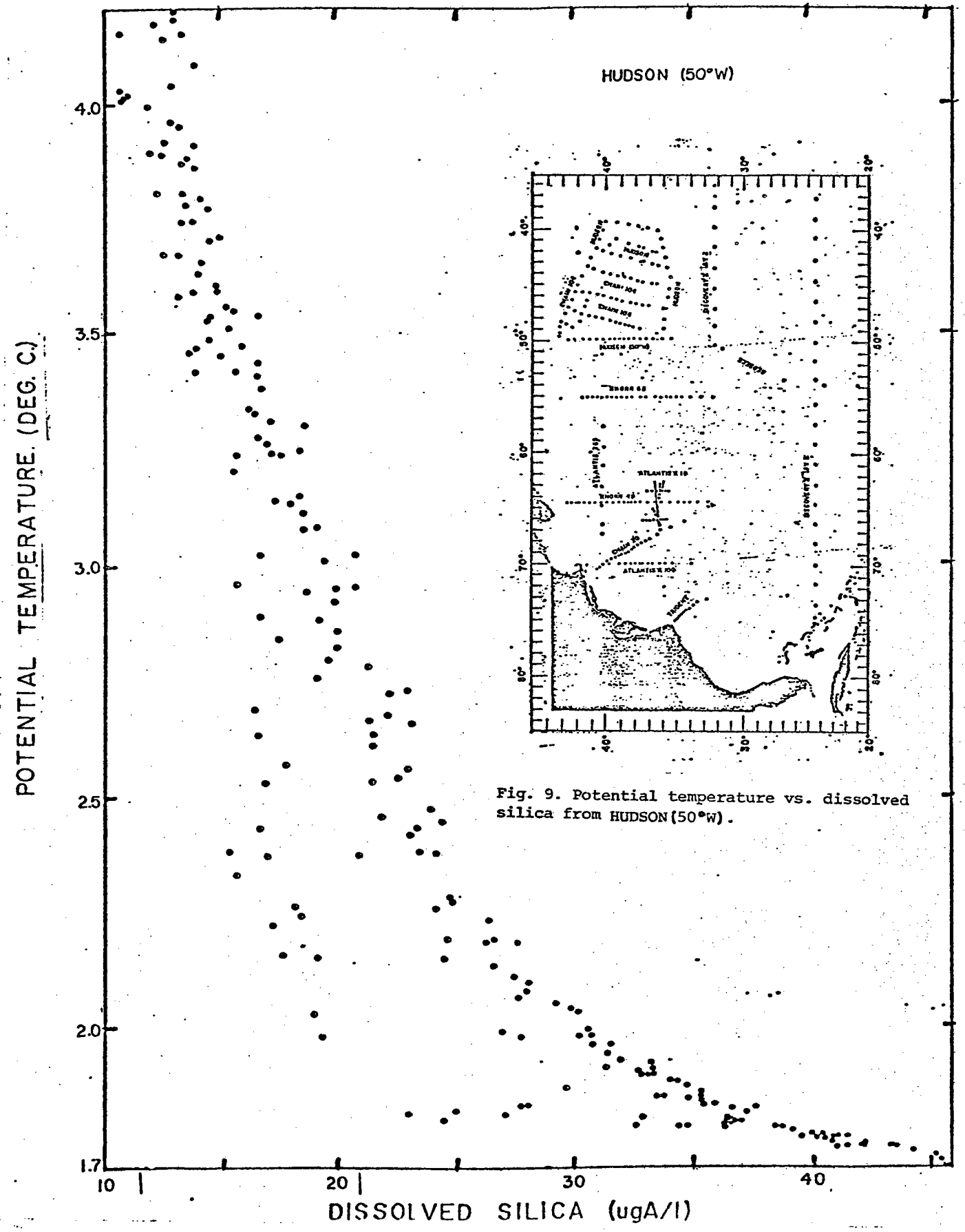

Fig. 9. Potential temperature vs. dissolved silica from HUDSON (50°W).

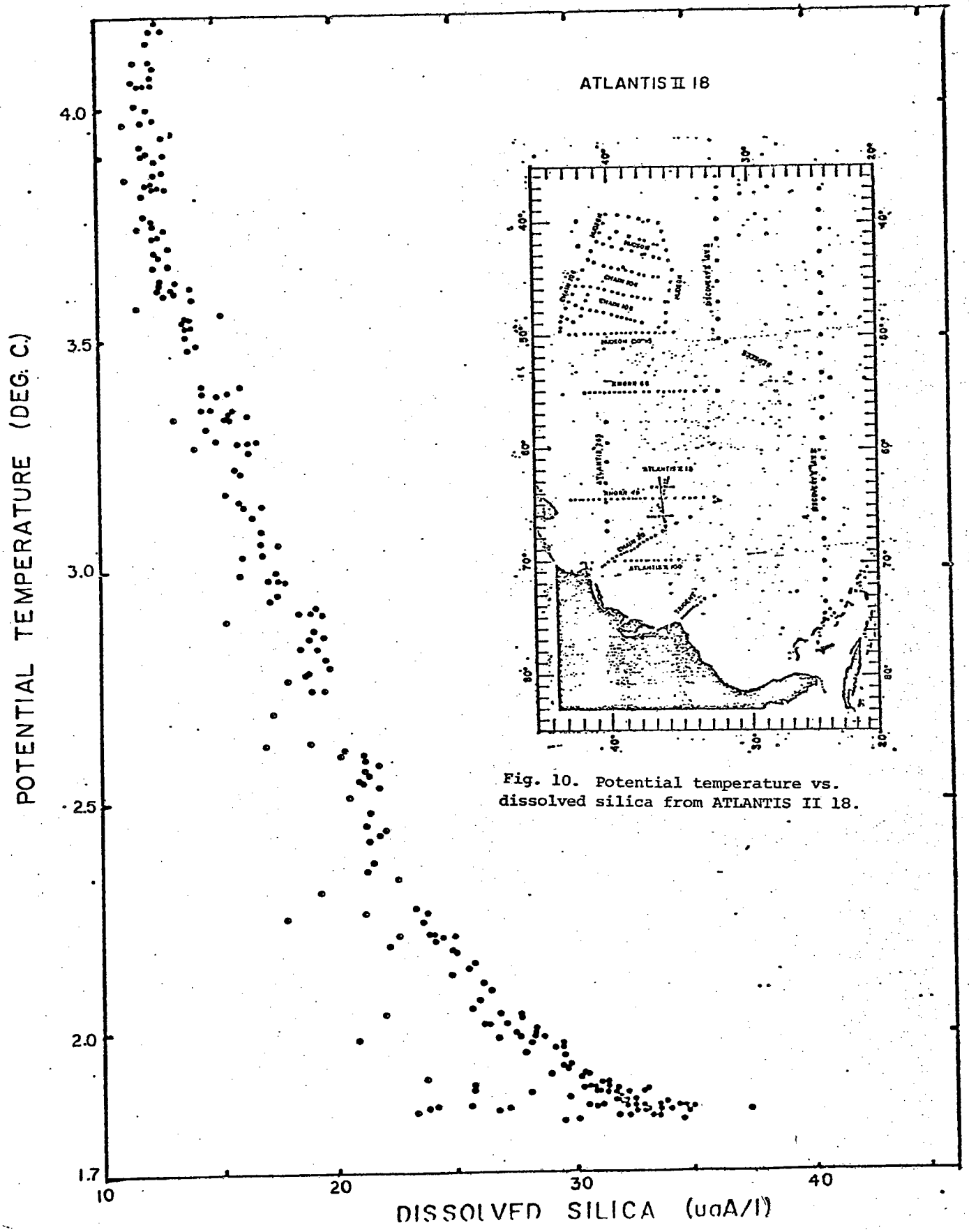

Fig. 10. Potential temperature vs. dissolved silica from ATLANTIS II 18.

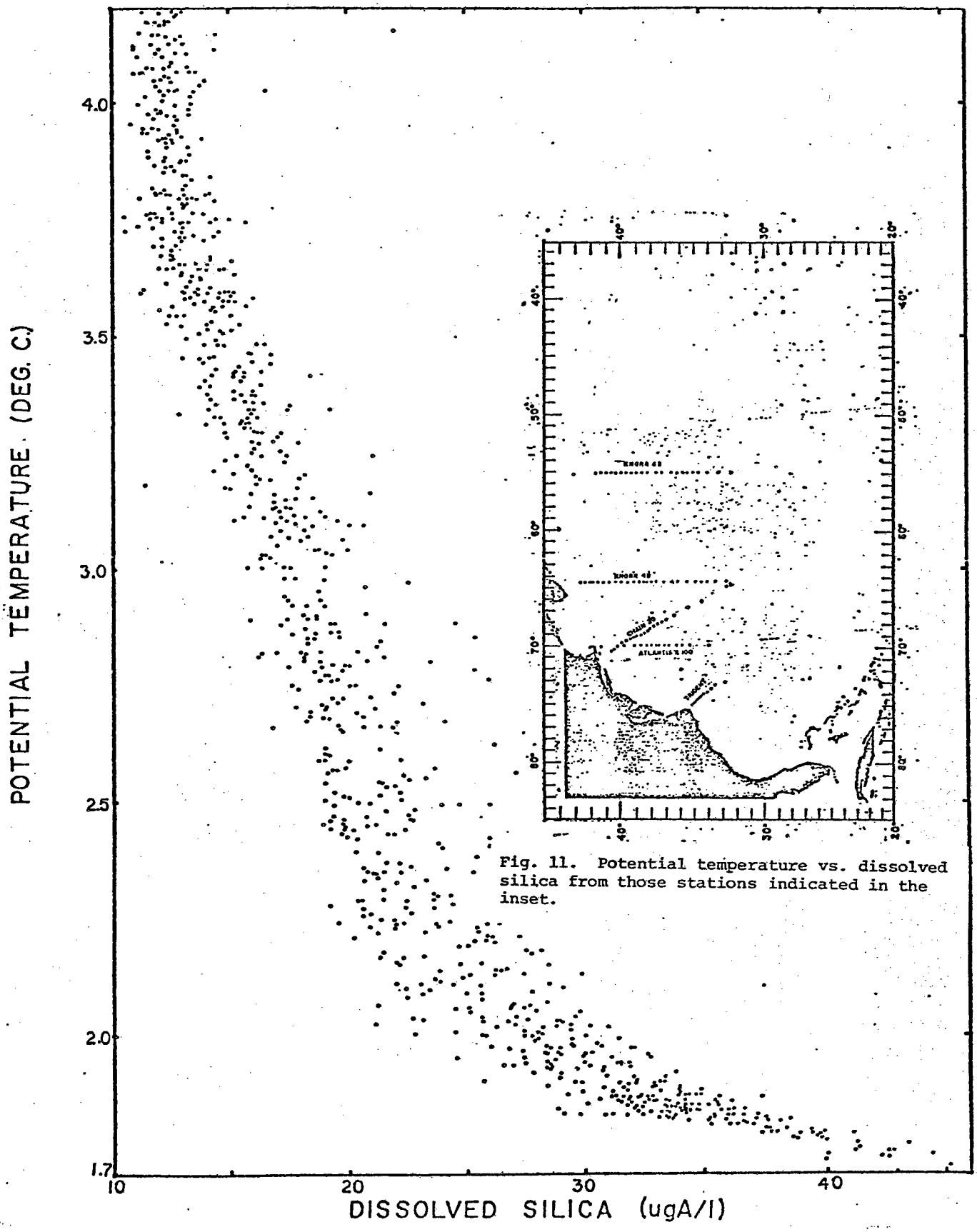

Fig. 11. Potential temperature vs. dissolved silica from those stations indicated in the inset.

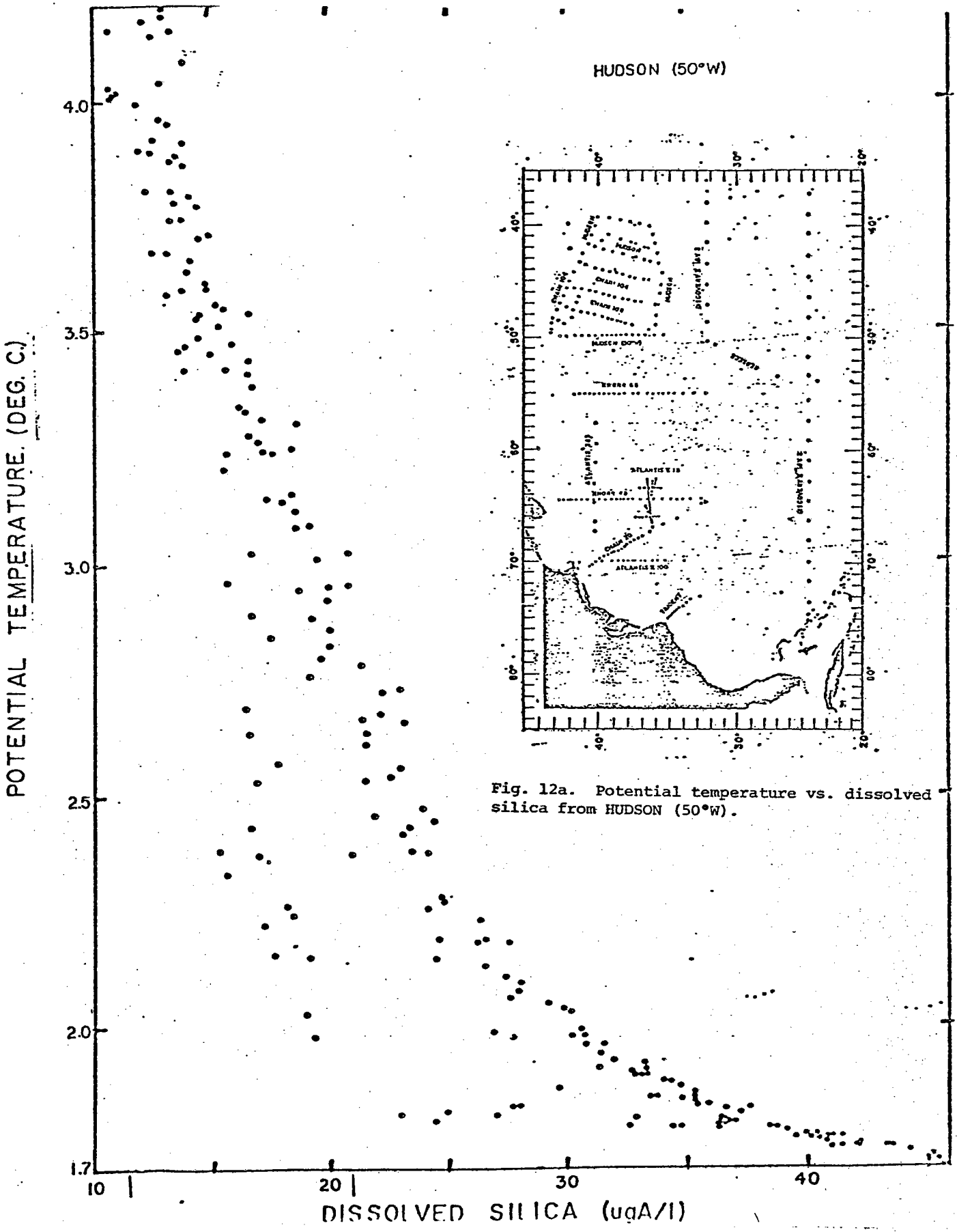

Fig. 12a. Potential temperature vs. dissolved silica from HUDSON (50°W).

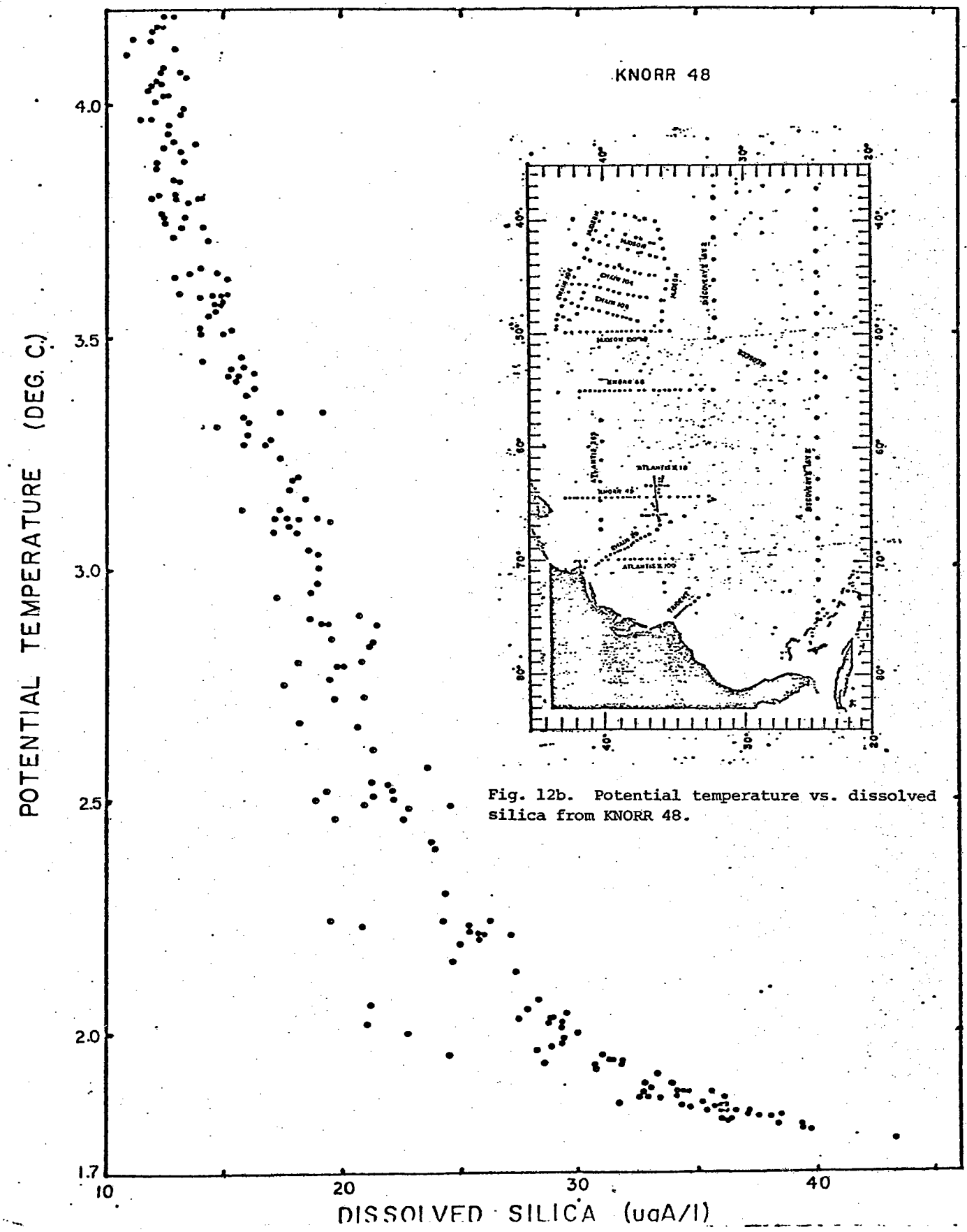

Fig. 12b. Potential temperature vs. dissolved silica from KNORR 48.

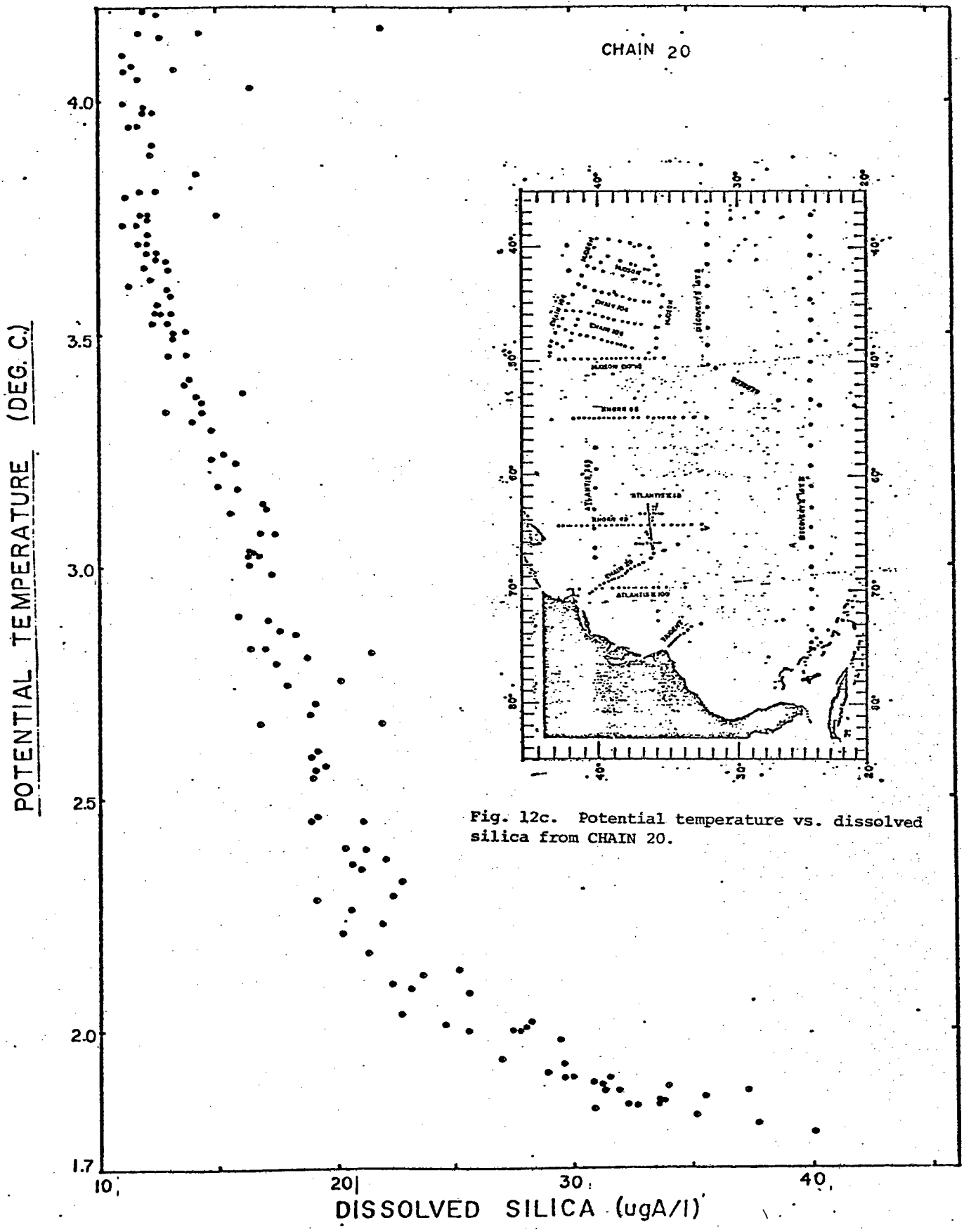

Fig. 12c. Potential temperature vs. dissolved silica from CHAIN 20.

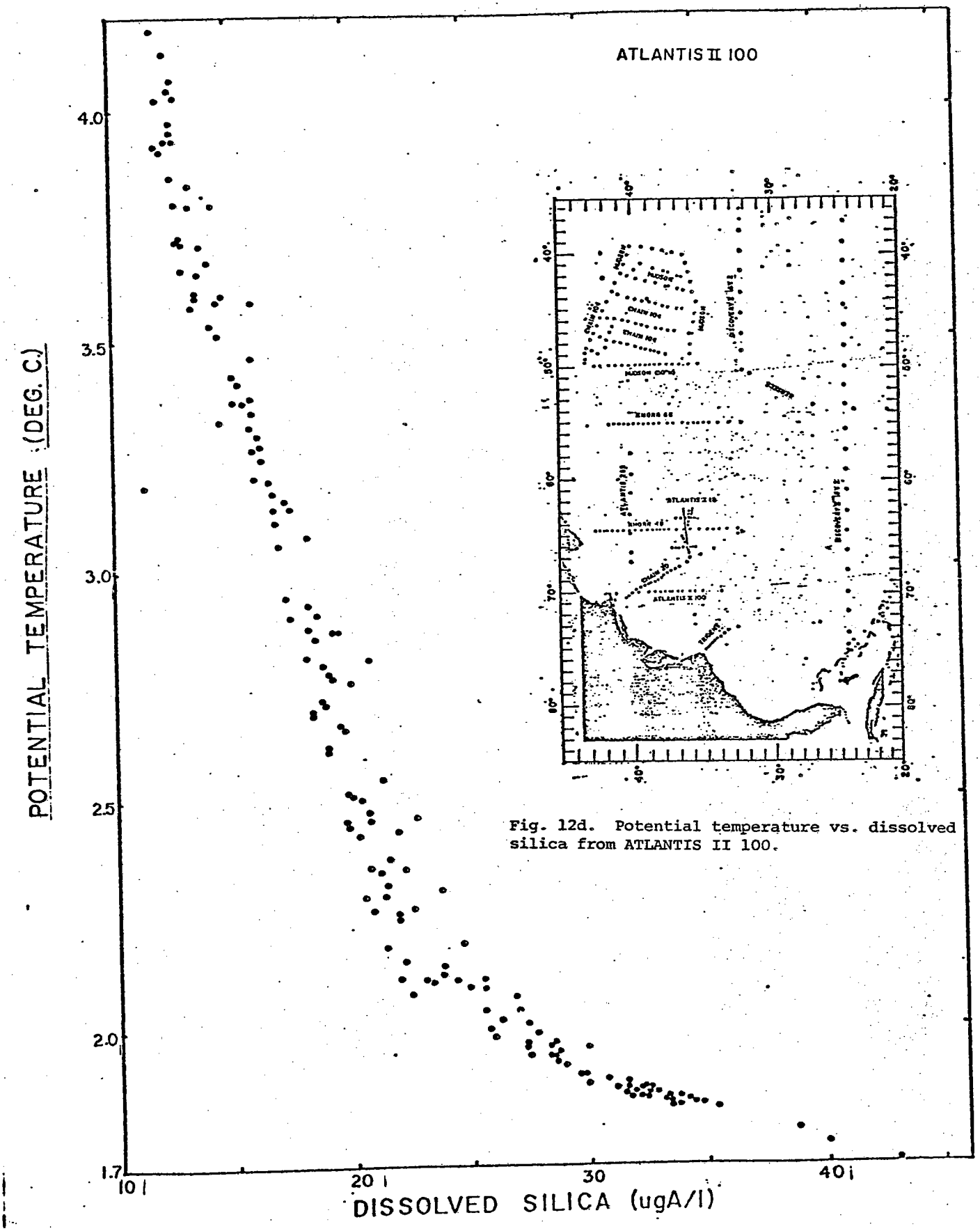

Fig. 12d. Potential temperature vs. dissolved silica from ATLANTIS II 100.

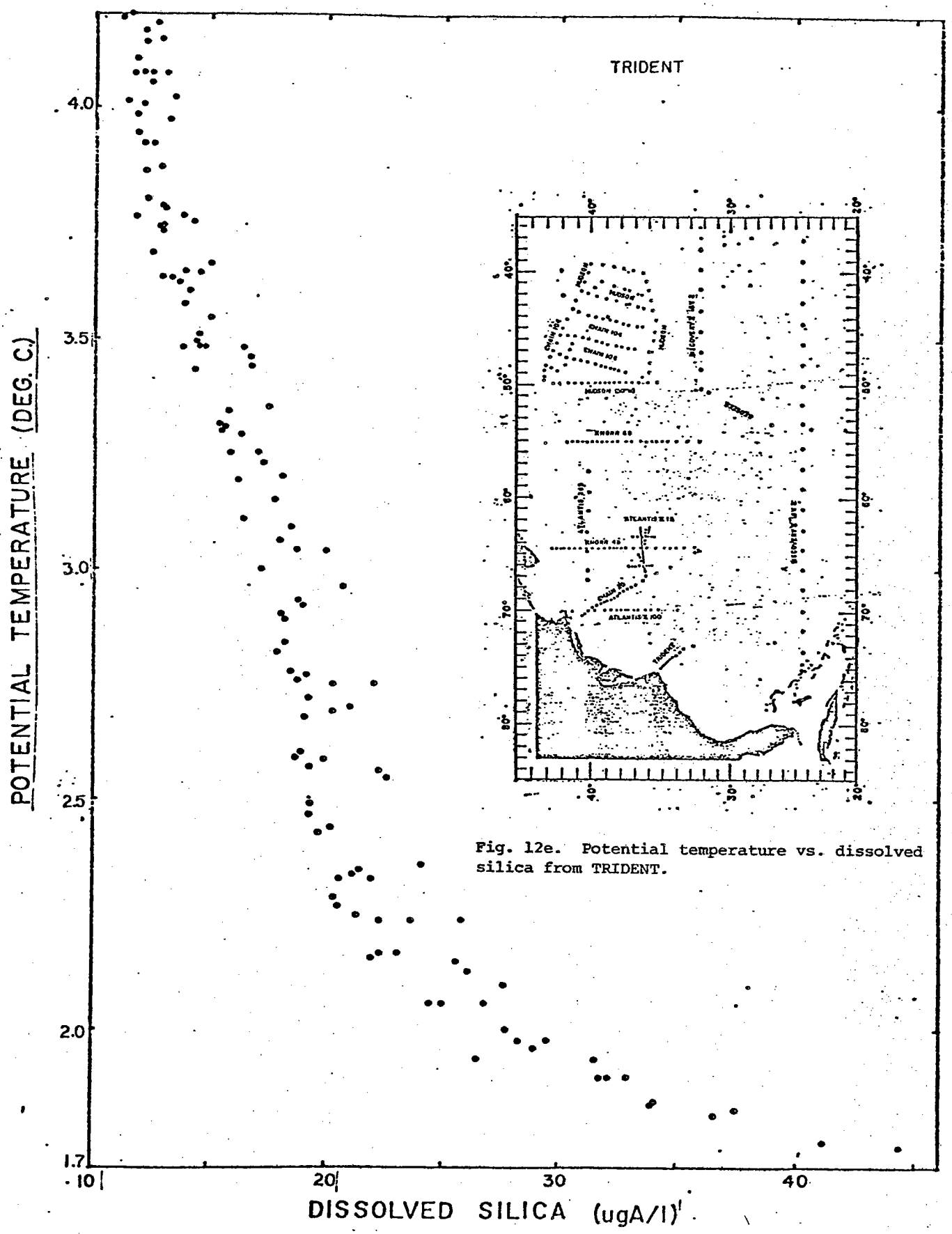

Fig. 12e. Potential temperature vs. dissolved silica from TRIDENT.

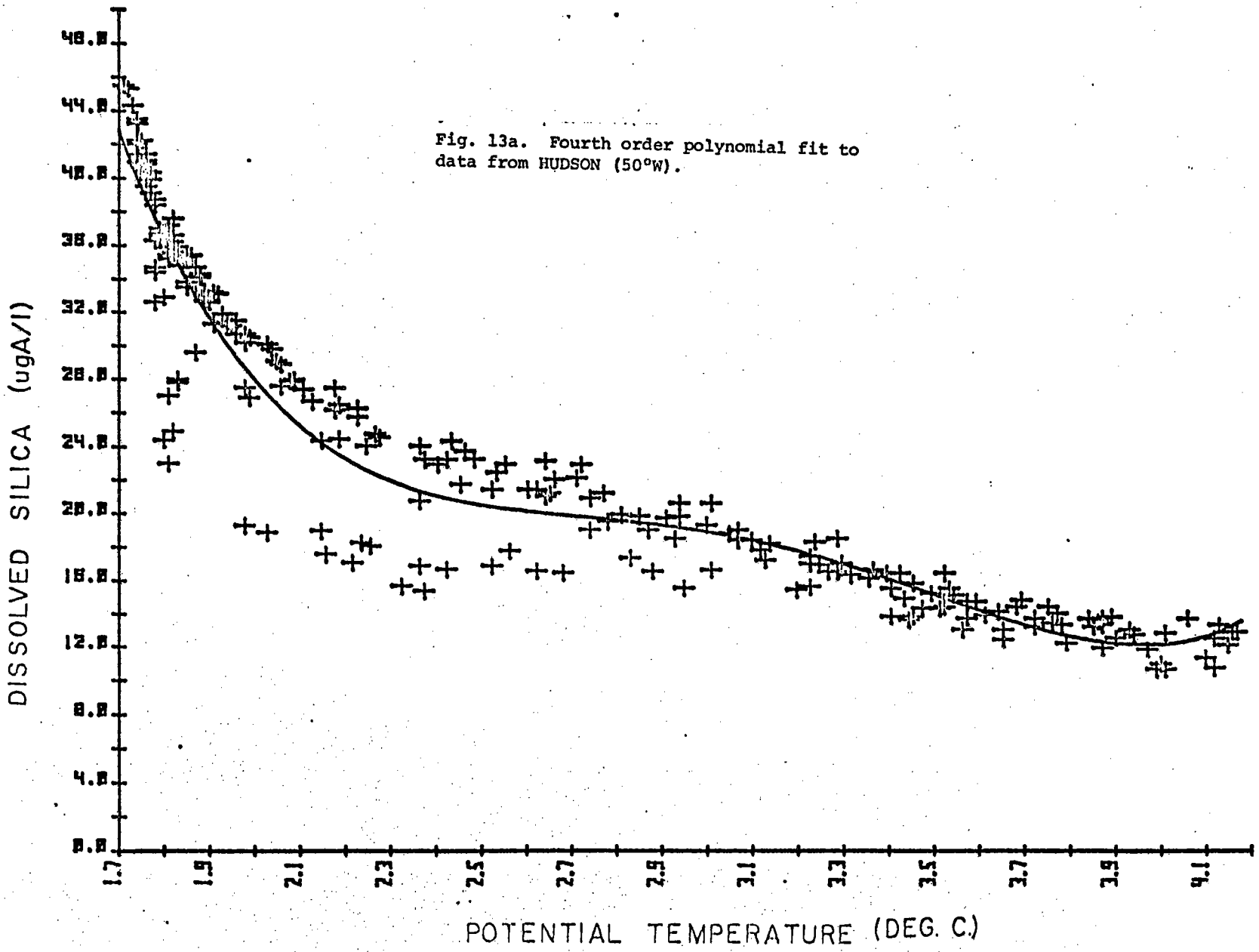

Fig. 13a. Fourth order polynomial fit to data from HUDSON (50°W).

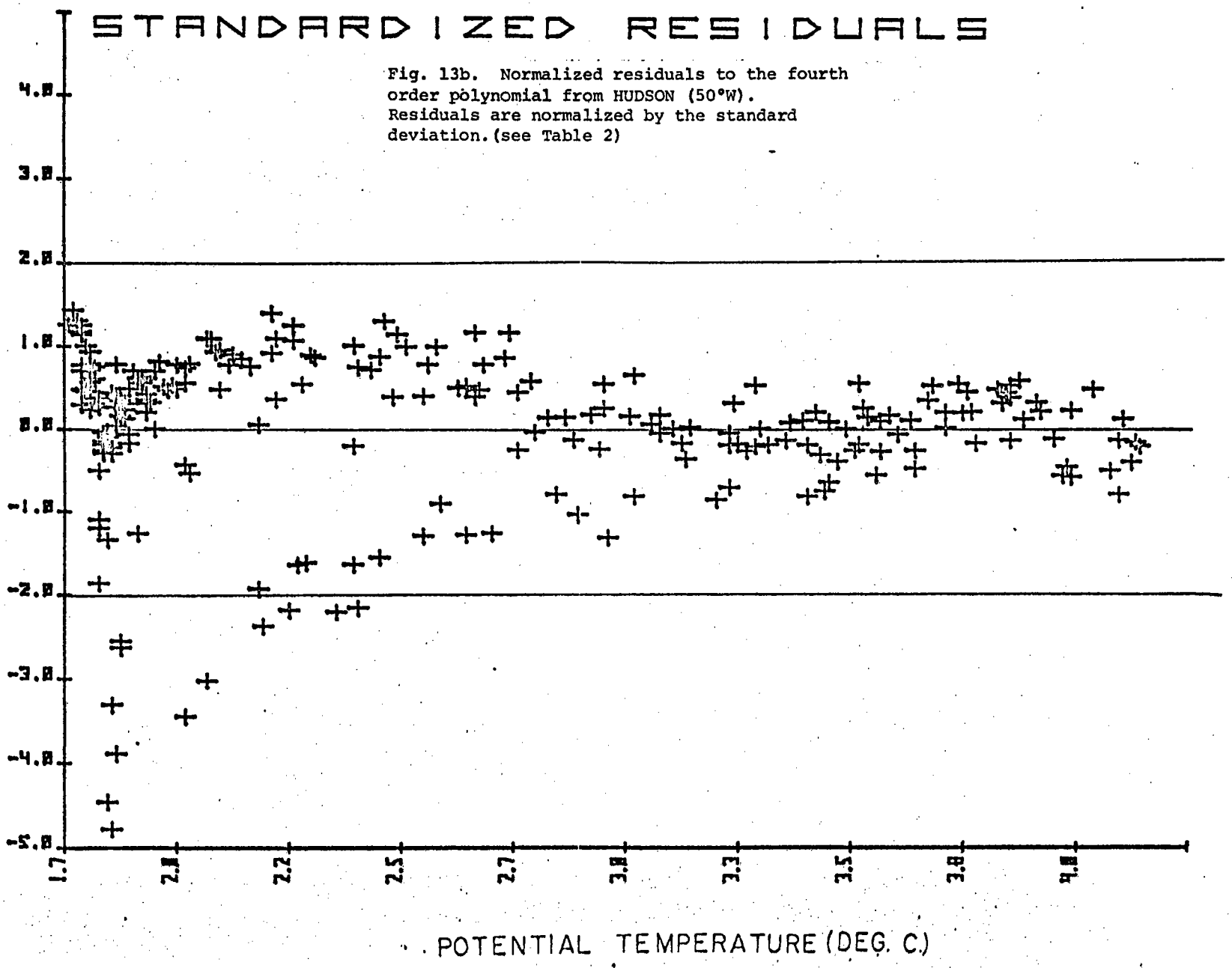

Fig. 13b. Normalized residuals to the fourth order polynomial from HUDSON (50°W). Residuals are normalized by the standard deviation. (see Table 2)

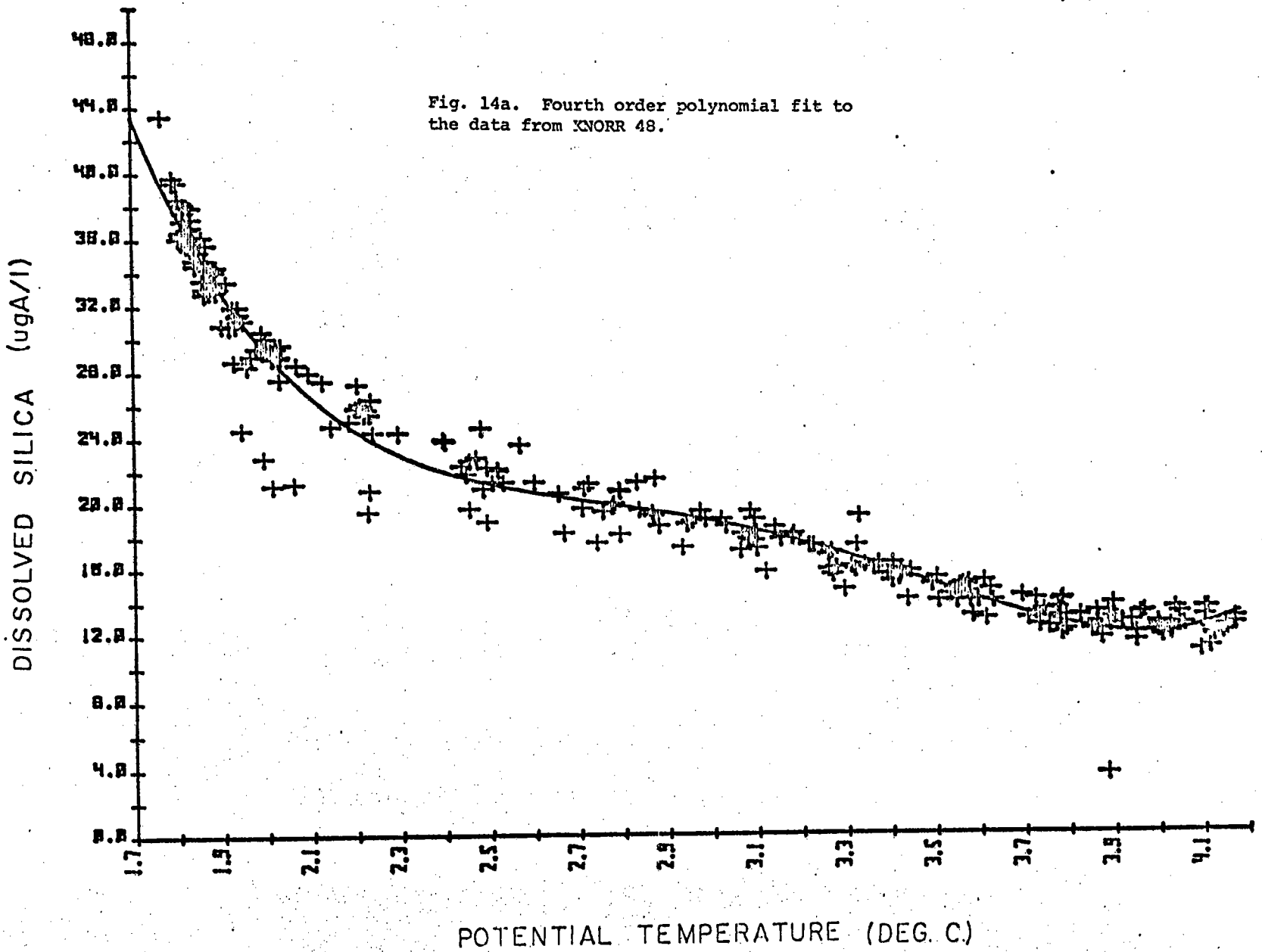

Fig. 14a. Fourth order polynomial fit to the data from KNORR 48.

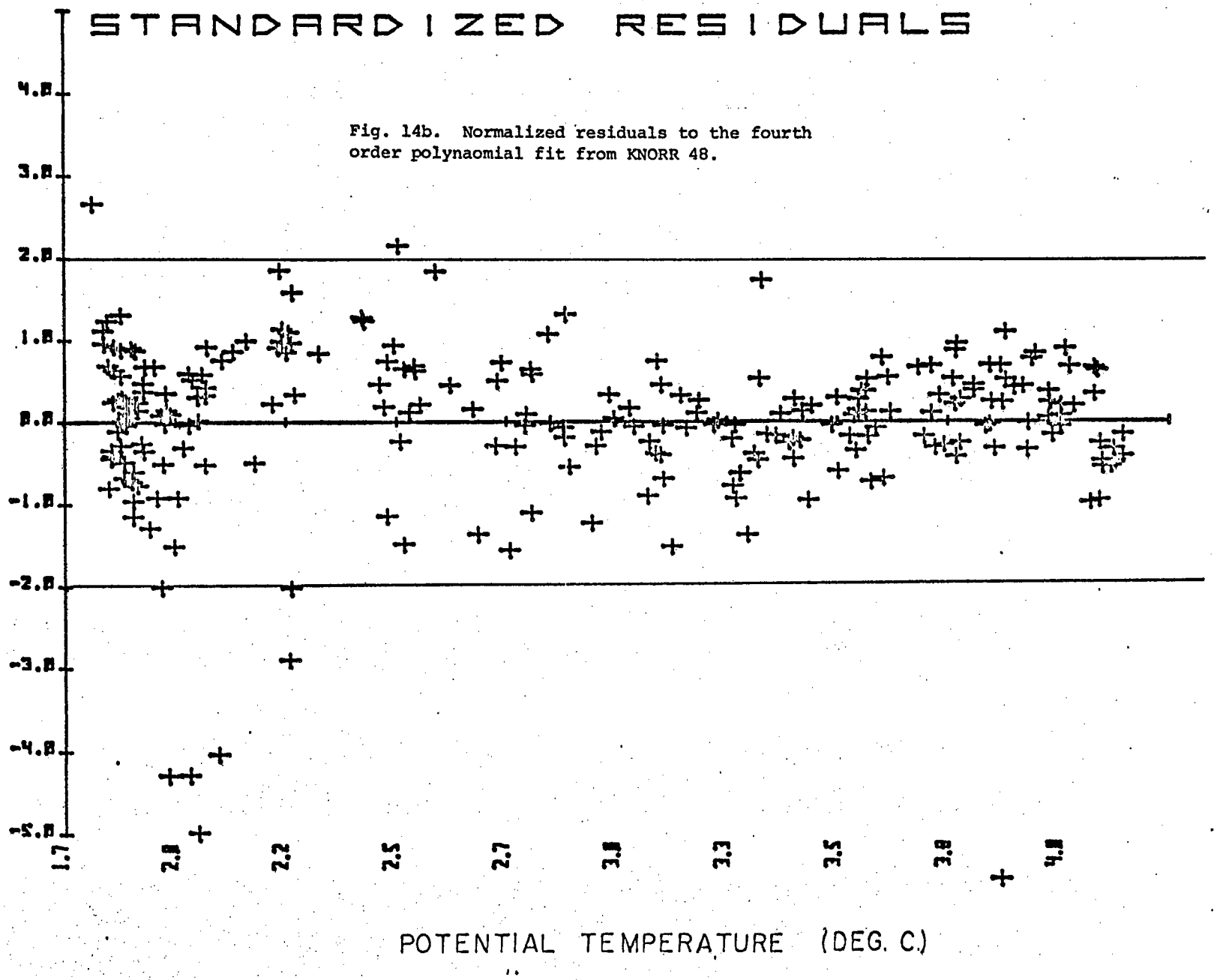

Fig. 14b. Normalized residuals to the fourth order polynaomial fit from KNORR 48.

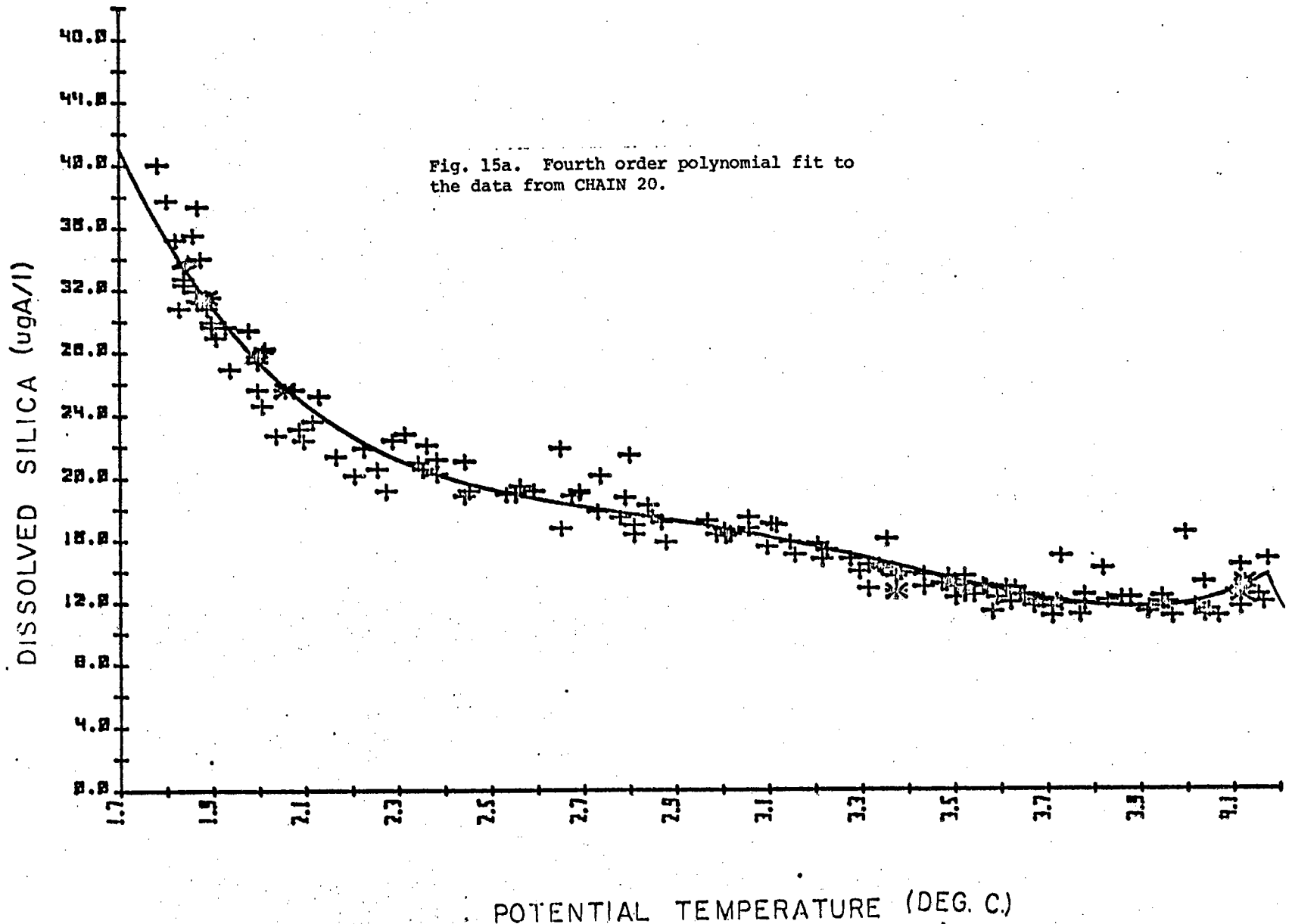

Fig. 15a. Fourth order polynomial fit to the data from CHAIN 20.

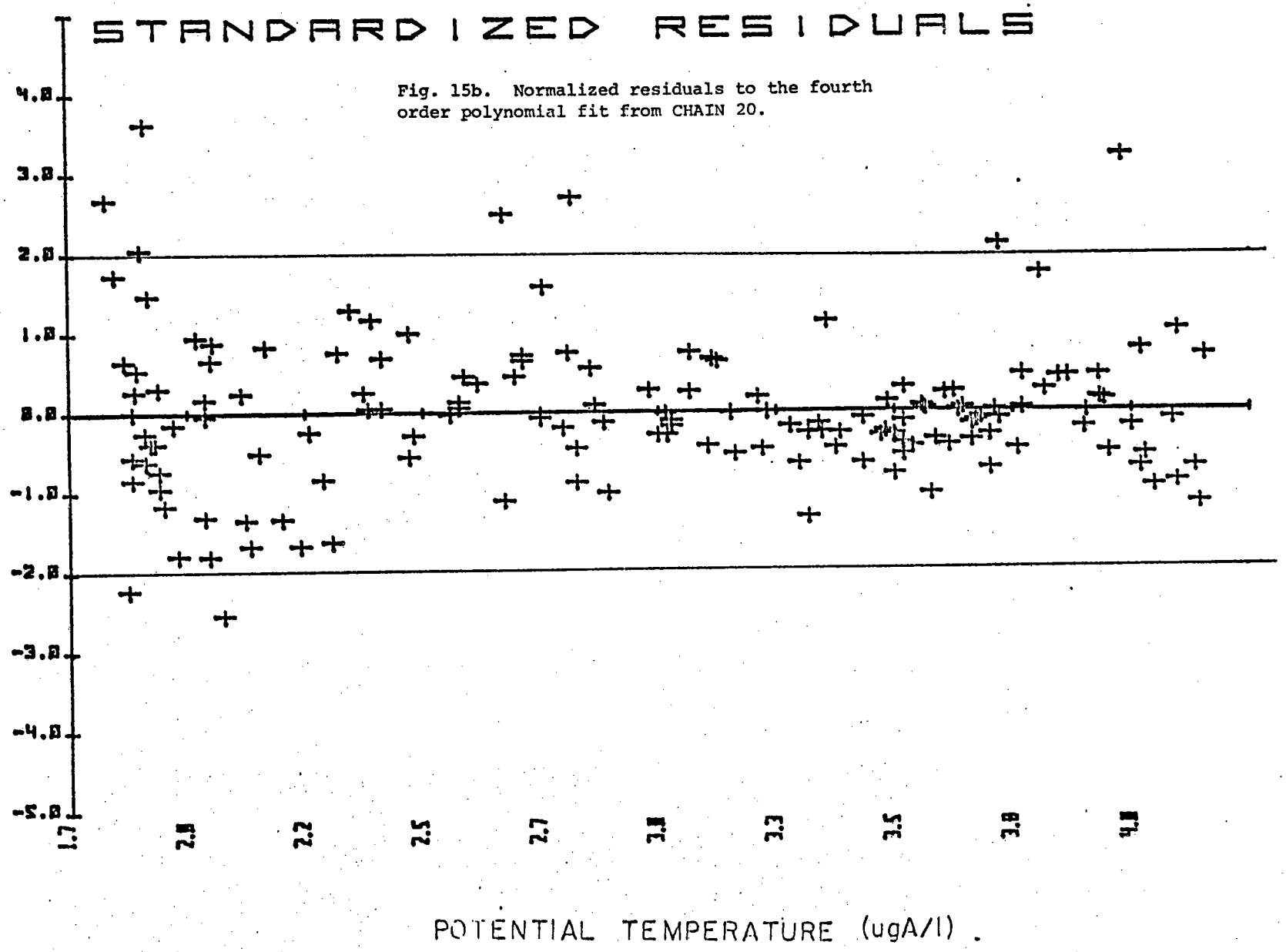

Fig. 15b. Normalized residuals to the fourth order polynomial fit from CHAIN 20.

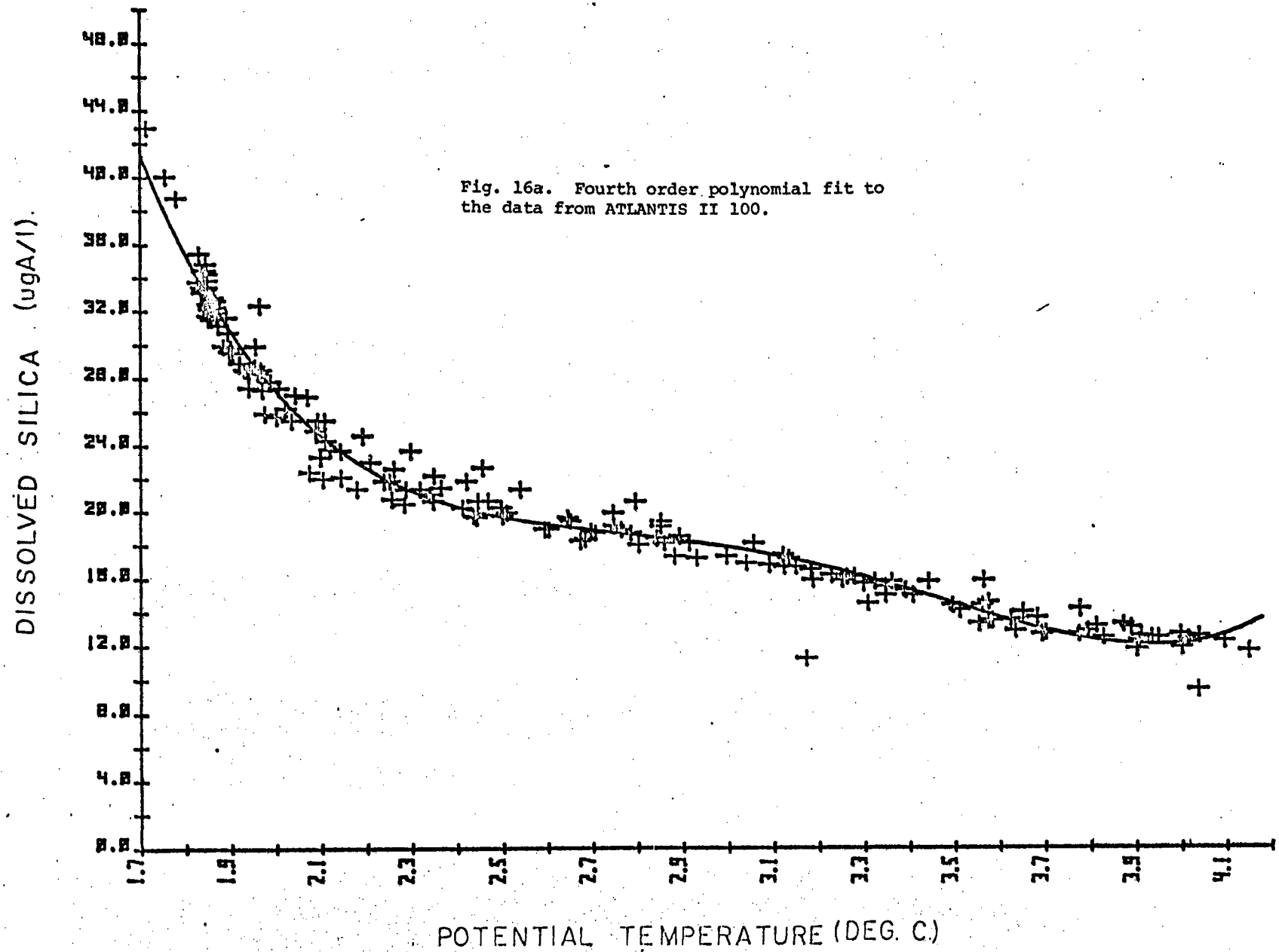

Fig. 16a. Fourth order polynomial fit to the data from ATLANTIS II 100.

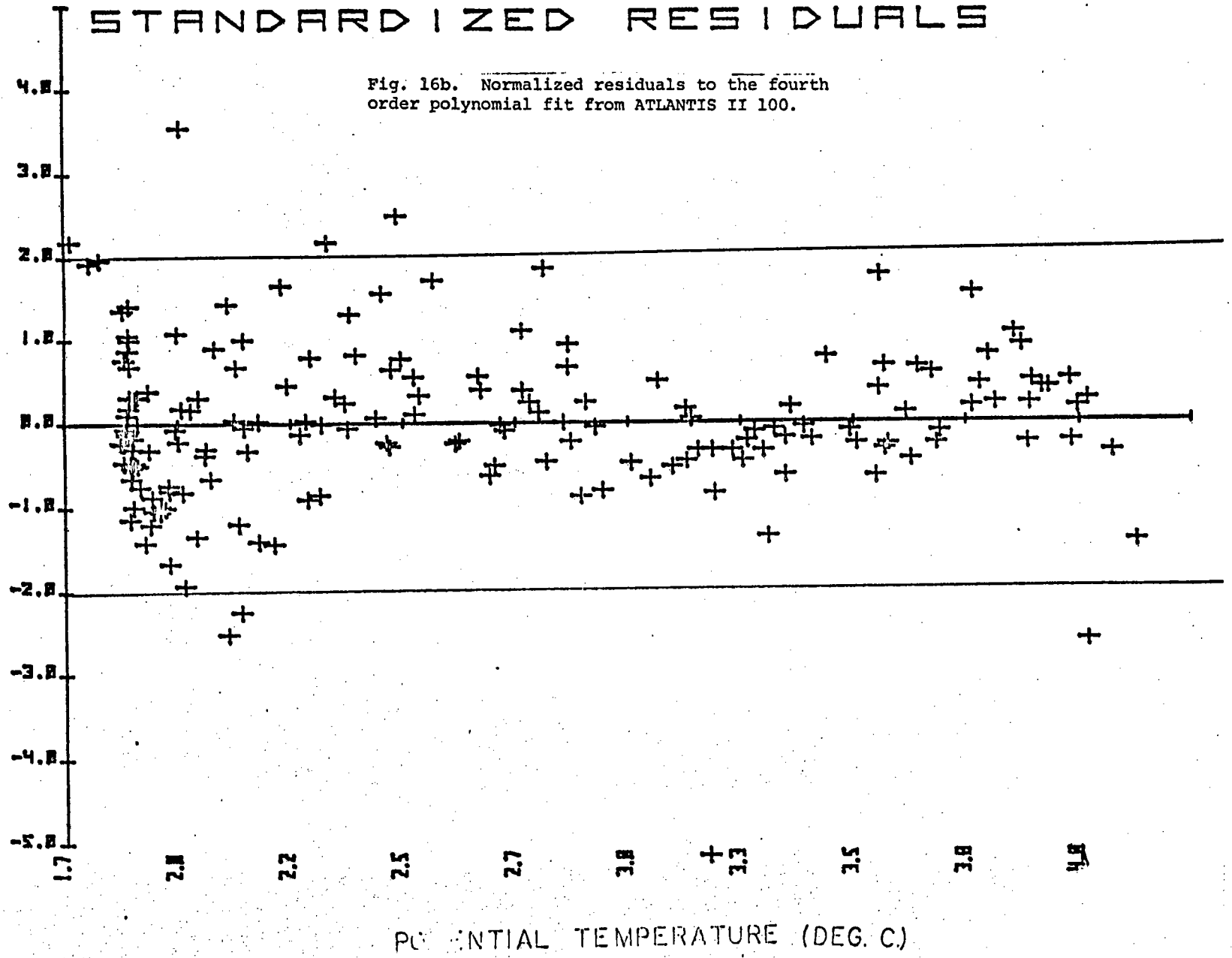

Fig. 16b. Normalized residuals to the fourth order polynomial fit from ATLANTIS II 100.

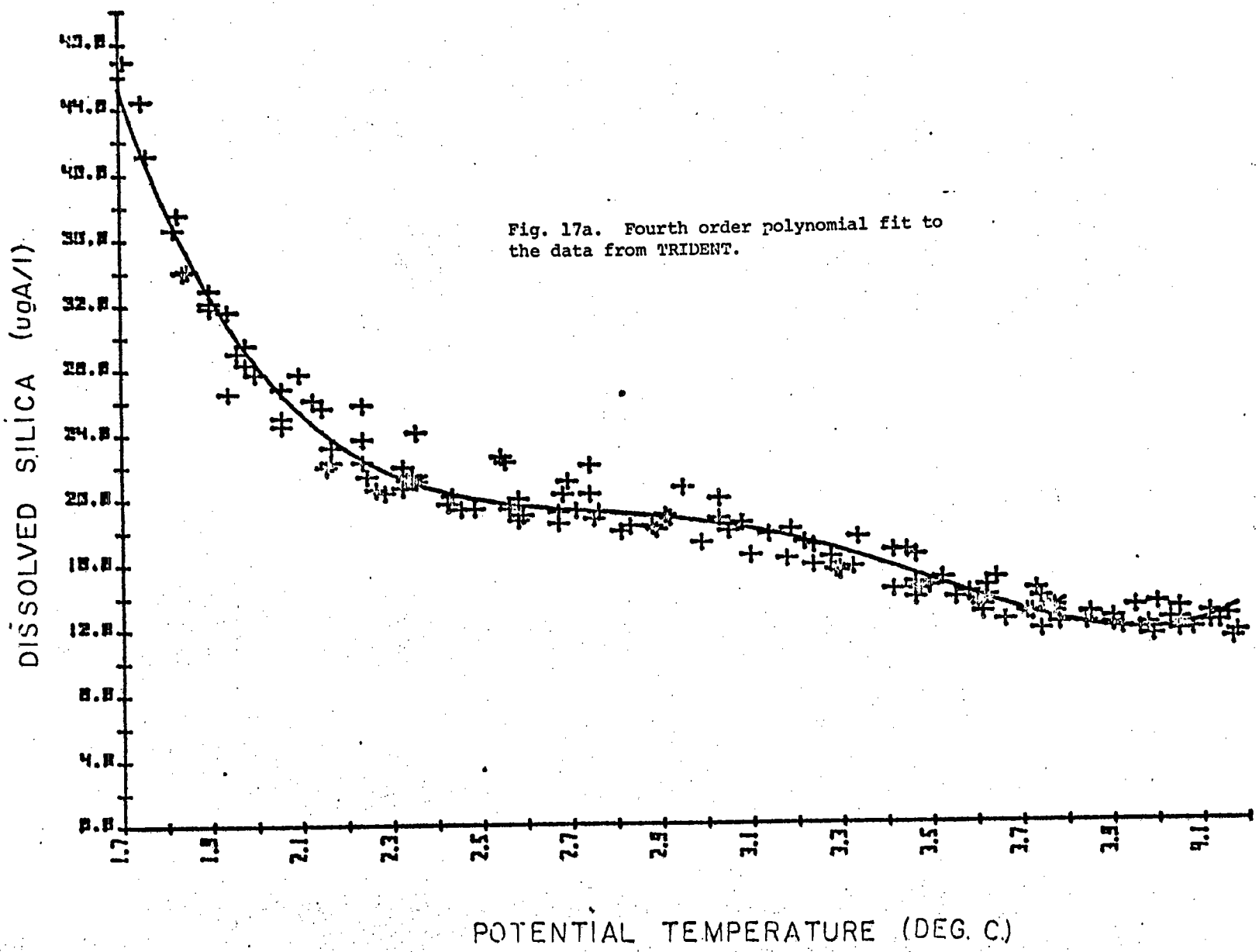

Fig. 17a. Fourth order polynomial fit to the data from TRIDENT.

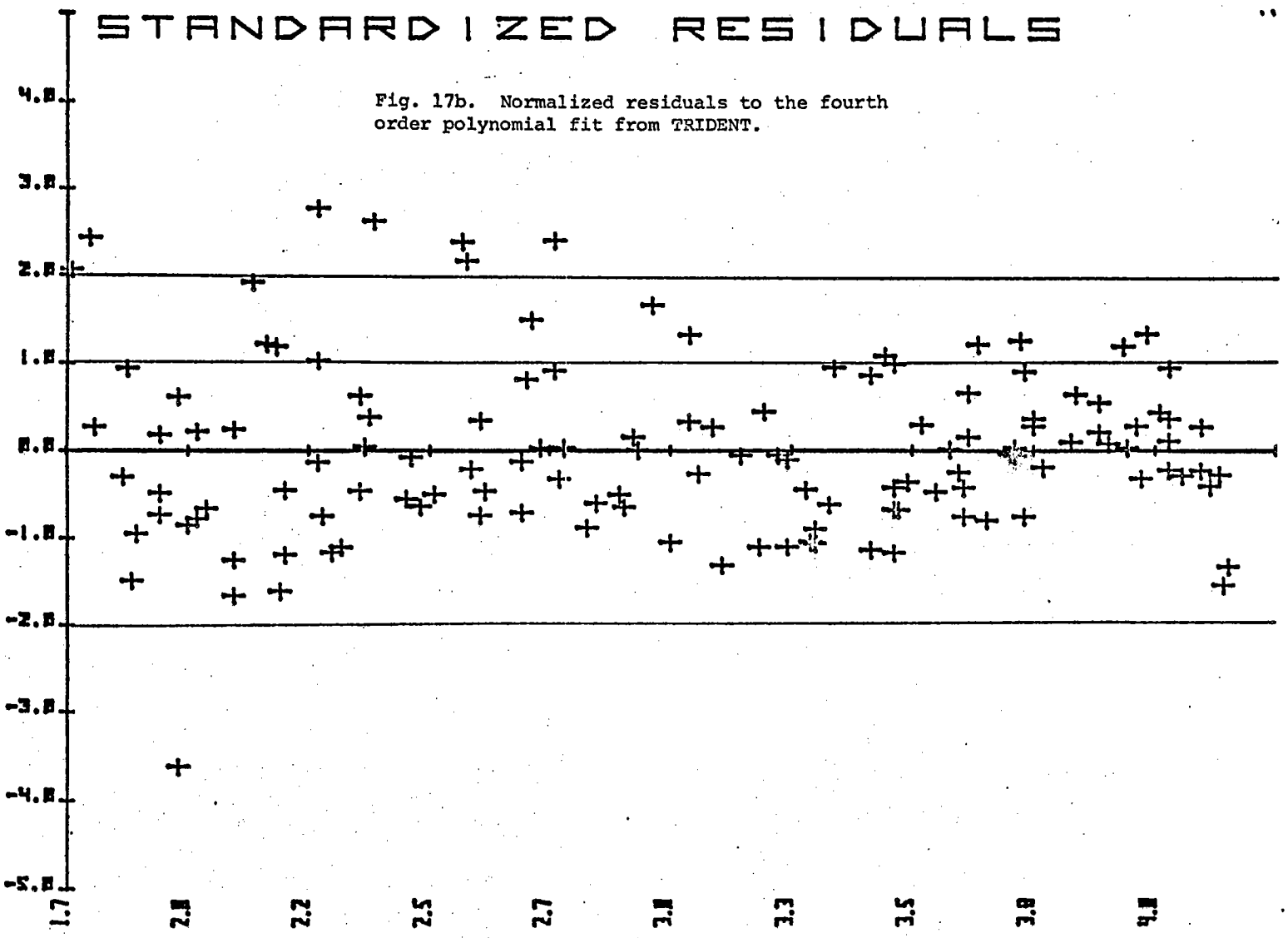

Fig. 17b. Normalized residuals to the fourth order polynomial fit from TRIDENT.

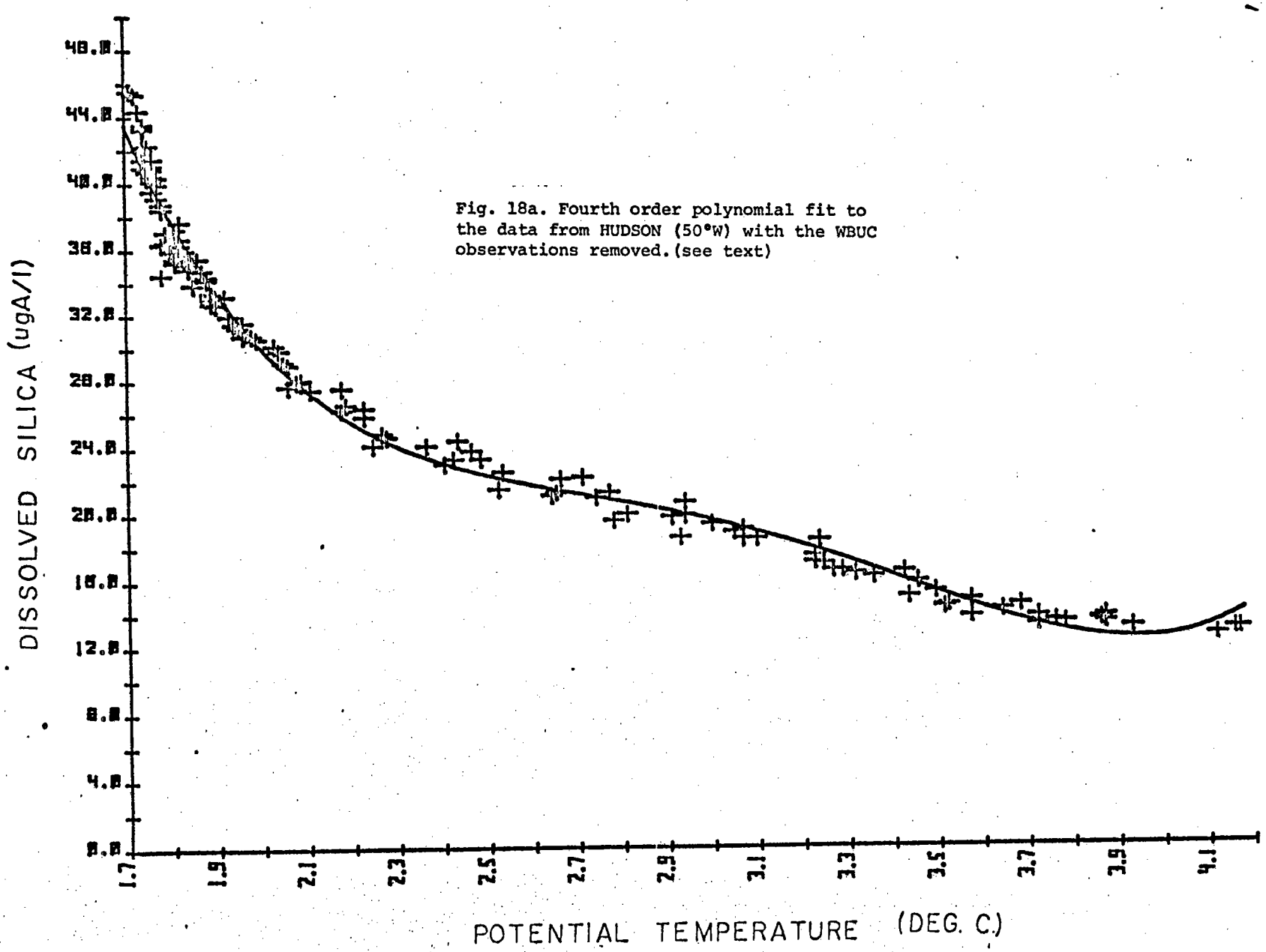

Fig. 18a. Fourth order polynomial fit to the data from HUDSON (50°W) with the WBUC observations removed. (see text)

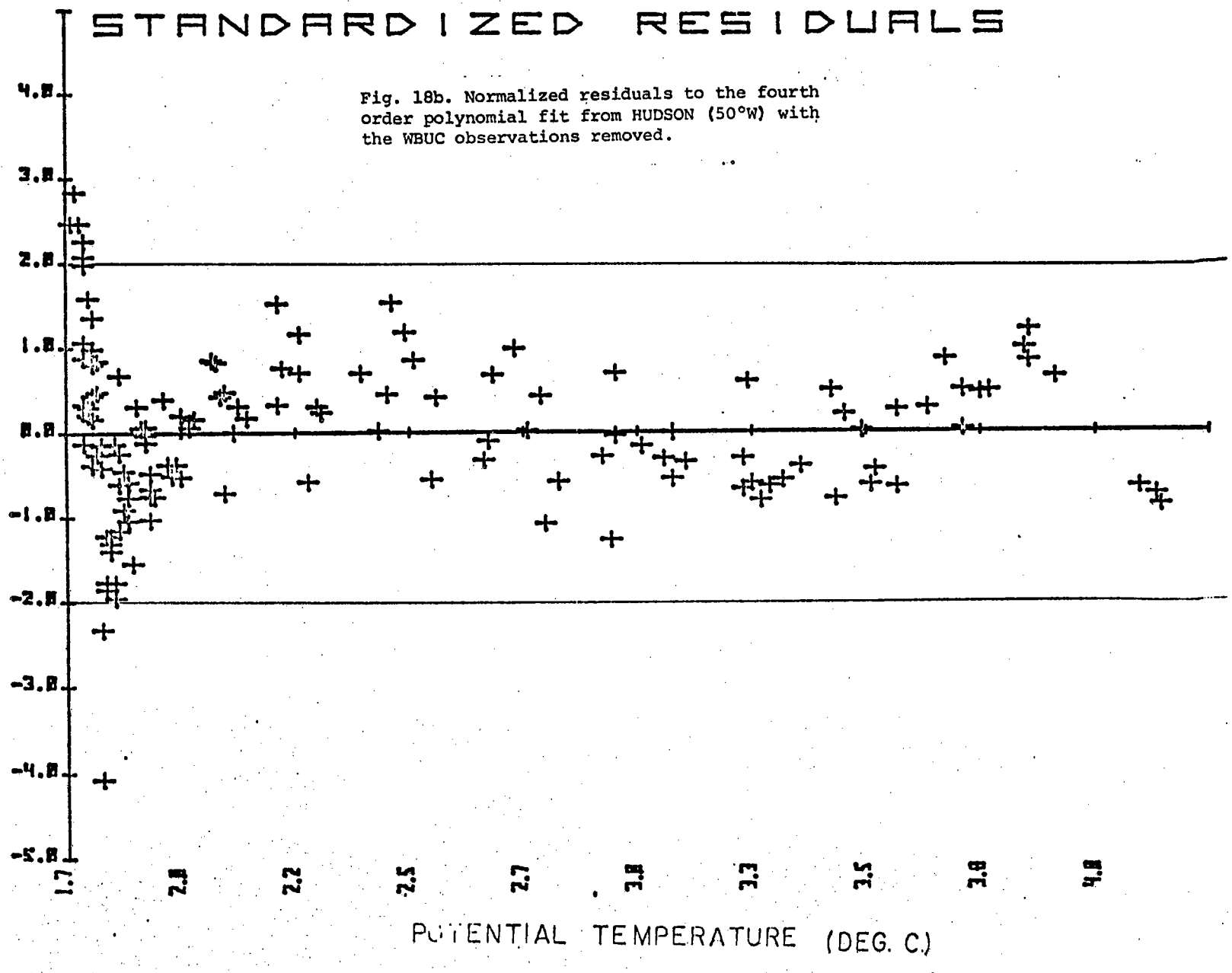

Fig. 18b. Normalized residuals to the fourth order polynomial fit from HUDSON (50°W) with the WBUC observations removed.

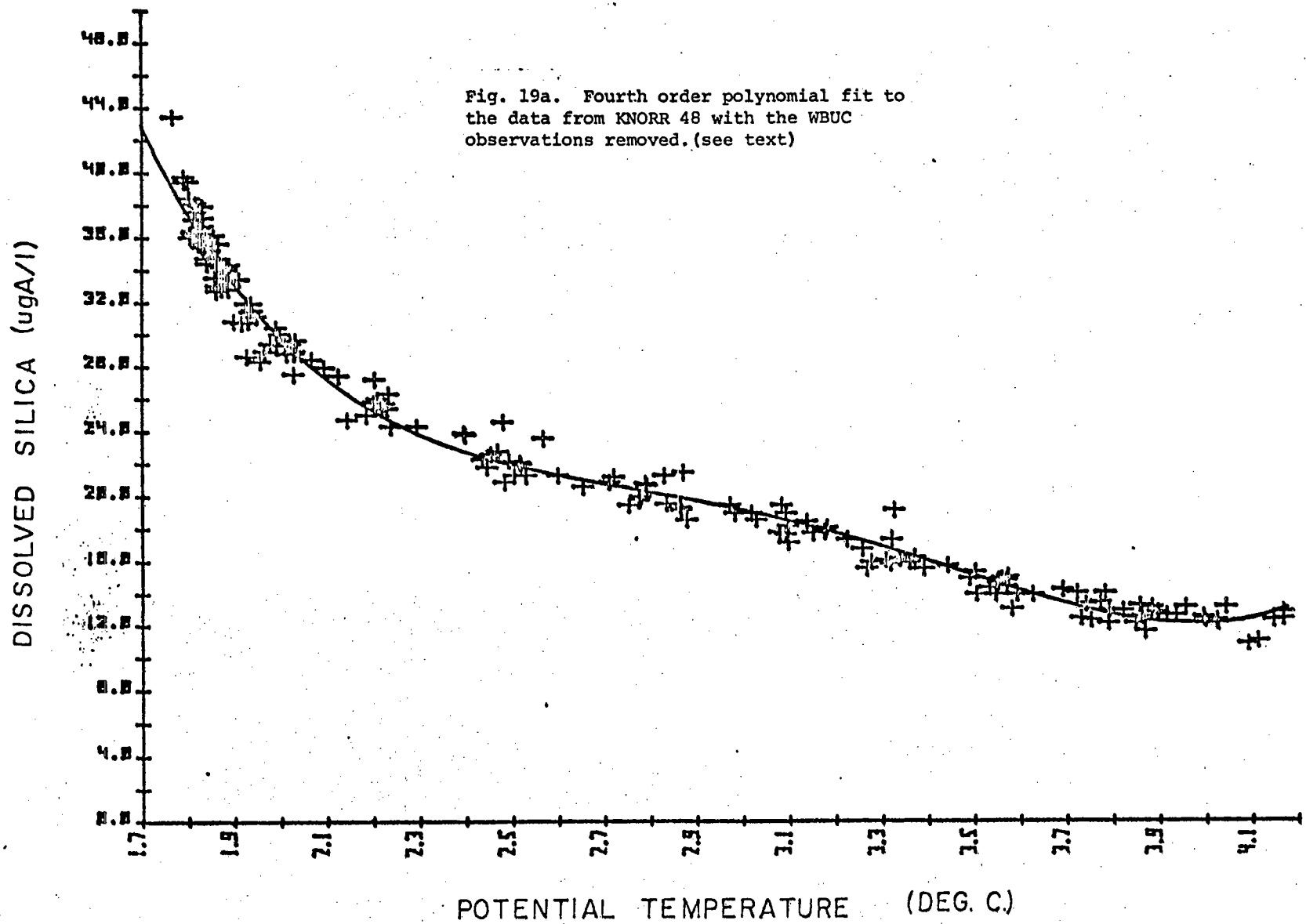

Fig. 19a. Fourth order polynomial fit to the data from KNORR 48 with the WBUC observations removed.(see text)

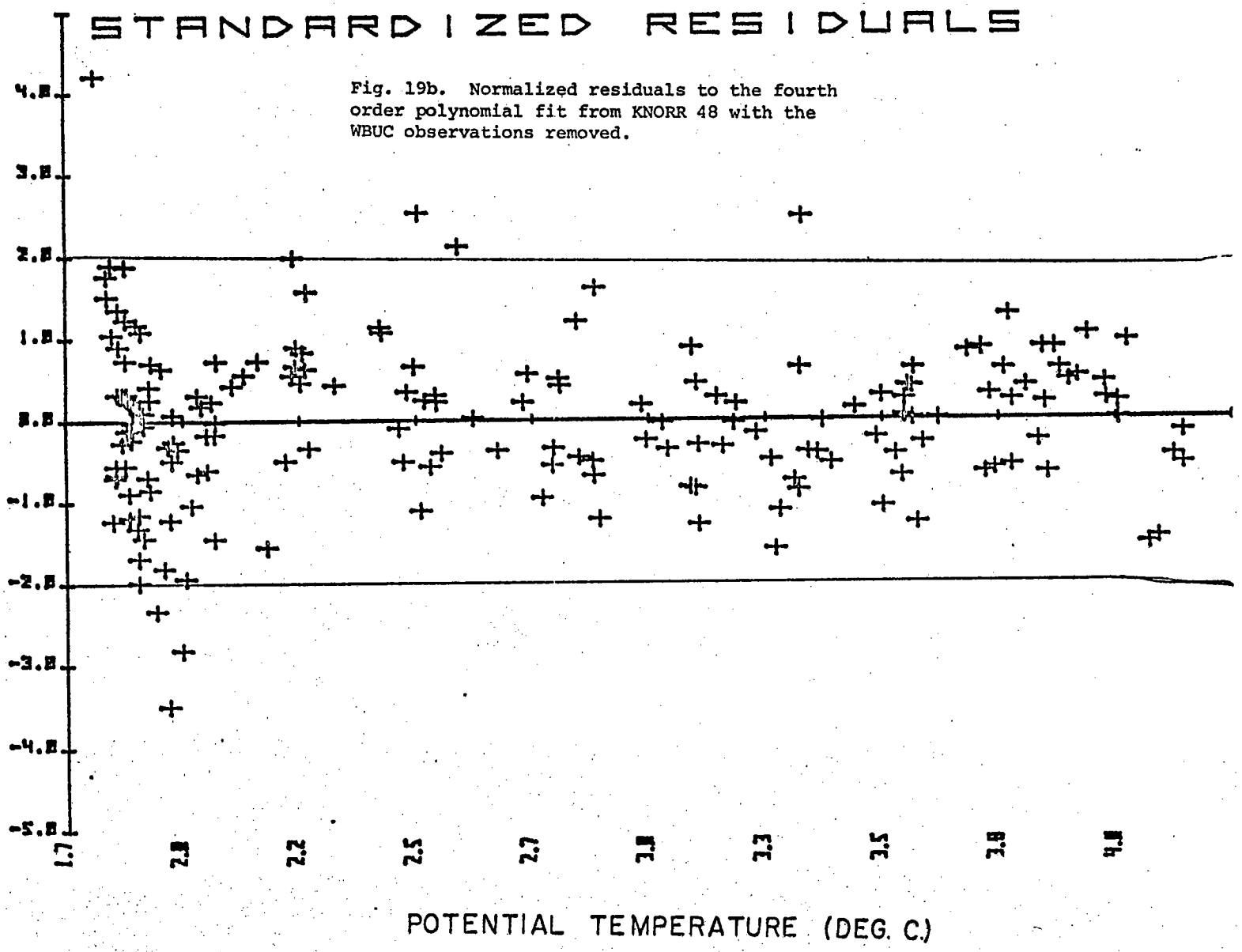

Fig. 19b. Normalized residuals to the fourth order polynomial fit from KNORR 48 with the WBUC observations removed.

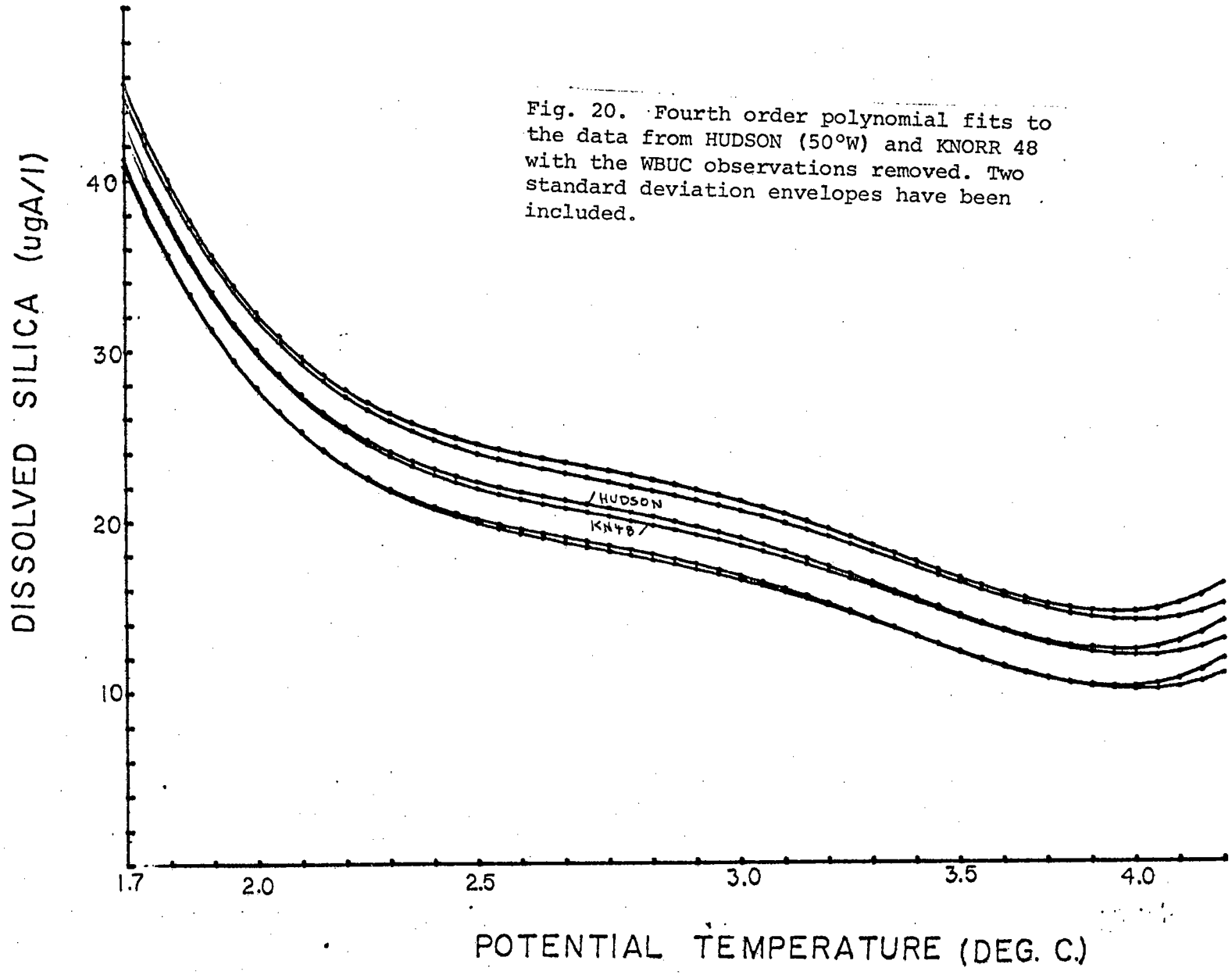

Fig. 20. Fourth order polynomial fits to the data from HUDSON (50°W) and KNORR 48 with the WBUC observations removed. Two standard deviation envelopes have been included.

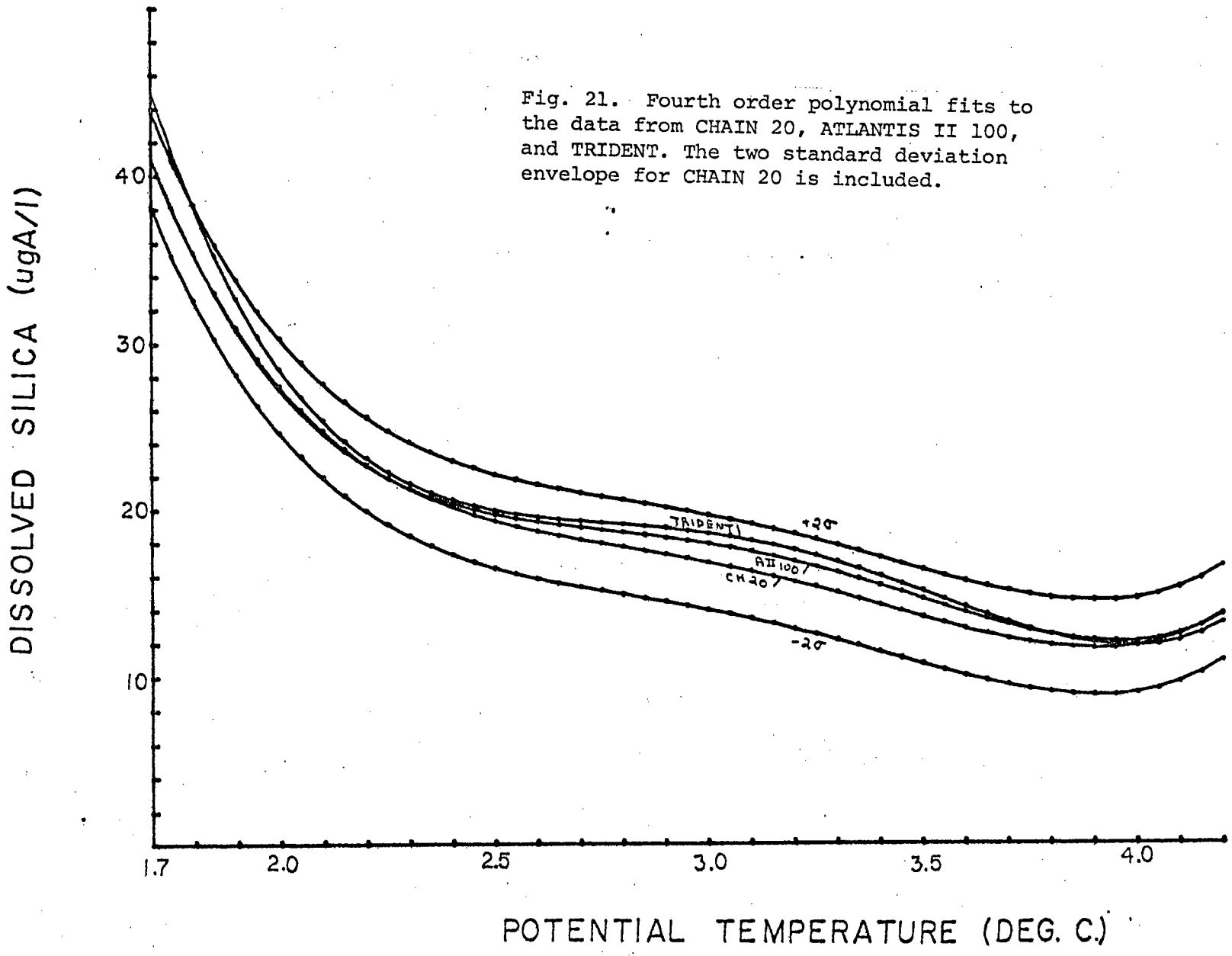

Fig. 21. Fourth order polynomial fits to the data from CHAIN 20, ATLANTIS II 100, and TRIDENT. The two standard deviation envelope for CHAIN 20 is included.

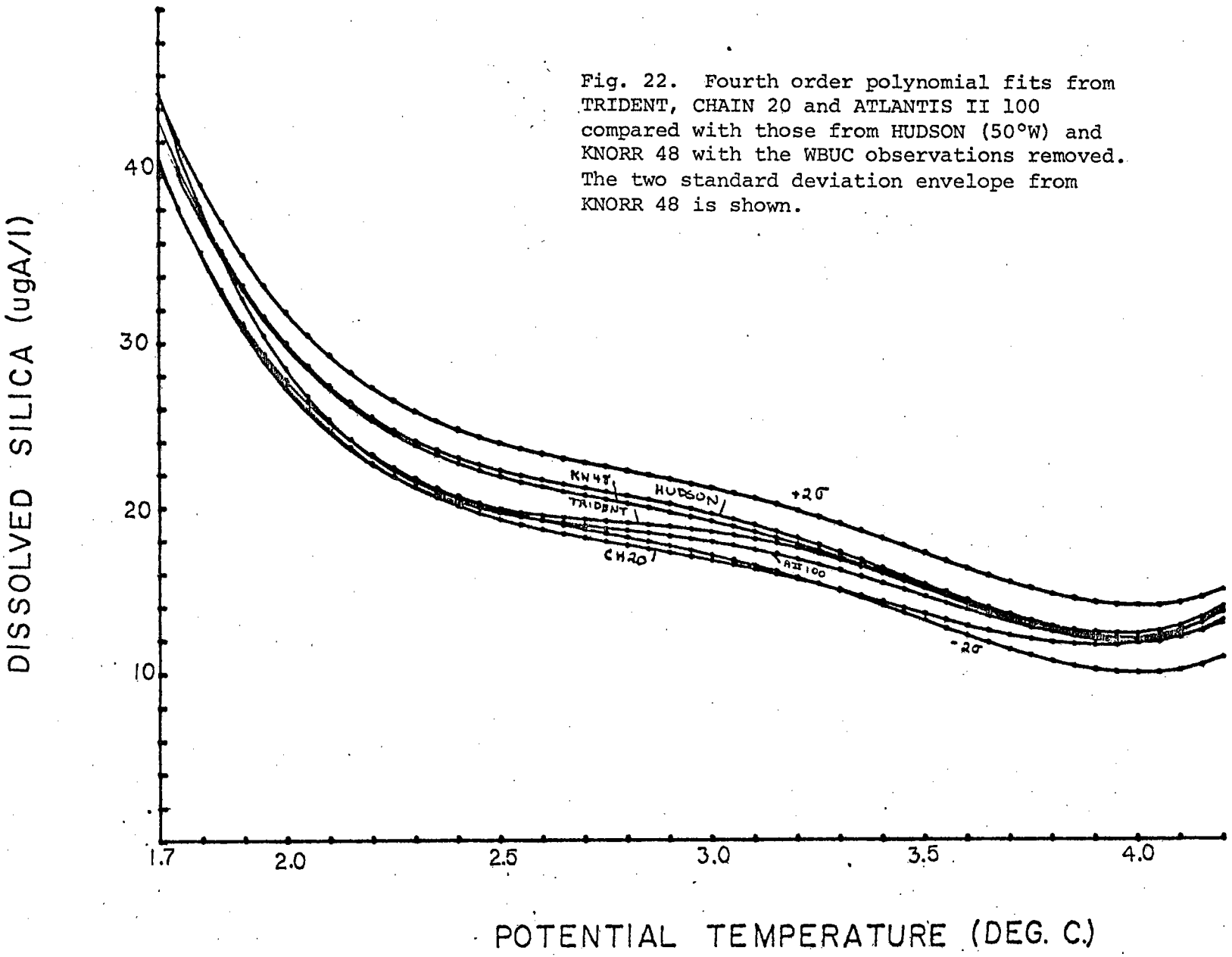

Fig. 22. Fourth order polynomial fits from TRIDENT, CHAIN 20 and ATLANTIS II 100 compared with those from HUDSON (50°W) and KNORR 48 with the WBUC observations removed. The two standard deviation envelope from KNORR 48 is shown.

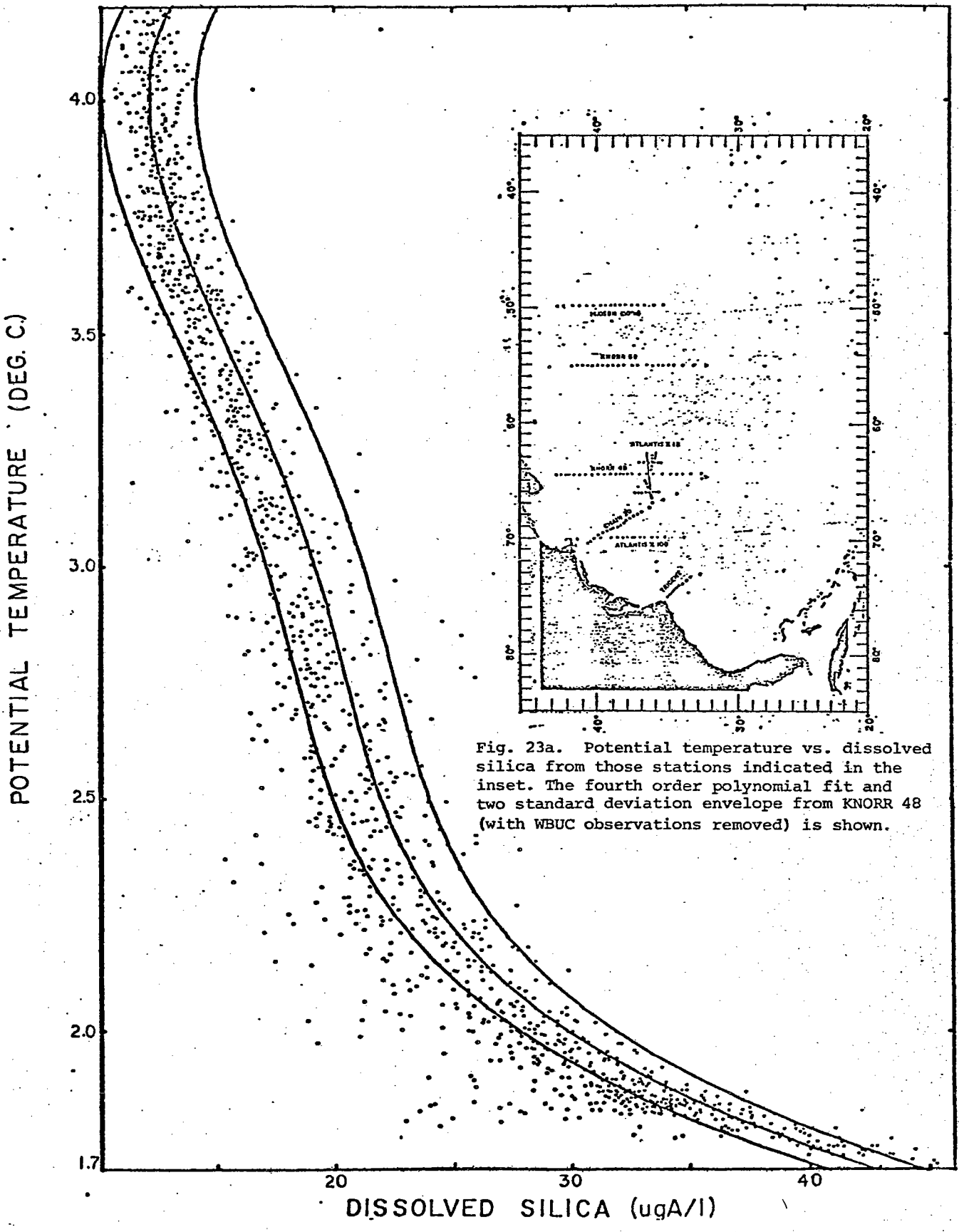

Fig. 23a. Potential temperature vs. dissolved silica from those stations indicated in the inset. The fourth order polynomial fit and two standard deviation envelope from KNORR 48 (with WBUC observations removed) is shown.

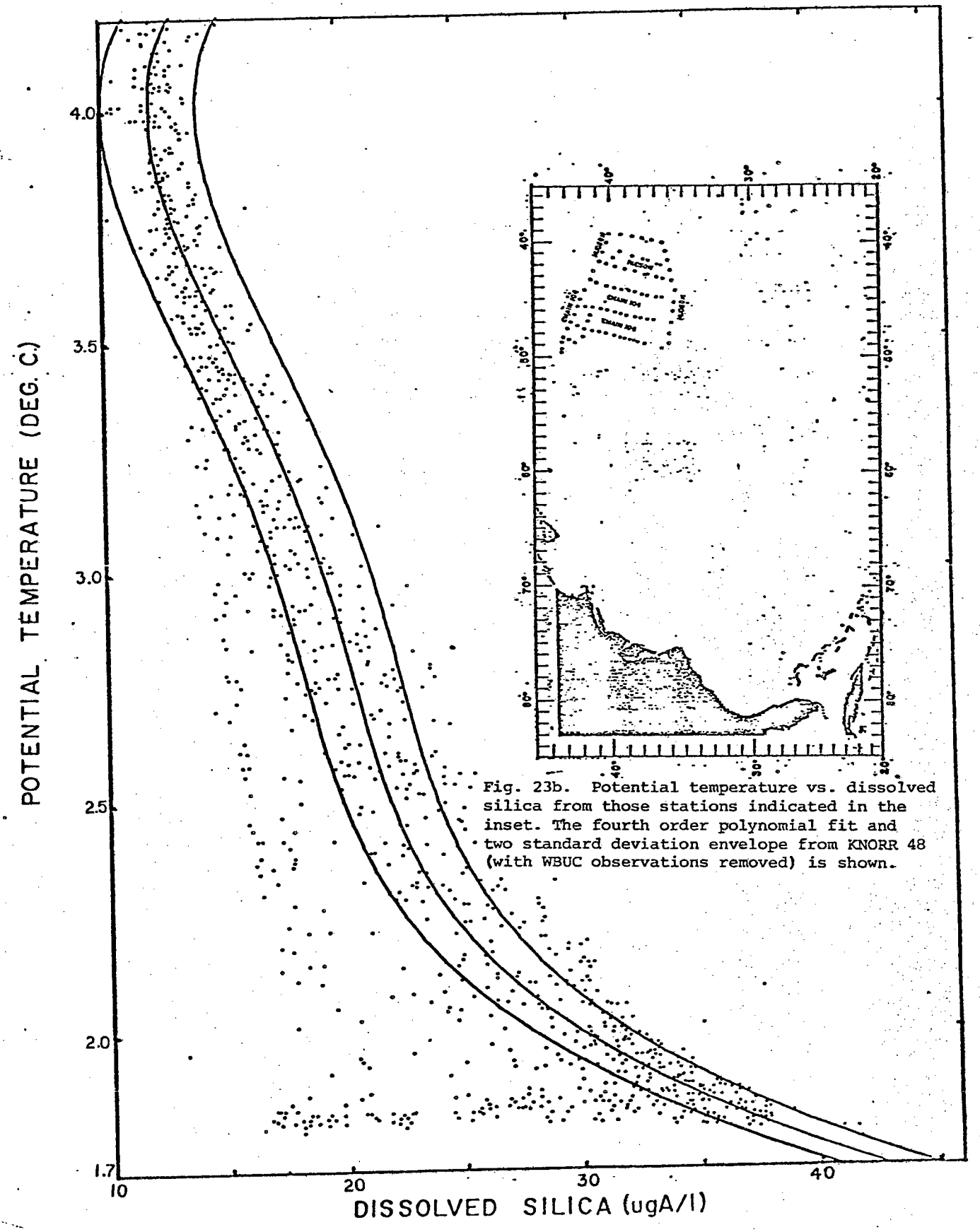

Fig. 23b. Potential temperature vs. dissolved silica from those stations indicated in the inset. The fourth order polynomial fit and two standard deviation envelope from KNORR 48 (with WBUC observations removed) is shown.

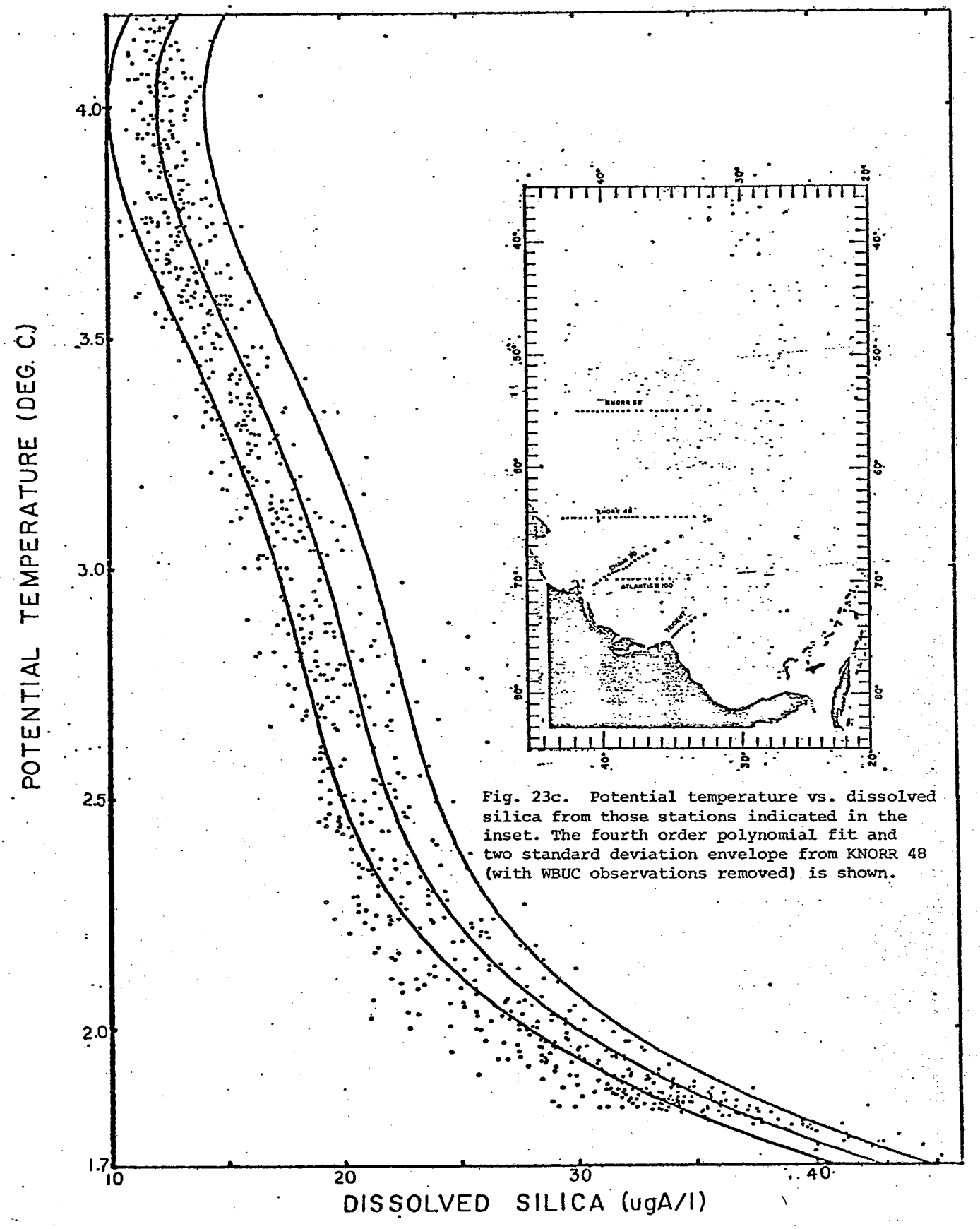

Fig. 23c. Potential temperature vs. dissolved silica from those stations indicated in the inset. The fourth order polynomial fit and two standard deviation envelope from KNORR 48 (with WBUC observations removed) is shown.

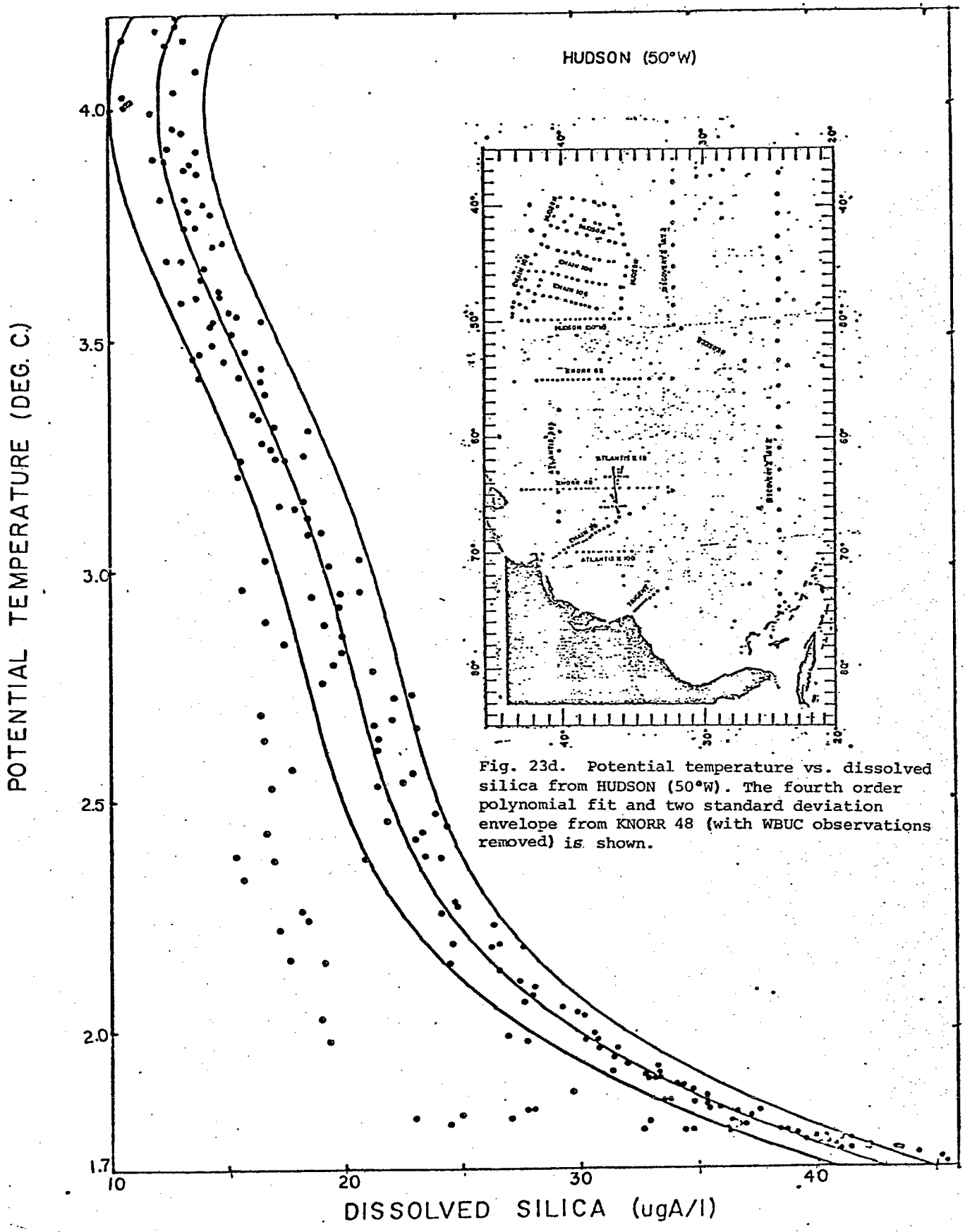

Fig. 23d. Potential temperature vs. dissolved silica from HUDSON (50°W). The fourth order polynomial fit and two standard deviation envelope from KNORR 48 (with WBUC observations removed) is shown.

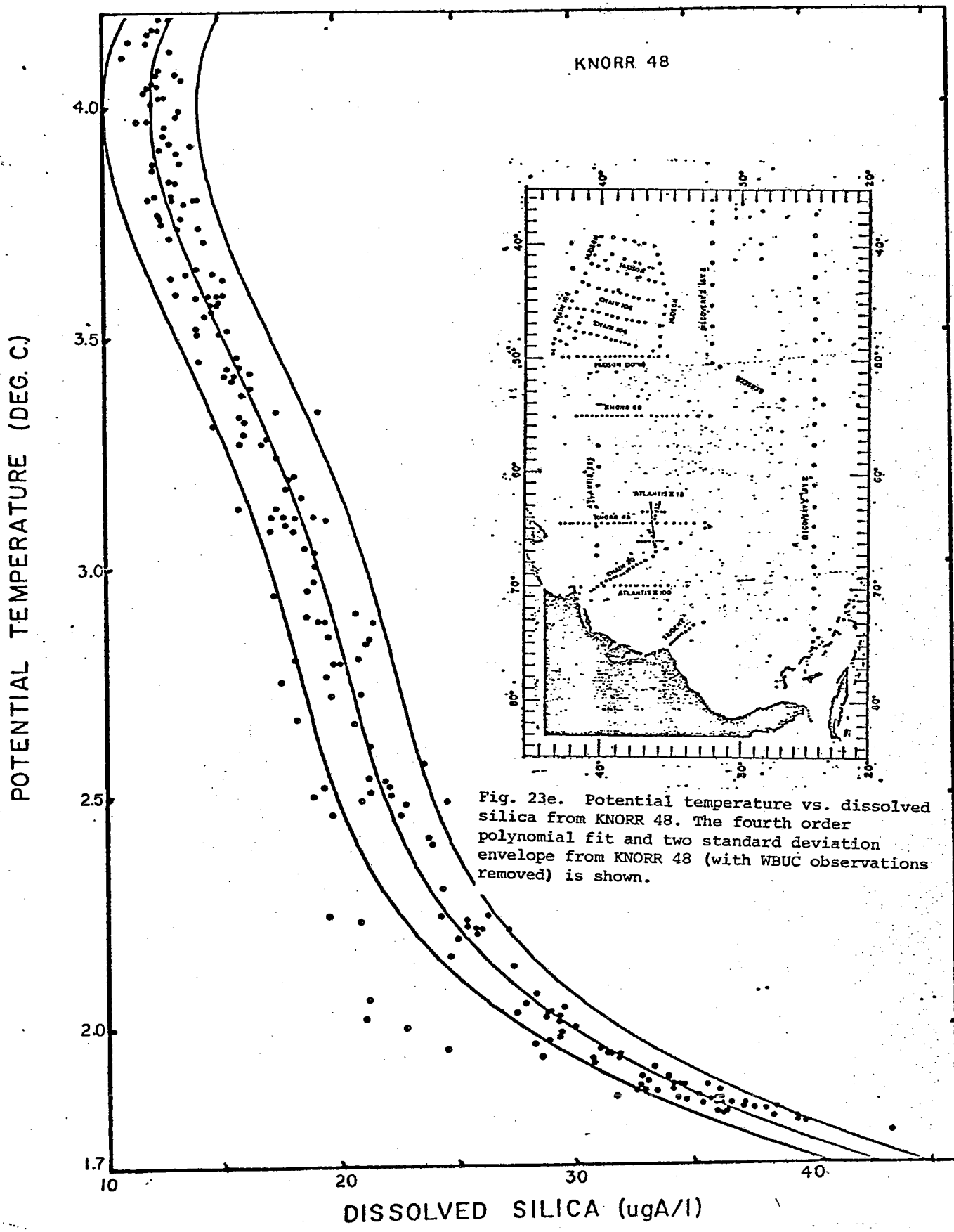

Fig. 23e. Potential temperature vs. dissolved silica from KNORR 48. The fourth order polynomial fit and two standard deviation envelope from KNORR 48 (with WBUC observations removed) is shown.

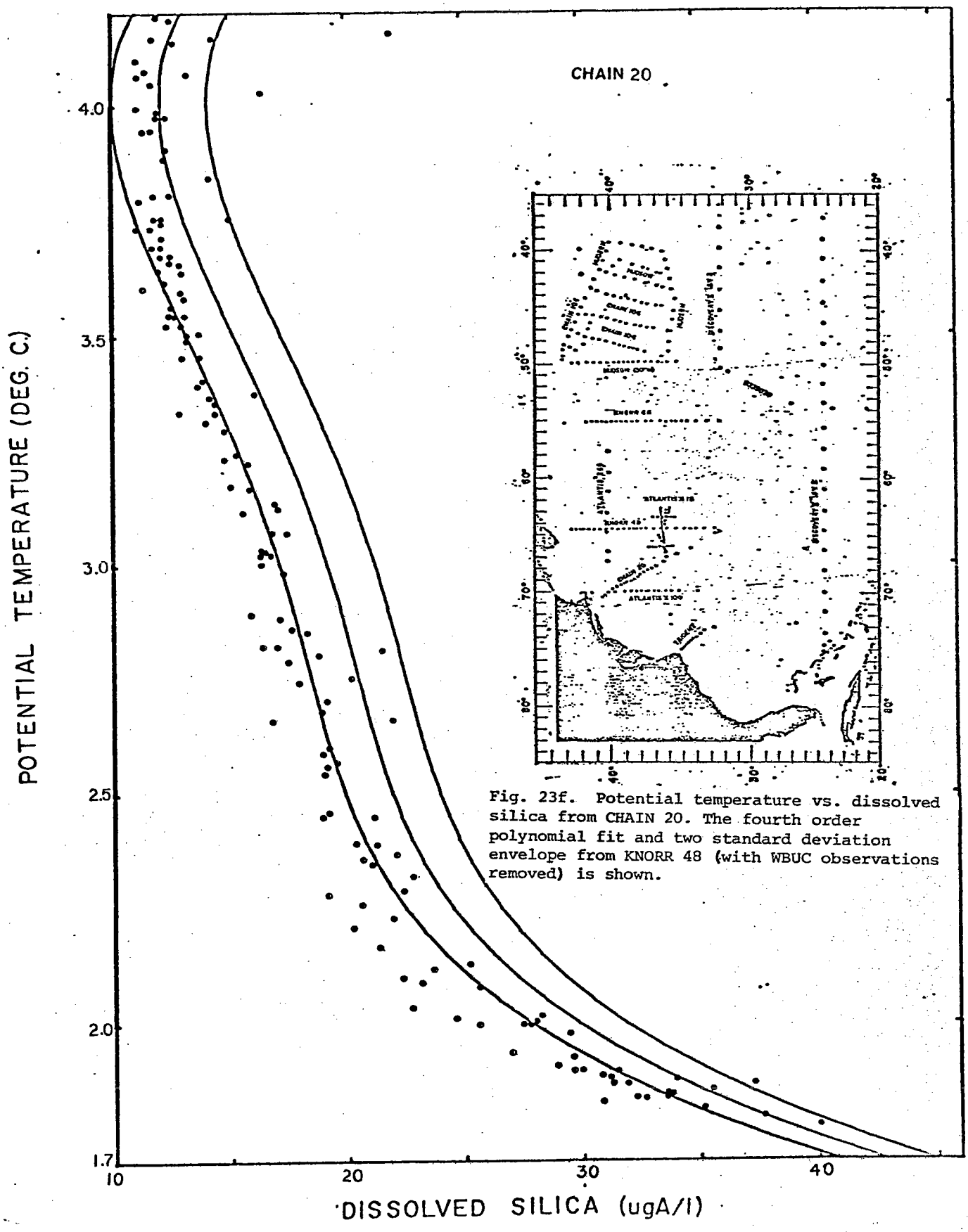

Fig. 23f. Potential temperature vs. dissolved silica from CHAIN 20. The fourth order polynomial fit and two standard deviation envelope from KNORR 48 (with WBUC observations removed) is shown.

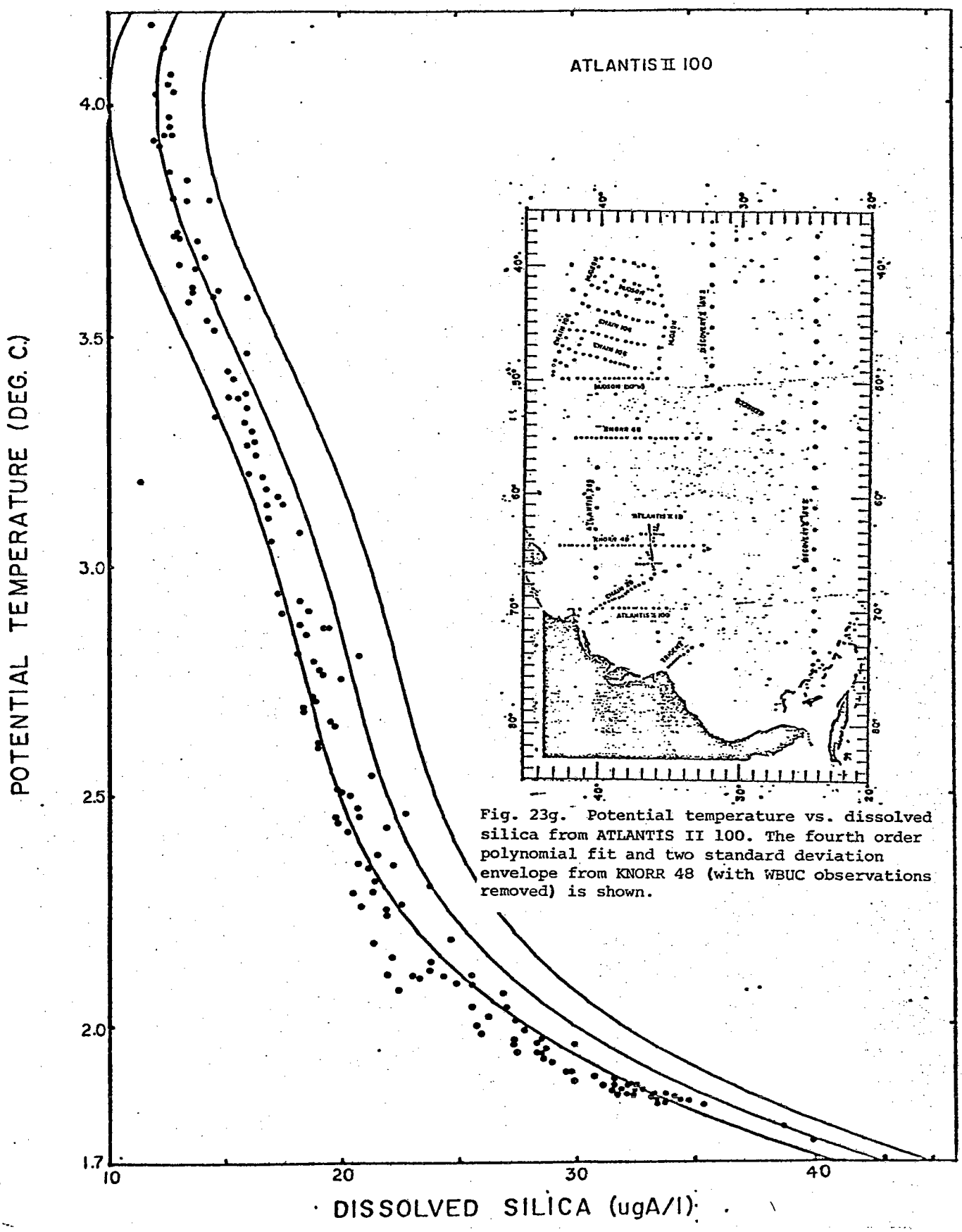

Fig. 23g. Potential temperature vs. dissolved silica from ATLANTIS II 100. The fourth order polynomial fit and two standard deviation envelope from KNORR 48 (with WBUC observations removed) is shown.

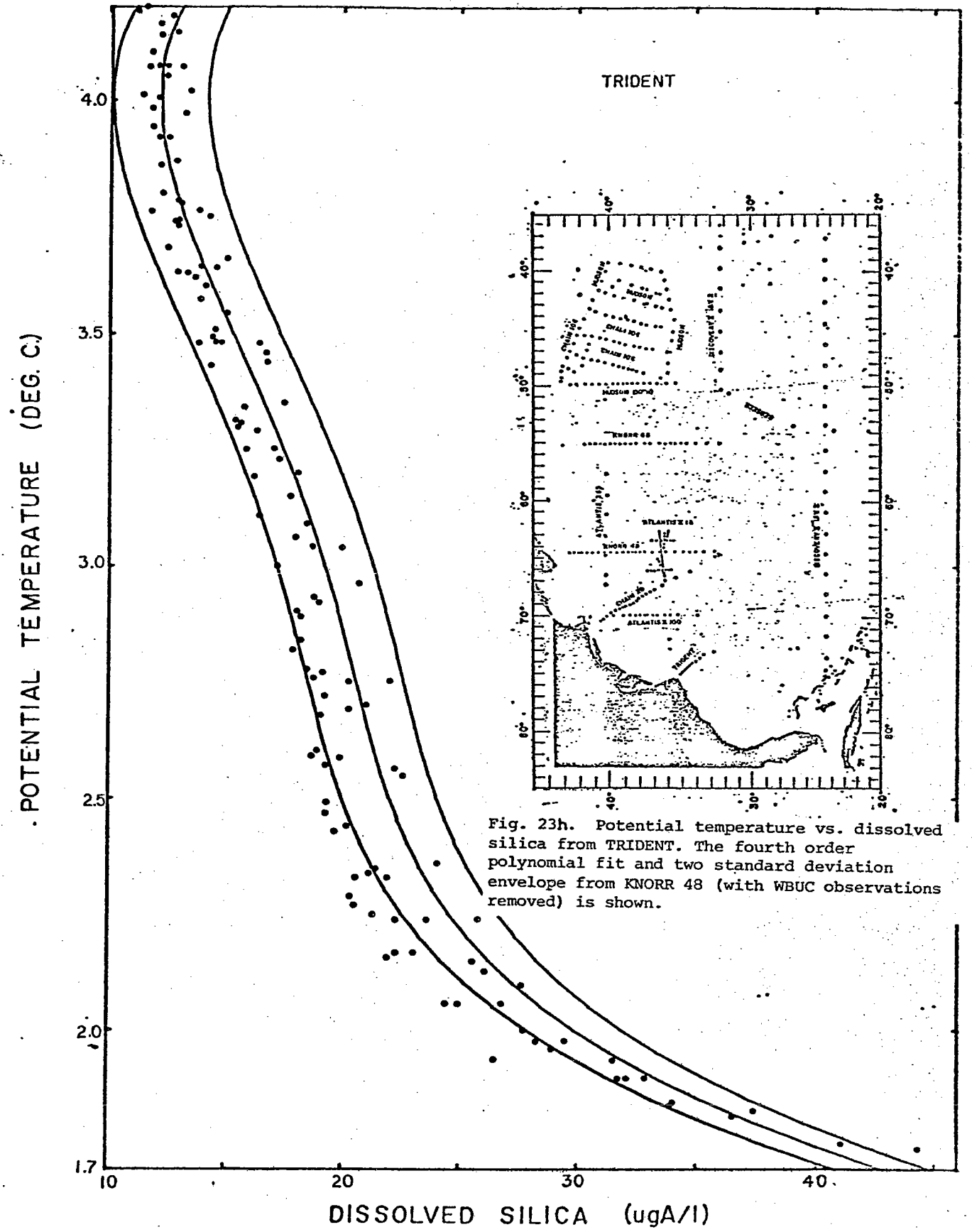

Fig. 23h. Potential temperature vs. dissolved silica from TRIDENT. The fourth order polynomial fit and two standard deviation envelope from KNORR 48 (with WBUC observations removed) is shown.

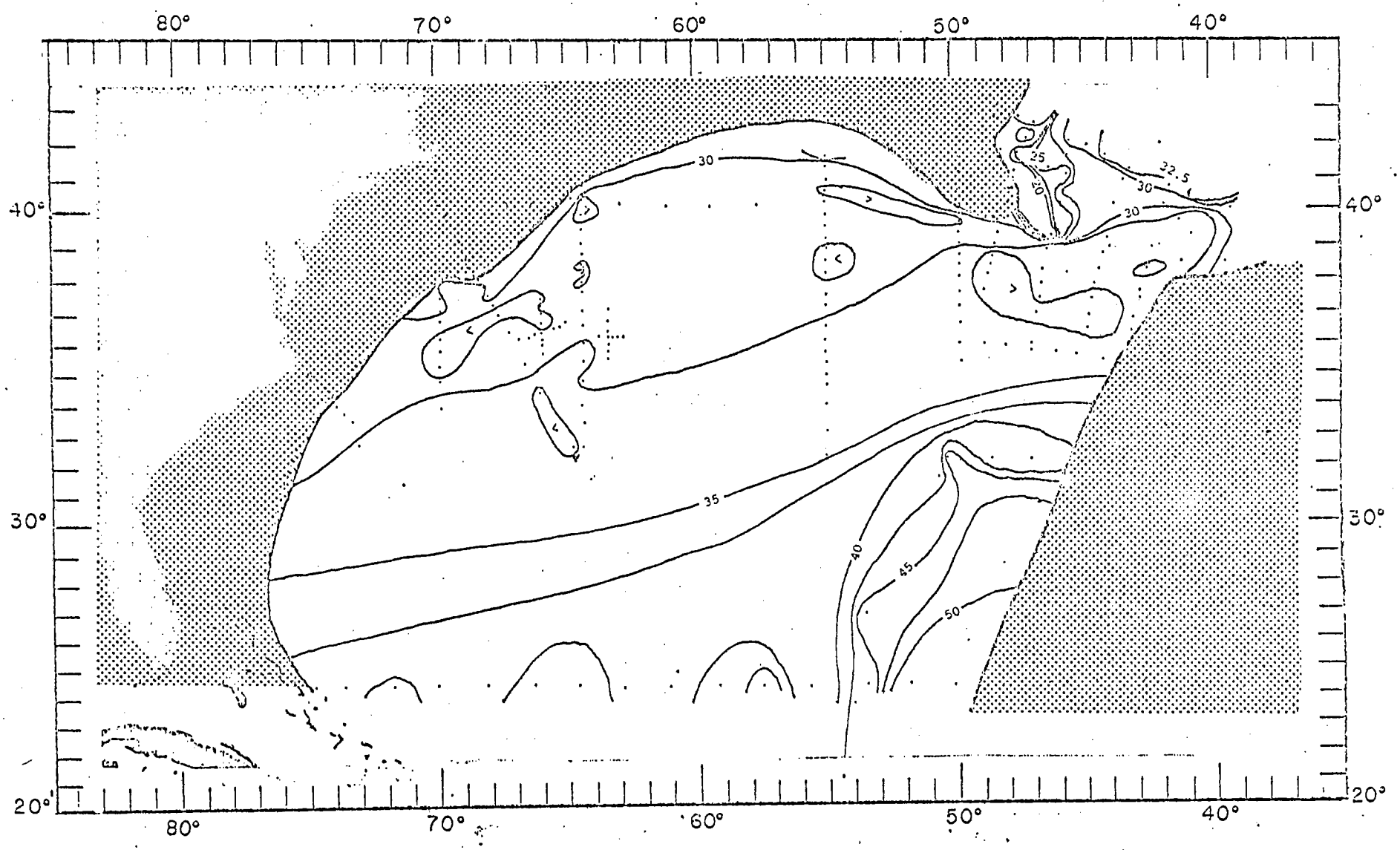

Fig. 24. Dissolved silica (ugA/l) on the 1.9°C potential temperature surface.

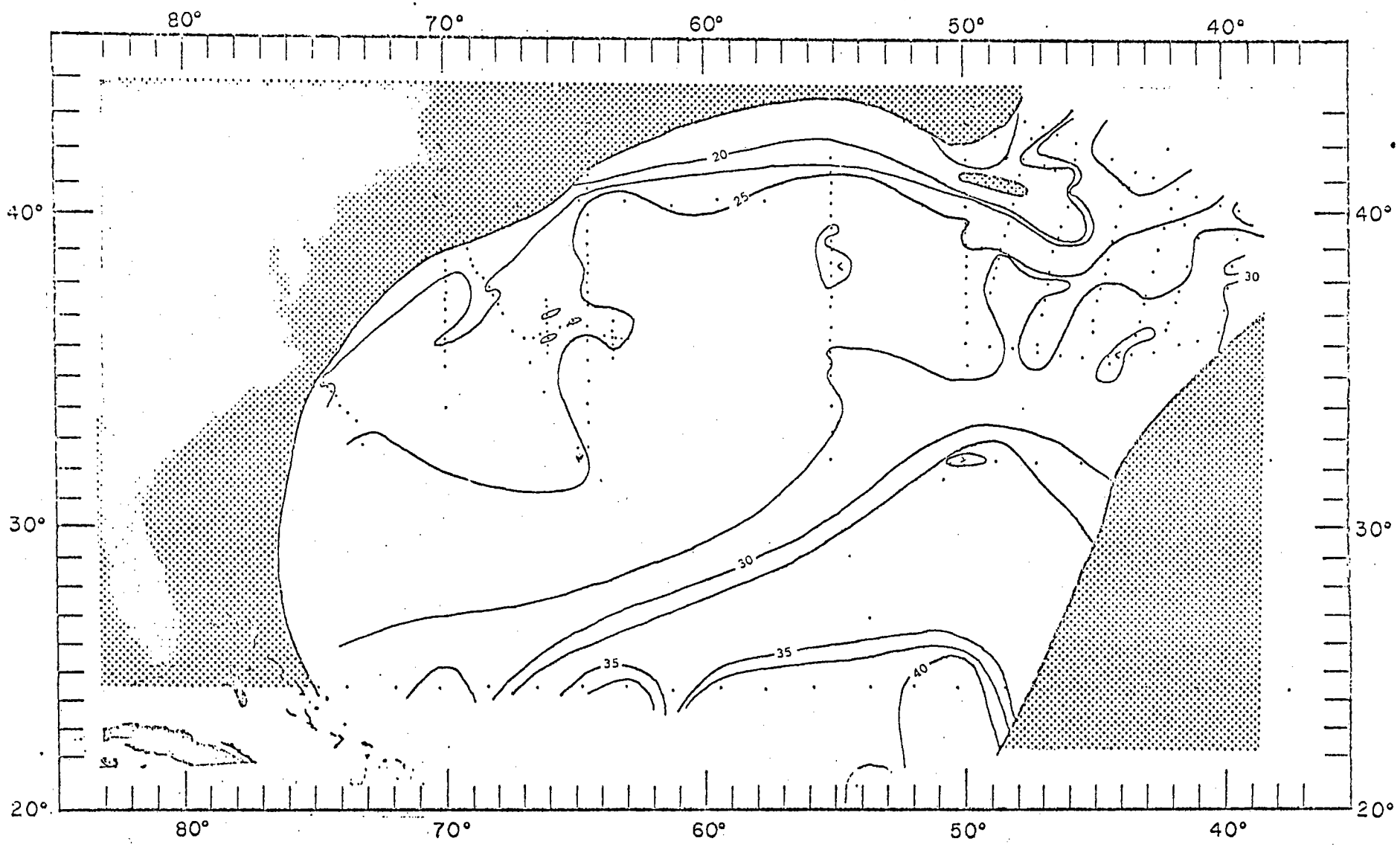

Fig. 25. Dissolved silica (ugA/l) on the 2.2°C potential temperature surface.

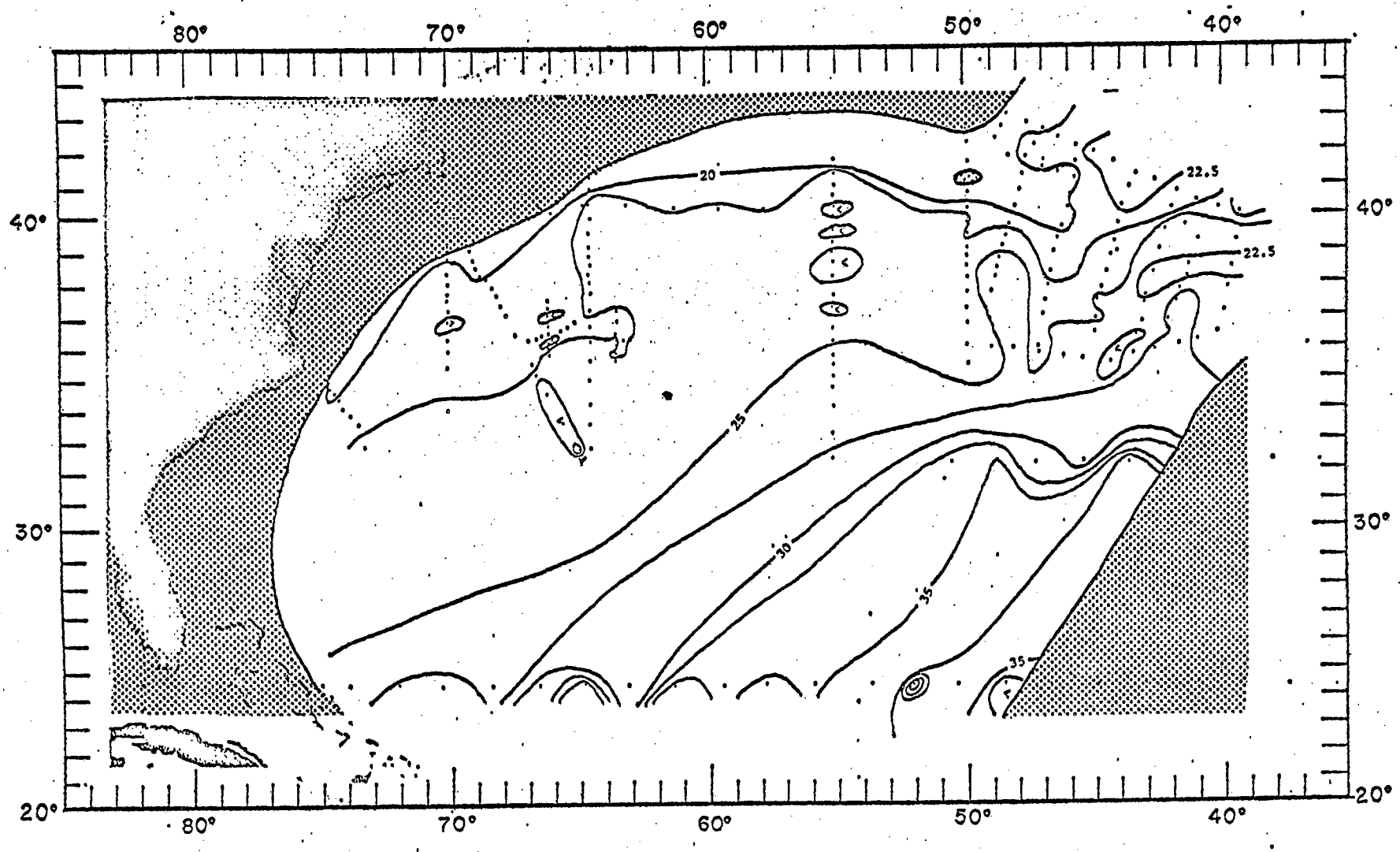

Fig. 26. Dissolved silica (ugA/l) on the 2.4°C potential temperature surface.

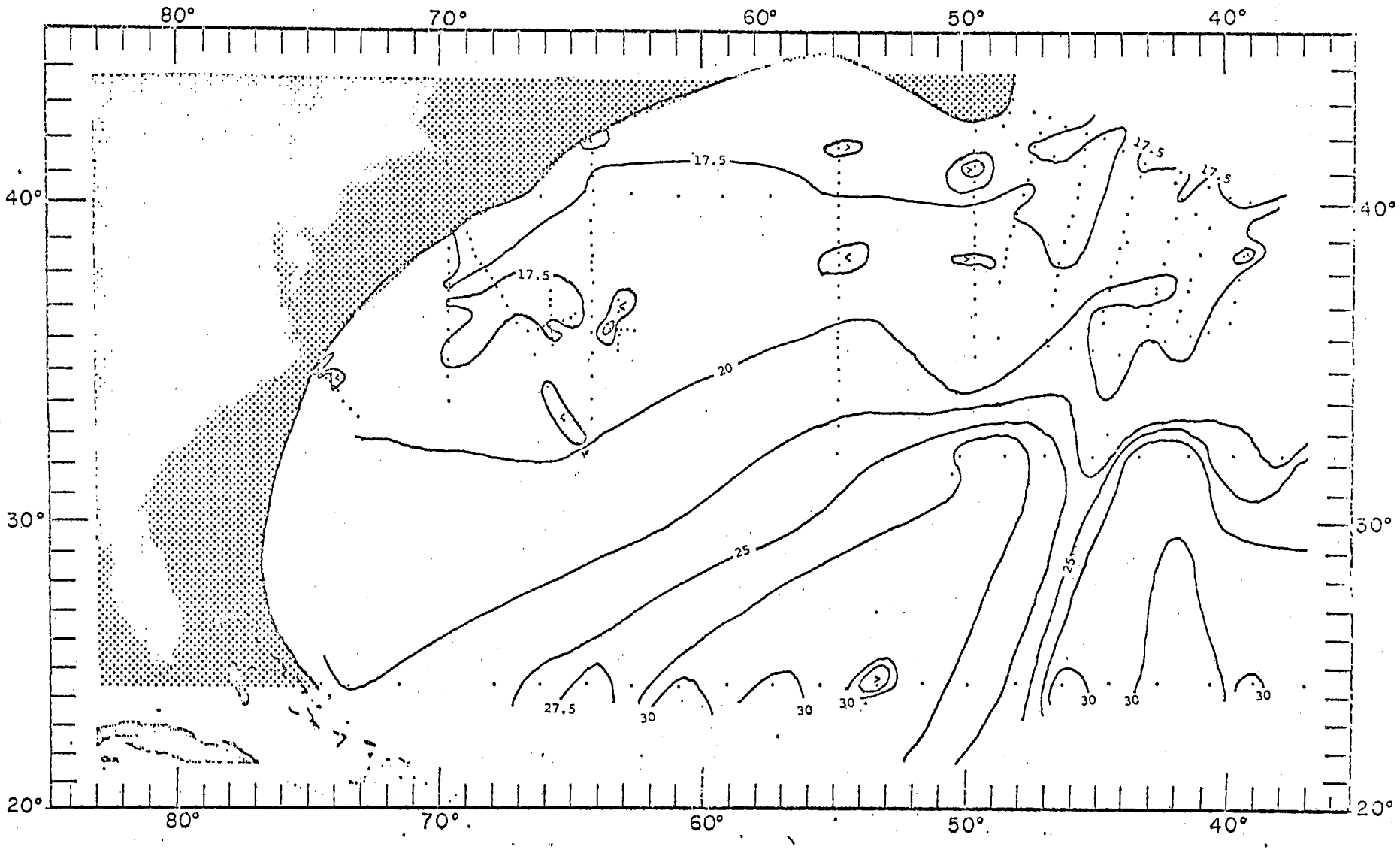

Fig. 27. Dissolved silica (ugA/l) on the 3.0°C potential temperature surface.

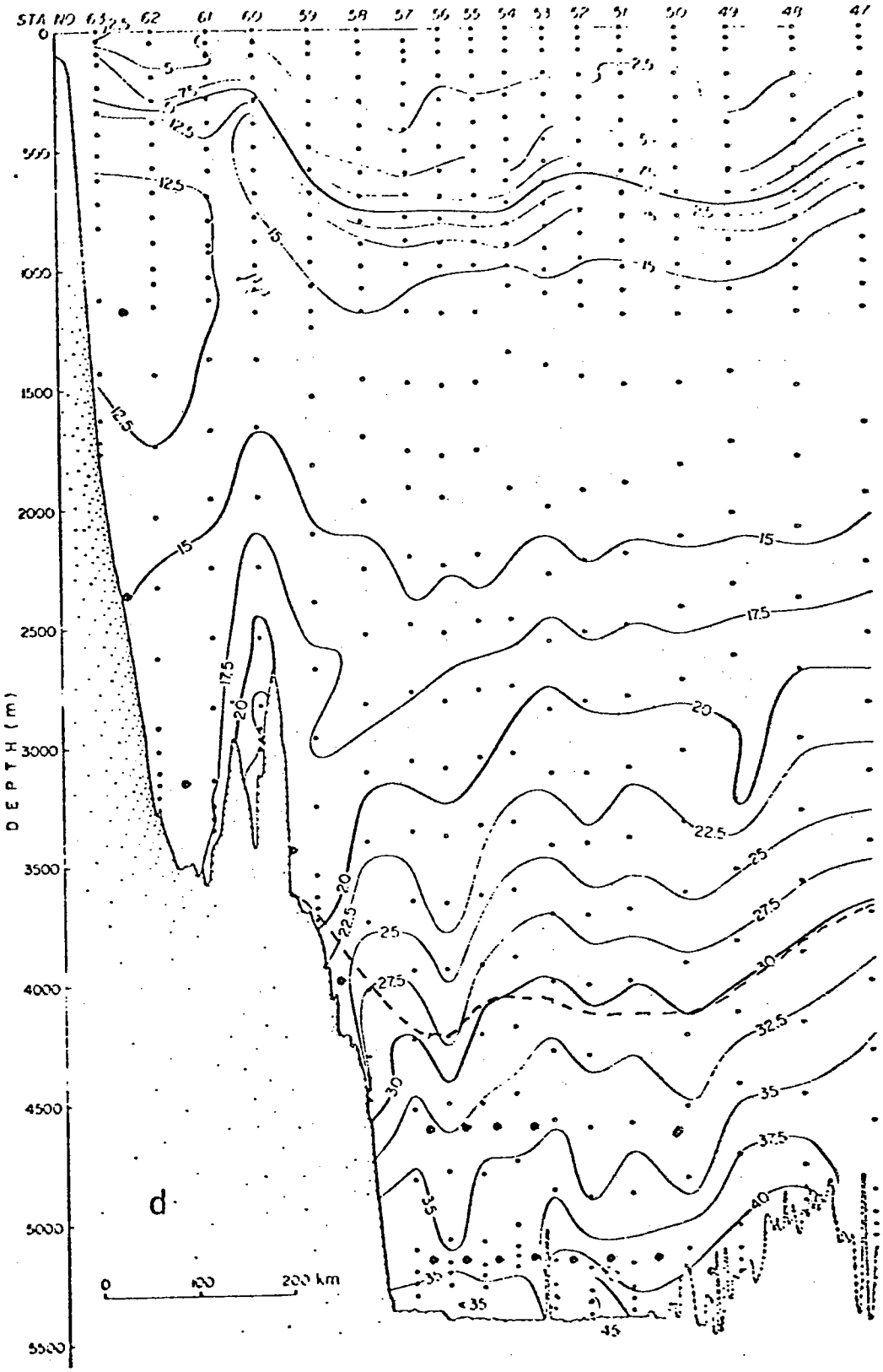

Fig 28. Section of dissolved silica (ugA/l) alon 50°W. The dotted line indicates the 2.0°C potential isotherm. The large dots indicate current meter locations (see text). (taken from Clarke, Hill, Reiniger and Warren (1978))

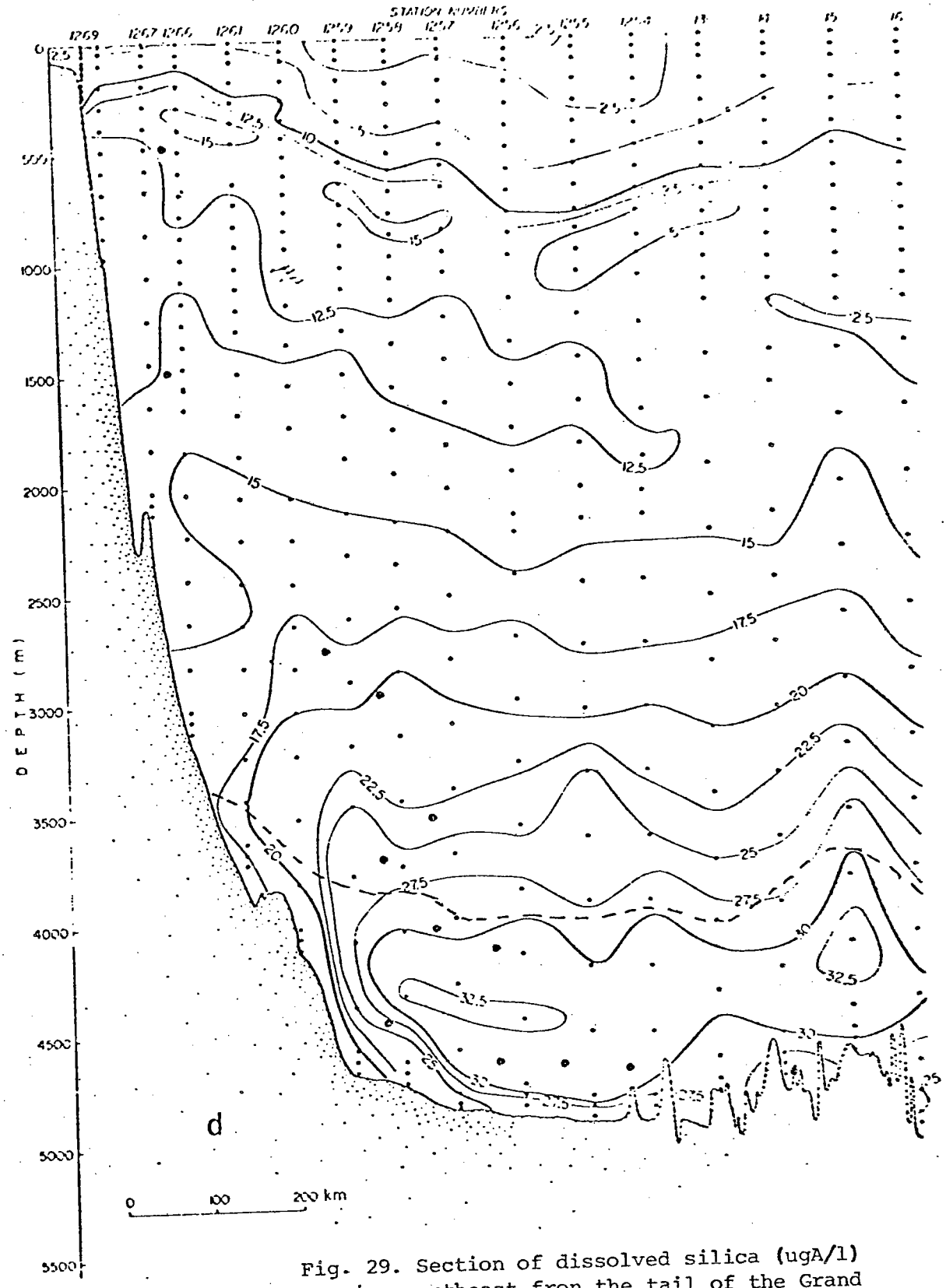

Fig. 29. Section of dissolved silica (ugA/l) running southeast fron the tail of the Grand Banks. The dotted line indicates the 2.0°C potential isotherm. The heavy dots indicate current meter positions (see text). (taken from Clarke, Hill, Reiniger and Warren (1978))

Fig. 30. Current meter record from the instrument along 50°W that was in the low silica water (see text).

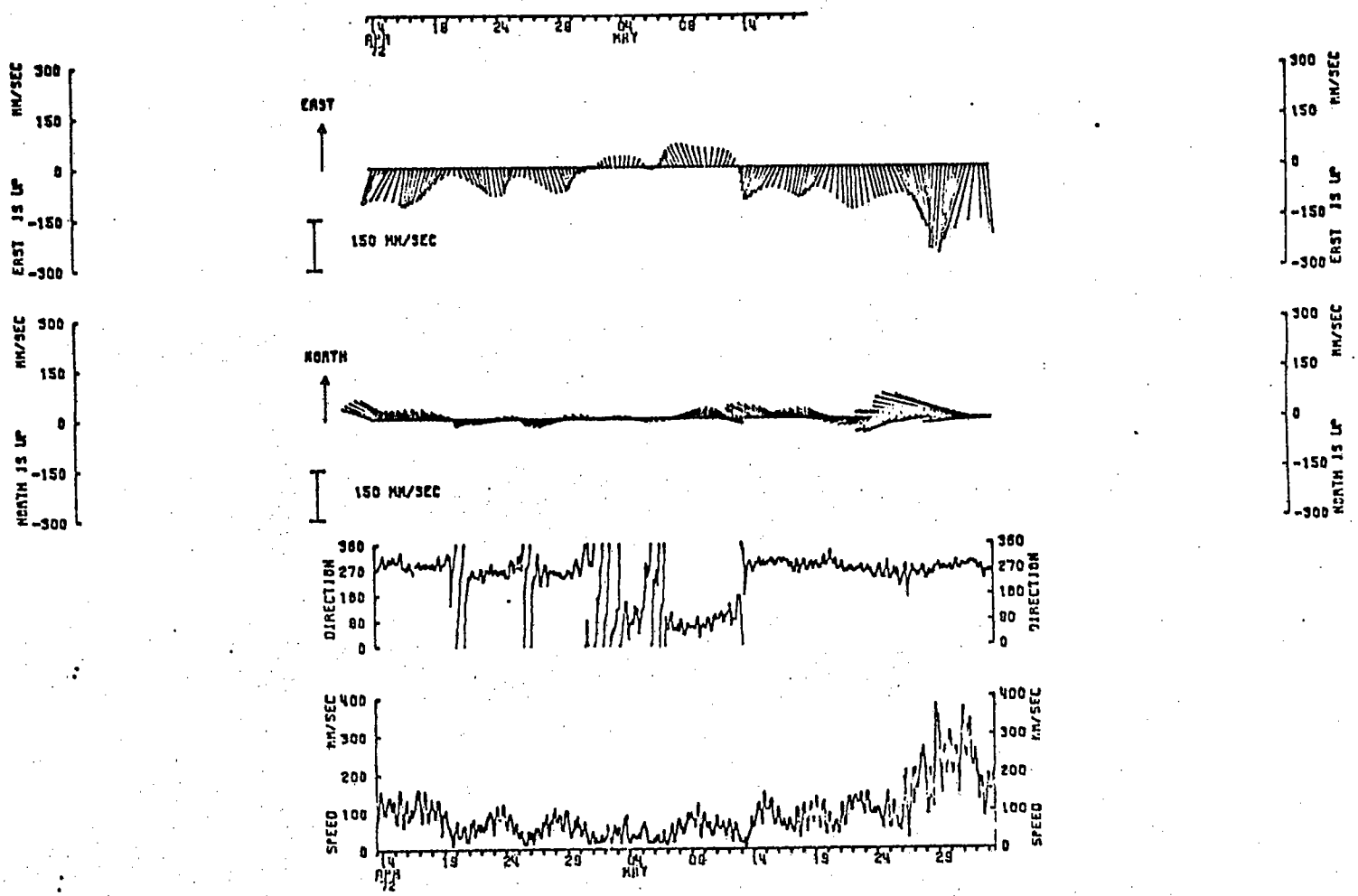

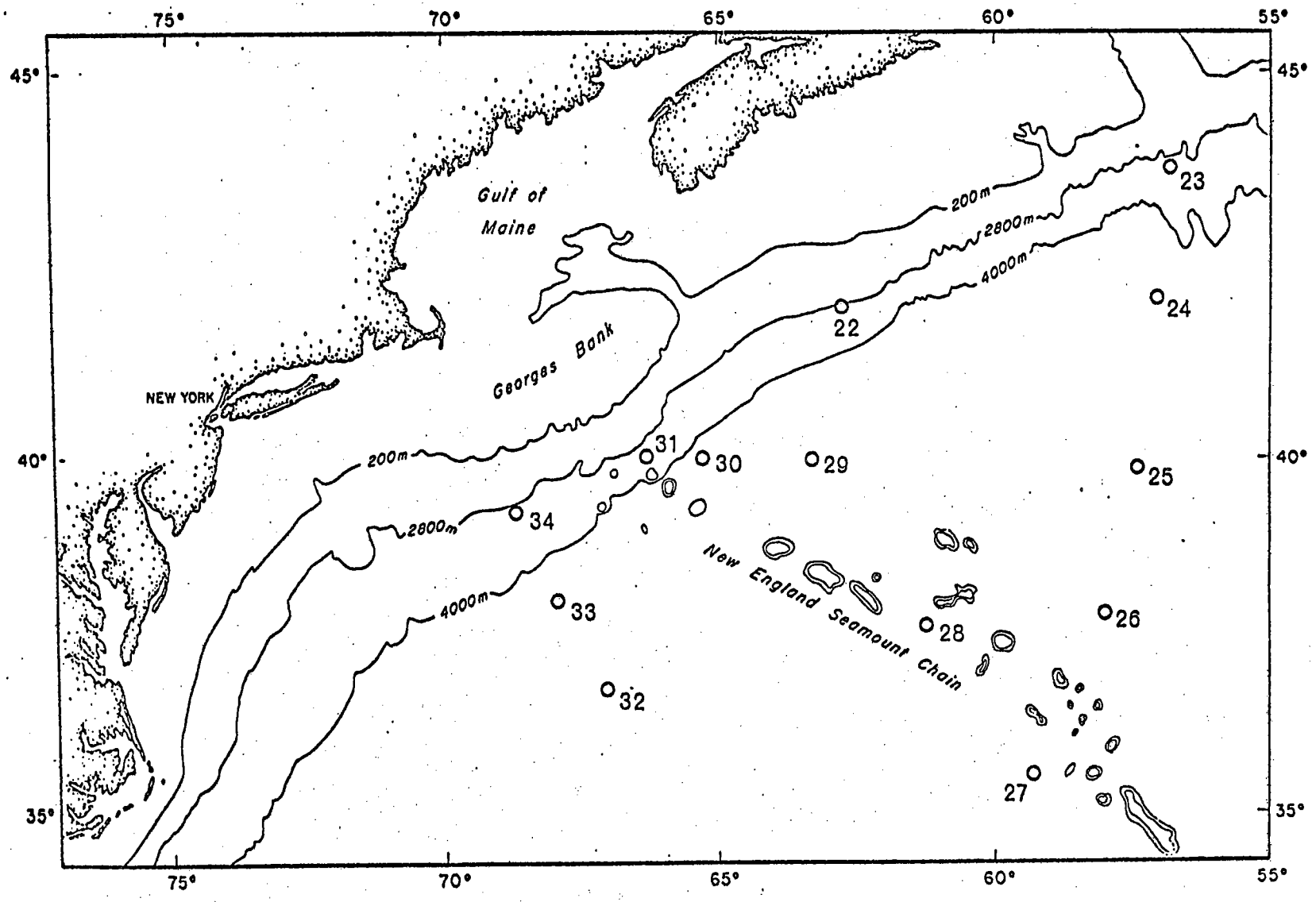

Fig. 31. Locations of stations from KNORR 12.

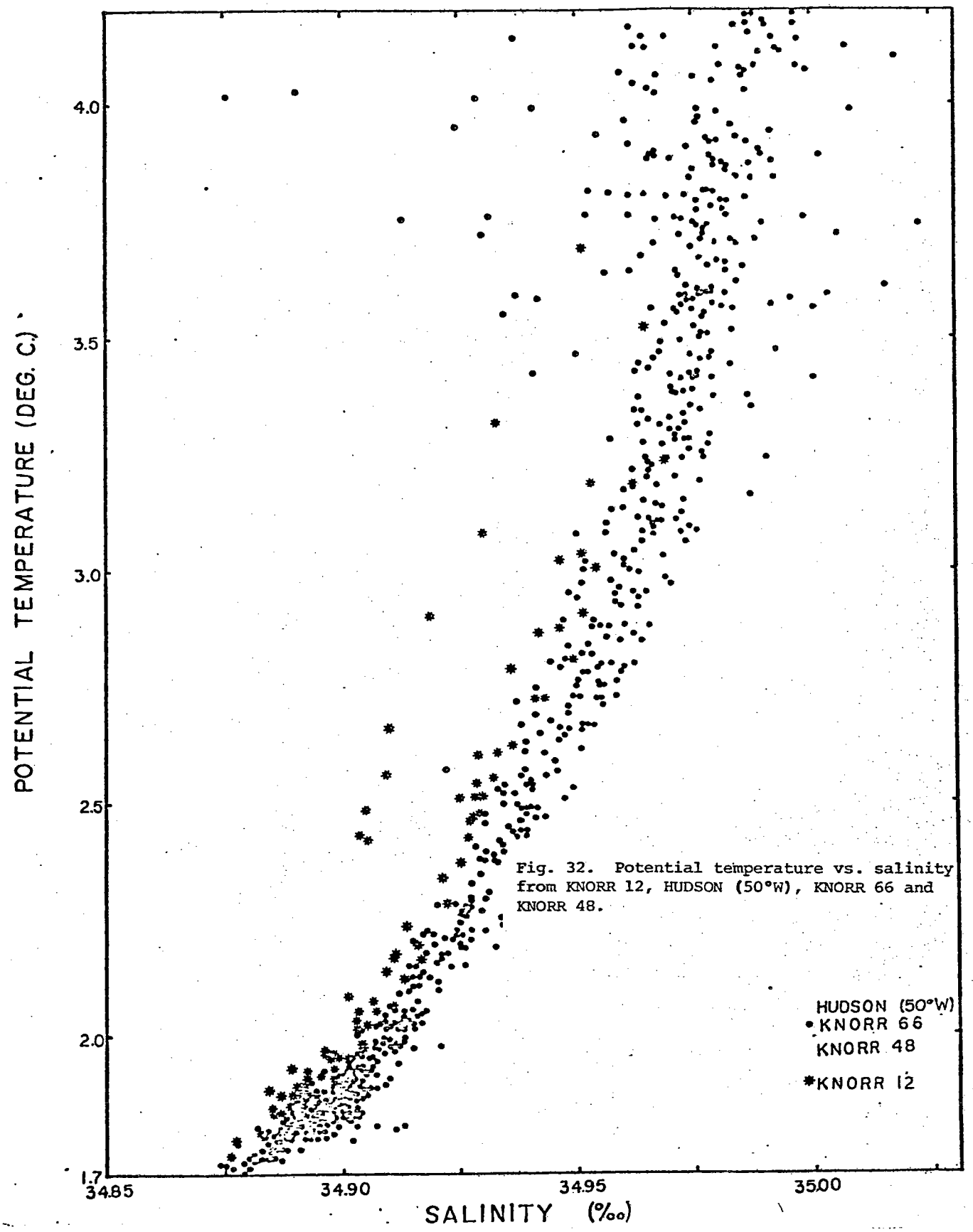

Fig. 32. Potential temperature vs. salinity from KNORR 12, HUDSON (50°W), KNORR 66 and KNORR 48.

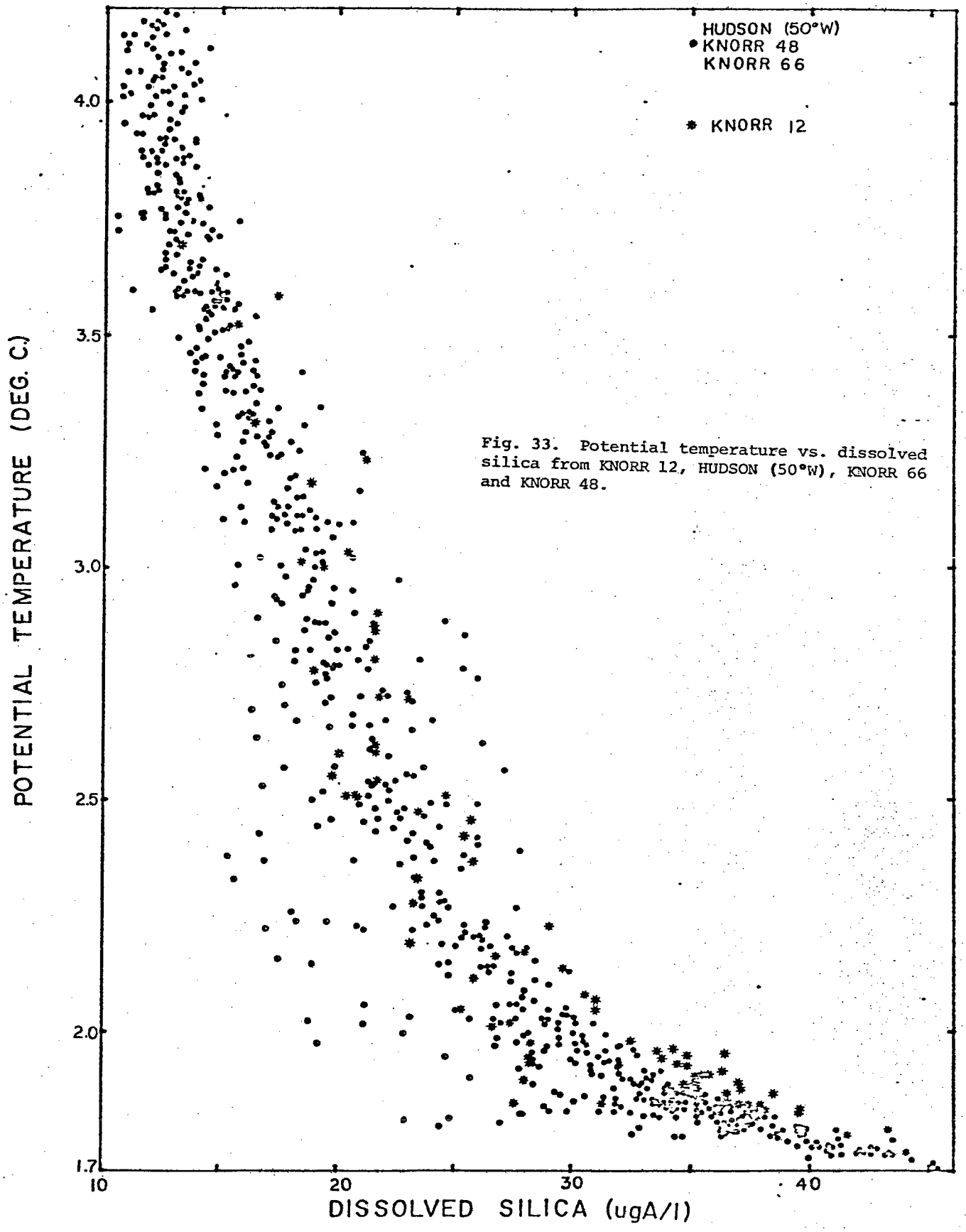

Fig. 33. Potential temperature vs. dissolved silica from KNORR 12, HUDSON (50°W), KNORR 66 and KNORR 48.